



3 4456 0269186 1

ORNL/TM-10504

ornl

OAK RIDGE NATIONAL LABORATORY

MARTIN MARIETTA

Long-Term Creep-Rupture Behavior of Modified 9Cr-1Mo Steel Base and Weldment Behavior

C. R. Brinkman
V. K. Sikka
J. A. Horak
M. L. Santella

OAK RIDGE NATIONAL LABORATORY
CENTRAL RESEARCH LIBRARY
CIRCULATION SECTION
4500N ROOM 175
LIBRARY LOAN COPY
DO NOT TRANSFER TO ANOTHER PERSON
If you wish someone else to see this
report, send in name with report and
the library will arrange a loan.
UCN-7969 (3-9-77)

~~APPLIED TECHNOLOGY~~

Any further distribution by any holder of this document or of the data therein to third parties representing foreign companies and foreign subsidiaries or foreign divisions of U.S. companies should be coordinated with the Deputy Assistant Secretary for Breeder Reactor Programs, Department of Energy.

No longer AT
Not ECI

David P. Harris 12/22/08

OPERATED BY
MARTIN MARIETTA ENERGY SYSTEMS, INC.
FOR THE UNITED STATES
DEPARTMENT OF ENERGY

Printed in the United States of America. Available from
the U.S. Department of Energy
Technical Information Center
P.O. Box 62, Oak Ridge, Tennessee 37830

This report was prepared as an account of work sponsored by an agency of the United States Government. Neither the United States Government nor any agency thereof, nor any of their employees, makes any warranty, express or implied, or assumes any legal liability or responsibility for the accuracy, completeness, or usefulness of any information, apparatus, product, or process disclosed, or represents that its use would not infringe privately owned rights. Reference herein to any specific commercial product, process, or service by trade name, trademark, manufacturer, or otherwise, does not necessarily constitute or imply its endorsement, recommendation, or favoring by the United States Government or any agency thereof. The views and opinions of authors expressed herein do not necessarily state or reflect those of the United States Government or any agency thereof.

ORNL/TM-10504
Distribution
Categories UC-79Th,
-Tk, -Tr

Metals and Ceramics Division

LONG-TERM CREEP-RUPTURE BEHAVIOR OF MODIFIED 9Cr-1Mo
STEEL BASE AND WELDMENT BEHAVIOR

C. R. Brinkman, V. K. Sikka, J. A. Horak,
and M. L. Santella

Date Published: November 1987

~~TECHNOLOGY~~
Other distribution by any holder of this document
or of the information contained therein to third parties representing
foreign companies and organizations or foreign
divisions of U.S. companies should be coordinated with
the Deputy Assistant Secretary for Breeder Reactor
Programs, Department of Energy.

NOTICE This document contains information of a preliminary nature.
It is subject to revision or correction and therefore does not represent a
final report.

Prepared for the
DOE Office of Technology Support Programs
AF 20 40 00 0

Prepared by the
OAK RIDGE NATIONAL LABORATORY
Oak Ridge, Tennessee 37831
operated by
MARTIN MARIETTA ENERGY SYSTEMS, INC.
for the
U.S. DEPARTMENT OF ENERGY
under Contract DE-AC05-84OR21400

MARTIN MARIETTA ENERGY SYSTEMS LIBRARIES

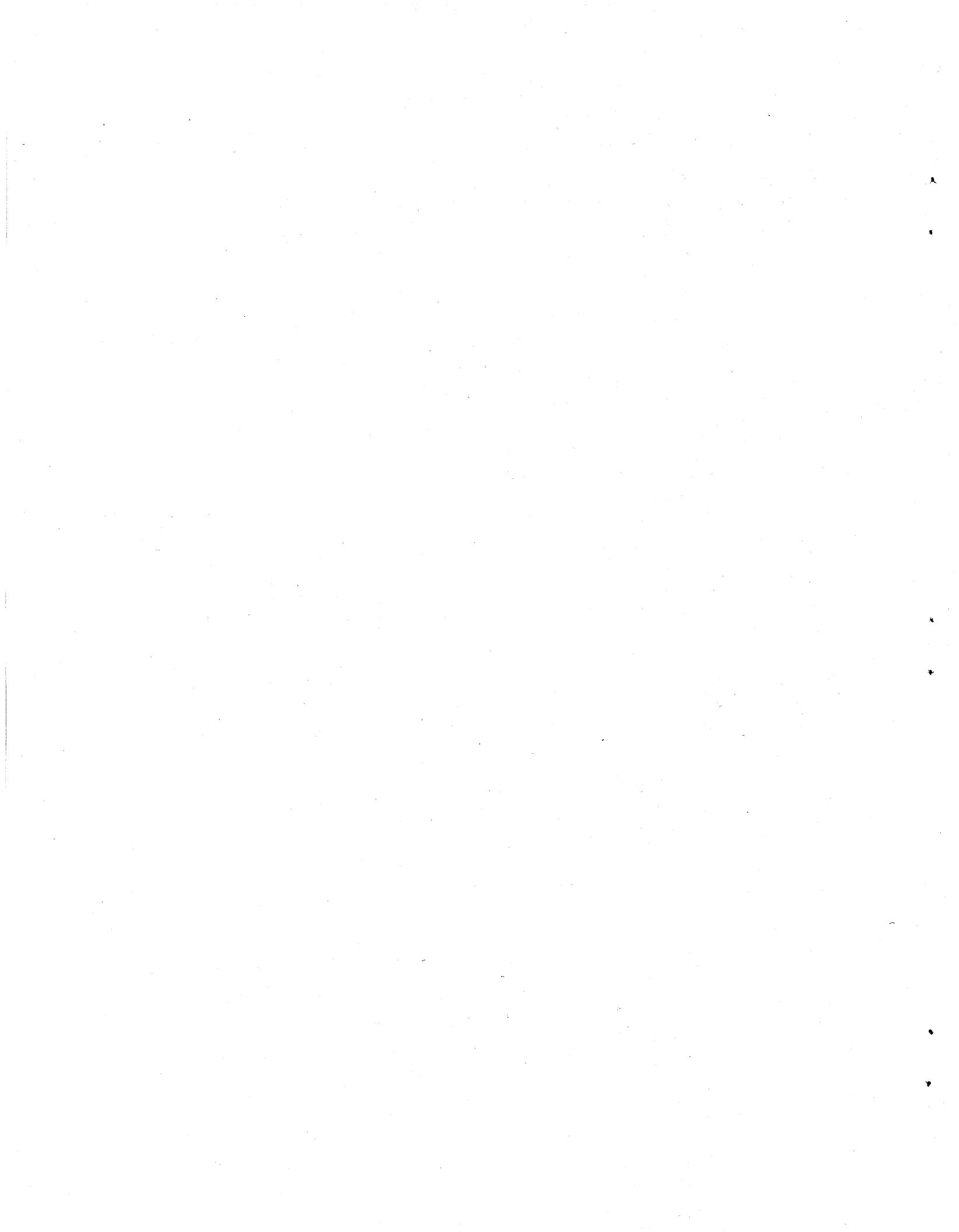


3 4456 0269186 1



CONTENTS

ABSTRACT	1
INTRODUCTION	1
MATERIALS AND EXPERIMENTAL PROCEDURE	2
RESULTS	8
DISCUSSION	11
CONCLUSIONS	35
ACKNOWLEDGMENTS	36
REFERENCES	36



LIST OF FIGURES

Fig. 1. Creep specimen used in the testing of modified 9Cr-1Mo steel.

Fig. 2. Stress-rupture data for commercial heats of modified 9Cr-1Mo steel tested in the normalized and tempered condition. Average curves from the time-temperature parameter are also included in these plots.

Fig. 3. Stress-minimum creep rate data for commercial heats of modified 9Cr-1Mo steel tested in the normalized and tempered condition. Average curves from the time-temperature parameter are also included in these plots.

Fig. 4. (a) Creep-rupture ductility data as a function of rupture time at various temperatures for commercial heats. (b) Reduction of area data from long-term creep-rupture tests at 593°C indicating reduced ductility at test times in excess of about 20,000 h. (c) Reduction of area vs time to failure for multiple wrought heats of modified 9Cr-1Mo and type 304 stainless steel.

Fig. 5. Effect of aging for 25,000 h on creep-rupture life of modified 9Cr-1Mo steel.

Fig. 6. Comparison of creep-rupture strength of modified 9Cr-1Mo sand castings with average curve for wrought material.

Fig. 7. Comparison of creep-rupture data on saddle forging with average curve developed from model for various product forms of several commercial heats. Maximum allowable design stress curve from ASME Code Case 1943 for Grade 91 is also included for comparison.

Fig. 8. Comparison of creep-rupture data on heats of modified 9Cr-1Mo steel melted and fabricated in Japan with average curve for commercial heats melted and tested in the United States

Fig. 9. Stress-rupture plot at 593°C comparing data on commercial heats of modified 9Cr-1Mo steel (tested in normalized and tempered condition) with average curves for standard British 9Cr-1Mo steel tested in normalized and tempered condition and standard American 9Cr-1Mo steel and 2.25Cr-1Mo steel tested in annealed conditions.

Fig. 10. Variation of 10^5 creep-rupture strength with temperature for several materials.

Fig. 11. Stress ratio (weldment to base metal average) as a function of time to rupture for SA weldments of both standard and modified 9Cr-1Mo filler wire compositions. Data are for test temperatures of 538 and 593°C. Stress ratios of unity, representing equal strength, and 0.67, the criterion for allowable stresses in ASME Code, Sect. VIII, are also included.

Fig. 12. Stress ratio (weldment to base metal average) as a function of time to rupture for GTA weldments of both standard and modified 9Cr-1Mo filler wire compositions. Data are for test temperatures 538, 593, 565, and 649°C. Stress ratios of unity, representing equal strength, and 0.67, the criterion for allowable stresses in ASME Code, Sect. VIII, are also included.

Fig. 13. Stress ratio (weldment to base metal average) as a function of time to rupture for SMA weldments of both standard and modified 9Cr-1Mo filler wire compositions. Data are for test temperatures of 538, 593, 649, and 677°C. Stress ratios of unity, representing equal strength, and 0.67, the criterion for allowable stresses in ASME Code, Sect. VIII, are also included.

Fig. 14. Stress ratio (weldment to base metal average) as a function of time to rupture. Weldment data are for both the standard and modified 9Cr-1Mo filler wire and for all three welding processes (GTA, SMA, and SA). Data are for test temperatures of 538, 565, 593, 649, and 677°C. Stress ratios of unity, representing equal strengths, and 0.67, representing the ASME Code, Sect. VIII, criteria for allowable stresses, are also included.

Fig. 15. Stress ratio (weldment to base metal minimum) as a function of time to rupture. Weldment data are for both the standard and modified 9Cr-1Mo filler wire and for all three welding processes (GTA, SMA, and SA). Data are for test temperatures of 538, 565, 593, 649, and 677°C. Stress ratios of unity, representing equal strengths; 0.80, the criterion for allowable stresses in ASME Code, Sect. VIII; and 0.67, the criterion for allowable stresses in ASME Code Case N-47, are also included.

Fig. 16. Hardness profile across several weldments illustrating strong and weak zones. (a) Gas tungsten arc (GTA). (b) Submerged arc (SA). (c) Submerged arc (SA). (d) Shielded metal arc (SMA).

Fig. 17. Hardness traverse data for GTA weld PC-116 showing that a 760°C PWHT is necessary to eliminate the overtempered region in partially tempered base plate.

Fig. 18. Comparison of post-tested weldment creep specimens given the standard and modified heat treatment prior to creep testing at 593°C. Note the slant fracture appearance of specimens given the standard heat treatment, i.e., 1038°C/760°C/732°C in comparison to the cup-cone fractures of those given the modified heat treatment, i.e., 1038°C/621°C/760°C.

Fig. 19. Stress-rupture properties of specimens taken across weldments with base, heat-affected-zone, and weld metal all within gage section of the specimen unless specified otherwise. Weldments prepared by SA, SMA, and GTA processes.

Fig. 20. Stress-rupture properties of specimens taken across weldments with base, heat-affected-zone, and weld metal all within gage section of the specimen unless specified otherwise. Weldments prepared by SA, SMA, and GTA processes.

Fig. A1.1

Fig. A1.2

Fig. A1.3

Fig. A1.4

Fig. A1.5

Fig. A1.6

Fig. A1.7

Fig. A1.8

Fig. A1.9

Fig. A3.1. Microstructures of 9Cr-1Mo (91887) showing subgrains as well as precipitates along prior austenite grain boundaries.

Fig. A3.2. Microstructures of 9Cr-1Mo (XA3370) showing subgrains as well as grain boundary precipitates along prior austenite boundaries.

Fig. A3.3. Micrograph of 9Cr-1Mo (91887) illustrating the distribution of precipitates in locations other than at prior austenite boundaries.

Fig. A3.4. Microstructure of 9Cr-1Mo (91887) showing the general dislocation distribution.

Fig. A3.5. Microstructure of 9Cr-1Mo (XA3370) showing heterogeneous dislocation distribution.

Fig. A3.6. Micrograph showing detail of dislocation networks in subgrain boundaries in alloy 91887.

Fig. A3.7. Micrograph showing detail of dislocation networks in subgrain boundaries in alloy 91887.

Fig. A3.8. Micrograph showing detail of dislocation networks in subgrain boundaries in alloy XA3370.

Fig. A3.9. Micrograph showing detail of dislocation networks in subgrain boundaries in alloy XA3370.

Fig. A3.10. Precipitate examined by in situ energy dispersive X-ray spectroscopy. Specimen is untilted.

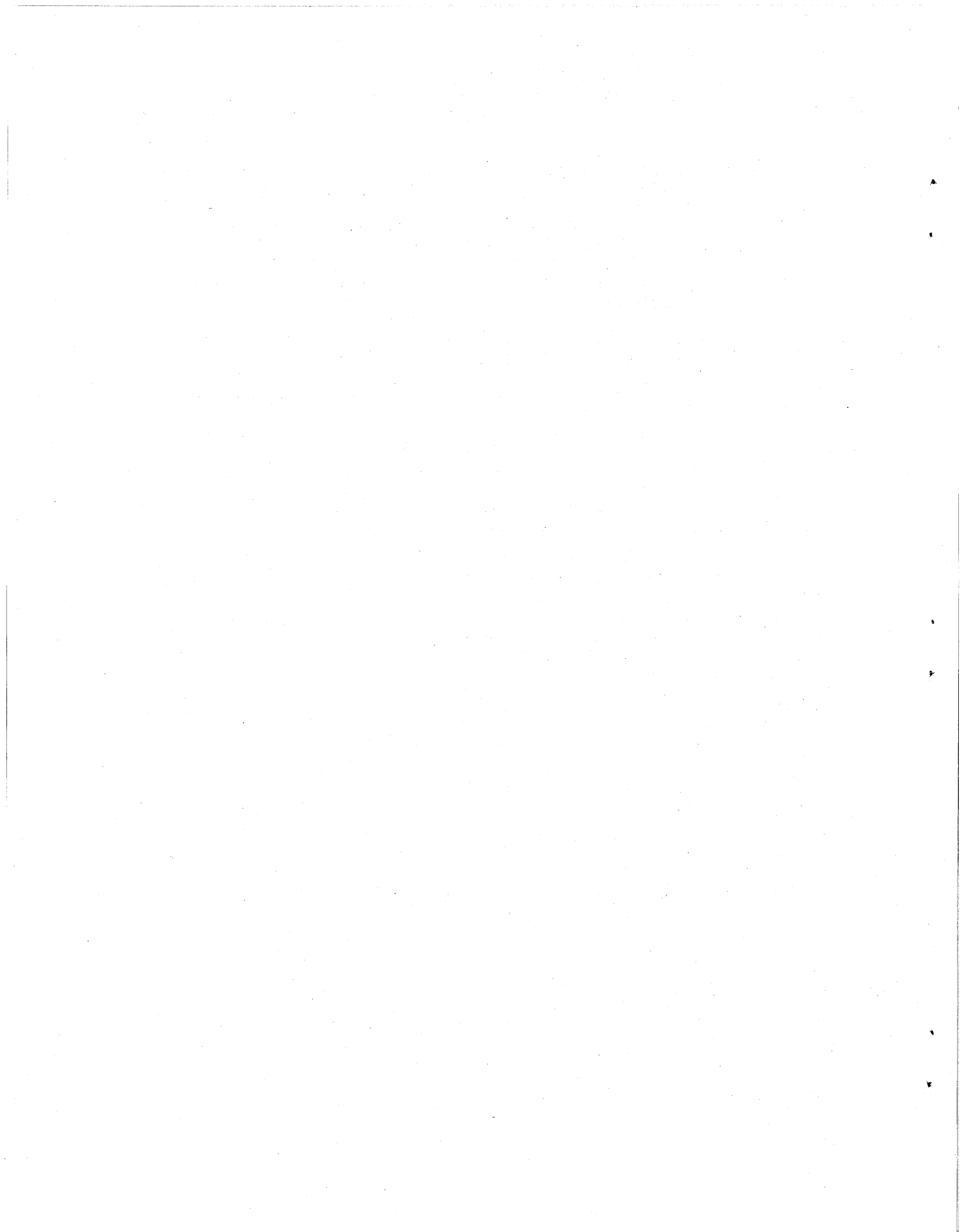
Fig. A3.11. Same precipitate shown in Fig. A3.10 with specimen tilted for X-ray microanalysis. Deterioration of the image quality is due to the interaction of the asymmetric magnetic field of the specimen with the objective lens field.

Fig. A3.12. X-ray spectra from MC precipitate analyzed in situ and adjacent matrix. Note the presence of Nb and V in the precipitate. Lower spectra show detail with expanded vertical scale.

Fig. A3.13. (a) Bright field, (b) dark field, and (c) selected area diffraction pattern illustrating the presence of small particles (~5 nm) in alloy XA3370. These may be precipitates or surface oxide particles.

LIST OF TABLES

- Table 1. Details on melting of commercial heats of modified 9Cr-1Mo steel
- Table 2. Summary of information of fabrication of commercial modified 9Cr-1Mo alloy.
- Table 3. Chemical analyses of various commercial heats of modified 9Cr-1Mo steel.
- Table 4. Commercial chemical composition specifications for modified 9Cr-1Mo steel.
- Table 5. Status of creep-rupture tests of modified 9Cr-1Mo steel
- Table 6. Status of creep-rupture tests of modified 9Cr-1Mo steel welds.
- Table 7. Comparison of measured and predicted rupture lives for modified 9Cr-1Mo steel weldments.
- Table A2.1. Welding procedures for modified 9Cr-1Mo steel
- Table A2.2. Results of creep-rupture tests on weldments of modified 9Cr-1Mo steel
- Table A3.1. Average of top and bottom ingot chemical composition (chromium equivalent numbers are also listed in this table)
- Table A3.2 Table A3.2



LONG-TERM CREEP-RUPTURE BEHAVIOR OF MODIFIED 9Cr-1Mo
STEEL BASE AND WELDMENT BEHAVIOR*

C. R. Brinkman, V. K. Sikka, J. A. Horak,
and M. L. Santella

ABSTRACT

Results are reported of long-term creep and creep-rupture tests from ongoing and completed tests conducted on modified 9Cr-1Mo steel in the normalized and tempered condition and its weldments. Test data are reported over the temperature range of 427 to 704°C obtained from multiple heats of wrought and cast material. Stress-rupture and creep data are given from tests on base material with test times to about 68,000 h (7.8 years to April 1987). Comparisons are made between long-term experimental data and predictions made with creep and rupture equations developed in 1984. Also given are results from rupture tests on specimens taken from weldments. These specimens were either all weld metal or taken transverse across a weldment such that the gage length contained weld, heat-affected-zone, and base material. Weldment materials were given either a standard or modified heat treatment. The objective of the modified heat treatment was to minimize a slightly weak or soft area in the heat-affected zone. Creep-rupture data indicate that the modified heat treatment improves the rupture behavior of weldments of this material.

INTRODUCTION

Development of modified 9Cr-1Mo steel began over 12 years ago.¹ It is now a commercially available alloy for long-term elevated temperature use in future Liquid Metal Reactor (LMR) plants. An important part of the justification of this new alloy for service in LMR systems has been the availability of a creep and creep-rupture data base to define

*Research sponsored by the U.S. Department of Energy, Office of Technology Support Programs, under contract DE-AC05-84OR21400 with Martin Marietta Energy Systems, Inc.

long-term rupture and deformation behavior. This is necessary for LMR components which may operate at temperatures where creep damage can occur for periods of up to 50 to 60 years. Hence, extensive creep characterization of multiple heats and product forms including weldments was initiated soon after the composition of this new alloy was fixed. Periodically, reports and papers have been written to define available properties and document results of ongoing tests on both base materials²⁻⁴ and weldments.^{5,6} Therefore, it is the objective of this report to present a status report of ongoing creep tests being conducted on wrought material (multiple heats and product forms), castings, and weldments (composite specimens) including all weld metal specimens.

MATERIALS AND EXPERIMENTAL PROCEDURE

Creep tests were performed on commercially available heats and product forms. Specifics about heat identification, melter, size, and melting practice are given in Table 1, while product form, identification, fabrication method, and fabricator are given in Table 2. Chemical composition of the various heats is given in Table 3. Most of the various heats and product forms met the target chemical composition, Table 4. However, there were some variations which allowed studies to be made of deviations in chemistry as follows. Heat F5349 was low in nitrogen, i.e., 0.011 vs a target range of 0.03 to 0.07 wt%. Heats 30176 and 30182 (same as 30176, see Table 1, footnote c) are low in silicon content, i.e., 0.11 vs a target range of 0.20 to 0.50 wt%. Heat 91887 has a high niobium content, i.e., 0.15 vs an allowed range of 0.06 to 0.10 wt%, and a low silicon content, i.e., 0.08 vs a target range of 0.20 to 0.50 wt%. Additional details concerning processing of heats and product forms can be found elsewhere.^{3,7-9}

All material was tested in the normalized and tempered (N&T) condition, i.e., a normalization heat treatment consisting of 1 h (up to 25 mm thick) at 1038°C followed by a tempering treatment of 732 to 760°C. Typical hardness values in the normalized condition were Rockwell C 40; and following tempering at 760°C for 1 h values in the range Rockwell B95 were common. This treatment produced a fully martensitic structure. An

Table 1. Details on melting of commercial heats of modified 9Cr-1Mo steel

Heat identification	Melter	Heat size (tons)	Melting practice ^a
XA3602	Quaker	4	AOD
F5349	CarTech	2.5	Electric/ESR
91887	CarTech	15	AOD
30383	CarTech	15	AOD/ESR
30394 ^b	CarTech	15	AOD/ESR
30176 ^c	CarTech	15	AOD/ESR
30182 ^c	Electralloy	15	AOD and AOD/ESR
10148 ^d	Electralloy	23	AOD and AOD/ESR
14361 ^d	Timken	65	Electric furnace
82631	Combustion Engineering	0.5	Air induction
YYC982C	Sumitomo ^e	2.0	VIM
59020	NKK ^f	5.0	VIM
A231001	Sumitomo ^e	50	VOD

^aAOD = argon-oxygen decarburization; ESR = electroslag remelting; VIM = vacuum induction melting; VOD = vacuum oxygen decarburization.

^bHeat 30394 is half of heat 30383 and was electroslag remelted.

^cHeats 30176 and 30182 are the same heat; their numbers are different because CarTech identifies each electroslag remelted ingot by a different number.

^dHeats 10148 and 14361 were originally AOD processed.

^eLocated in Japan.

^fNippon Kokan K. K., located in Japan.

Table 2. Summary of information on fabrication of commercial heats of modified 9Cr-1Mo alloy

Heat	Melter	Melting practice ^a	Product	Product size (mm)		Fabrication method	Fabricator
				OD	Thickness		
F5349	Quaker	AOD	Plate		16	Hot forged, hot rolled	ORNL, ^b Y-12
30383	CarTech	AOD	Plate		51	Hot forged, hot rolled	Jessop
30383	CarTech	AOD	Bar	95		Hot forged, hot rolled	CarTech
30383	CarTech	AOD	Tube	102	15	Hot extruded	Amax
30394	CarTech	AOD-ESR	Plate		25	Hot forged, hot rolled	Jessop
30394	CarTech	AOD-ESR	Bar	232		Hot forged	Cartech
30394	CarTech	AOD-ESR	Tube	102	15	Hot extruded	Amax
30394	CarTech	AOD-ESR	Tube	76	13	Hot rotary pierced	Timken
30182	CarTech	AOD-ESR	Plate		16	Hot forged, hot rolled	Combustion Engineering
30182	CarTech	AOD-ESR	Bar	232		Hot forged	CarTech
30182	CarTech	AOD-ESR	Tube	102	15	Hot extruded	Amax
30182	CarTech	AOD-ESR	Tube	76	13	Hot rotary pierced	Timken
30176	CarTech	AOD-ESR	Plate		25	Hot forged, hot rolled	Jessop
10148	Electralloy	AOD	Plate		16	Hot forged, tempered, cold rolled	ORNL
10148	Electralloy	AOD	Bar	44		Hot extruded	ORNL
10148	Electralloy	AOD	Bar	107		Hot rolled	Bethlehem
10148	Electralloy	AOD	Pipe	245	15	Hot pilgered	Phoenix
10148	Electralloy/ Universal Cyclops	AOD-ESR	Plate	203		Hot rolled	Universal Cyclops
10148	Electralloy Universal Cyclops	AOD-ESR	Plate	51		Hot rolled	Universal Cyclops
10148	Electralloy Universal Cyclops	AOD-ESR	Octagon box	200		Hot forged	Universal Cyclops
10148	Electralloy Universal Cyclops	AOD-ESR	Round	232		Hot forged	Universal Cyclops

Table 2. (continued)

Heat	Melter	Melting practice ^a	Product	Product size (mm)		Fabrication method	Fabricator
				OD	Thickness		
10148	Electralloy Universal Cyclops	AOD-ESR	Tube	54	9.45	Hot extruded, cold reduced	TI Stainless ^c
10148	Electralloy Universal Cyclops	AOD-ESR	Pipe	406	25	Hot extruded	Cameron Iron Works
14361	Electralloy/ Special Metals	AOD-ESR	Saddle forging	781	166	Hot forged	National Forge
14361	Electralloy/ Special Metals	AOD-ESR	Pipe	584	102	Hot extruded	Cameron Iron Works
XA3602	Combustion Engineering	Air induction	Tube	51	8.03	Centrifugally cast and cold pilgered	Combustion Engineering
YYC982C	Sumitomo ^d	VIM	Tube	76	13	Hot extruded, cold drawn	Sumitomo
YYC982C	Sumitomo	VIM	Tube	51	6.4	Hot extruded, cold drawn	Sumitomo
59020	NKK ^d	VIM	Plate		25	Hot forged, hot rolled	NKK
59020	NKK	VIM	Tube	76	13	Hot extruded, cold drawn	NKK
59020	NKK	VIM	Tube	51	6.4	Hot extruded, cold drawn	NKK

^aAOD = argon-oxygen decarburization; ESR = electroslag remelting; VIM = vacuum induction melting.

^bOak Ridge National Laboratory.

^cLocated in the United Kingdom.

^dLocated in Japan.

Table 3. Chemical analyses of various commercial heats of modified 9Cr-1Mo steel

Element	Content (wt %) for each heat ^a										
	F5349	30383		30394		30176 Plate	30182 Tube ^c	10148	XA3602	91887	YYC982C
		Plate	Tube ^b	Plate	Tube ^c						
C	0.10	0.083	0.075	0.084	0.094	0.081	0.081	0.089	0.089	0.097	0.105
Mn	0.39	0.46	0.46	0.46	0.45	0.37	0.36	0.47	0.40	0.38	0.43
P	0.007	0.010	0.009	0.010	0.014	0.010	0.013	0.021	0.005	0.007	0.006
S	0.015	0.004	0.004	0.003	0.004	0.003	0.003	0.006	0.009	0.005	0.006
Si	0.35	0.41	0.40	0.40	0.37	0.11	0.11	0.28	0.19	0.08	0.42
Ni	0.10	0.09	0.08	0.09	0.09	0.09	0.09	0.16	0.05	0.08	0.02
Cr	8.80	8.46	8.17	8.57	8.11	8.61	8.32	9.24	9.21	9.22	8.52
Mo	0.94	1.02	0.99	1.02	1.03	0.89	0.90	0.96	0.93	1.01	0.98
V	0.205	0.198	0.195	0.198	0.200	0.209	0.208	0.21	0.197	0.22	0.20
Nb	0.060	0.072	0.064	0.073	0.072	0.072	0.076	0.054	0.059	0.15	0.075
Ti	0.006	0.005	0.005	0.005	0.002	0.004	0.002	0.002	0.005	<0.01	
Co	0.018	0.055	0.055	0.055	0.056	0.010	0.011	0.019	0.019	0.018	
Cu	0.09	0.03	0.03	0.04	0.04	0.04	0.04	0.08	0.02	0.01	0.003
Al	<0.001	0.002	0.003	0.014	0.024	0.007	0.004	0.002	0.003	0.003	0.003
B	0.001	<0.001		<0.001		<0.09		<0.001	<0.001		
W	<0.01	0.05		0.05		<0.01		0.01	<0.01	<0.01	
As	0.002	<0.001		<0.001		0.001		0.002	<0.001		
Sn	0.004	<0.001		<0.001		<0.001		0.004	0.001		
Zr	<0.001	<0.001		<0.001		<0.001		<0.001	<0.001	<0.001	
N	0.011	0.051	0.050	0.053	0.053	0.055	0.053	0.035	0.065	0.038	0.0465
O	0.012							0.008		0.005	

^aAll chemical analysis was carried out at Combustion Engineering, Inc., Chattanooga, Tenn.

^bHot extruded.

^cHot rotary pierced.

Table 4. Commercial chemical composition specifications for modified 9Cr-1Mo steel

Element	Concentration (wt %)		Element	Concentration (wt %)	
	Target	Allowed range		Target	Allowed range
C	0.10	0.08-0.12	Nb	0.08	0.06-0.10
Mn	0.40	0.30-0.50	N	0.05	0.03-0.07
Si	0.20	0.20-0.50	Al	<0.02	0.04 max. ^a
P	<0.01	0.02 max.	Ti	<0.01	0.01 max.
S	<0.01	0.01 max.	B	<0.001	<0.001
Cr	8.5	8-9	W	<0.01	<0.01
Ni	<0.10	0.2 max.	Zr	<0.01	<0.01
Mo	0.95	0.85-1.05	O	<0.02	<0.02
Cu	<0.10	0.2 max.	Sb	<0.001	<0.001
V	0.21	0.18-0.25			

^aMax. = maximum.

exception to the above heat treatment practice occurred in the case of some weldments in which case the preweld tempering was done at 671°C.

Almost all specimens from wrought material were taken transverse to the rolling direction and had a 6.35-mm gage diameter as shown in Fig. 1. Specimens taken from castings and weldments sometimes differed in that the gage length was extended from 31.8 to 57.25 mm to incorporate additional material. Weldment specimens were taken with their major specimen axis transverse to the fusion line such that the gage section contained base, heat-affected-zone (HAZ), and weld metal. All weld metal specimens were taken with their major axis parallel to the fusion line.

The creep test methods used conformed to the requirements of ASTM E 139-70 (3). Lever-arm creep machines were calibrated to a load accuracy of $\pm 0.5\%$. The temperature was measured by three Chromel vs Alumel thermocouples ($\pm 0.4\%$ accuracy) wired to the gage section. The temperature variation among these was less than $\pm 1.0^\circ\text{C}$, and the highest temperature

ORNL-DWG 76-2499RI

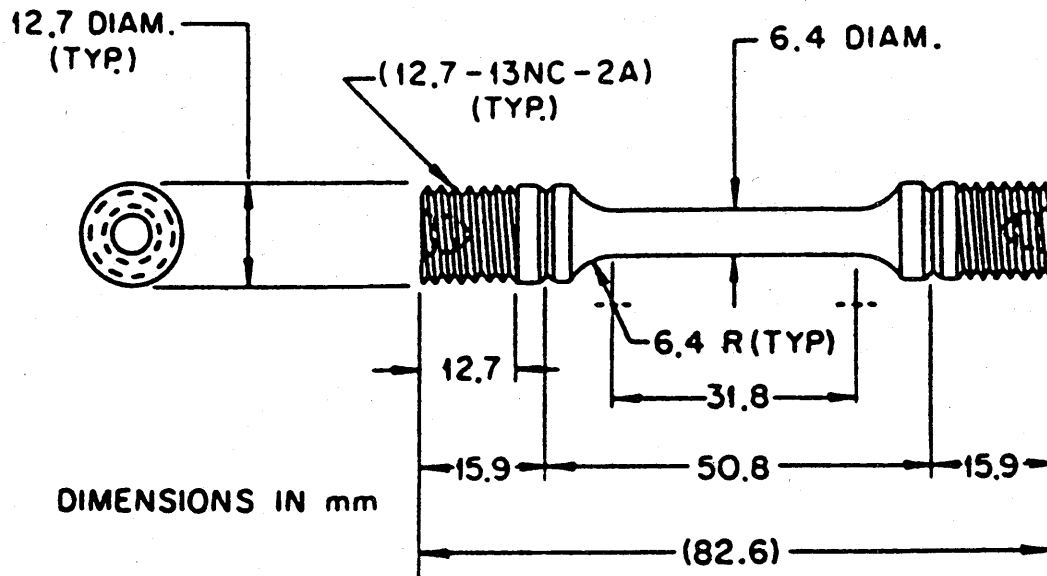


Fig. 1. Creep specimen used in the testing of modified 9Cr-1Mo steel.

was taken as the nominal test temperature. Proportioning temperature controllers were used to obtain control to $\pm 1.0^{\circ}\text{C}$, with the highest temperature being the nominal test temperature.

Length changes were measured by an averaging extensometer attached by set screws to a small groove in the specimen shoulder. The extension readings were converted to strains by dividing by the reduced section length. The dial gage used in measuring the extension had a resolution of $2.5\ \mu\text{m}$ ($0.0001\ \text{in.}$).

Currently (July 1987), there are 28 tests on base materials, 19 on weldments, and one on casting material currently ongoing in the laboratory.

RESULTS

Results are given in Table 5 of recently completed and currently ongoing (April 1987) creep and creep-rupture tests conducted on wrought base material. Appendix 1 gives examples of creep deformation as measured in the laboratory in comparison to predictions of creep strain using an equation derived in 1984. This creep equation was defined as follows:

Table 5. Status of creep-rupture tests of modified 9Cr-1Mo steel^a

Test number	Heat number	Test temperature (°C)	Stress (MPa)	Test time (h)	Primary creep strain (%)	Minimum creep rate (%/h) (10 ⁻⁴)	Total creep strain (%)	Reduction of area (%)	Time to tertiary creep (0.2%) (h)	Rupture time (h)	Predicted rupture life ^d (h)
23628	394-E/420T ^c	704	28	21,809	1.00	2.0	14.33	19	13,400	21,809	13,124
24299	394-E/5871	649	76	6,620	0.06	9.67	12.35	56	4,000	6,620	7,032
20842	F5349-Y	538	179	68,637	1.85	0.10	2.24				
21769	394B	538	186	60,925	0.87	0.222	2.42				
21822	394B	427	413	59,509	0.10	0.04	0.52				
22502	148A	538	186	47,475	0.80	0.10	0.40				
22770	394E	454	379	48,449	0.23	0.08	1.65				
23790	001	593	124	26,787	0.70	1.15	20.45	77	19,000	26,787	19,715
22855	383B	593	110	49,514	0.50	0.714	13.0	32	34,200	49,514	55,274
22936	394E	593	103	46,171	0.25	0.30	2.75				
22973	394E	538	155	45,117	0.25	5.55	4.11				
22974	394E	538	234	45,101	0.15	0.17	0.92				
23698	394E	427	379	33,409	0.08	0.51	0.19				
23816	582 ^b	649	55	28,490.3	0.62	1.25	7.47	9	20,000	28,490	49,499
24043	143-61 ^f	649	76	29,363	0.50	1.25	4.91	13	19,000	29,363	5,370
24073	394E ^c	593	110	24,767	0.40	0.53	1.53				
24079	176 ^c	593	110	24,456	0.18	0.67	1.26				
24101	143-61 ^f	593	124	23,533	0.09	0.03					
24118	582 ^b	593	110	23,533	1.20	1.88	4.07				
24252	101	649	62	21,670	0.38	0.68	1.63				
24351	394E ^c	538	207	19,286	0.80	0.63	1.90				
24357	176 ^c	538	207	19,124	0.45	0.58	1.29				
24359	176 ^c	538	186	19,052	0.40	0.17	0.70				
24577	394E	538	165	40,652 + 9,885	0.15	0.03	0.73 + 0.31				
24721	565163	593	145	10,419	0.80	2.29	16.93				
24746	383 ^e	482	276	40,632 + 11,951	0.22	0.15	1.45 + 0.28				
24749	394 ^e	482	276	40,753 + 9,311	0.21	0.10	0.96 + 0.17				
24752	176 ^e	482	276	40,751 + 10,127	0.30	0.13	1.16 + 0.31				
24772	148A ^e	482	276	40,802 + 9,235	0.22	0.08	0.950 + 0.17				
24820	383B ^e	538	165	40,942 + 9,416	0.14	0.04	0.87 + 0.27				
24847	176 ^e	538	165	40,652 + 9,624	0.14	0.04	0.83 + 0.42				
24899	148A ^e	538	165	40,901 + 8,732	0.12	0.03	0.67 + 0.21				
24990	565163	593	124	5,253	0.04		0.44				
24995	565163	649	76	5,231			0.19				
25371	565163	538	83	4,550		3.12	0.66				
24083	143-61 ^f	593	145	12,273	0.7	8.13	21.50	60	10,000	12,273	5,597
24689	565/63	593	172	2,540			13.5	85	1,750	2,540	839
25731	565/63	538	83	4,549			0.67				
Battelle	383B-27T	593	124	21,337		1.31	20.0	61	12,800	21,337	25,981
Battelle	394E-9T	593	124	30,545		0.98	12.8	39	15,700	30,544	25,981
Battelle	176-9T	593	124	14,732		0.89	22.2	84	12,000	14,732	25,981
Battelle	148A-9T	593	124	24,387		0.71	16.4	59	15,000	24,387	25,981

^aTest time and total creep strain through April 2, 1987. Primary and minimum creep rates calculated May 1986.

^bCasting.

^cSample aged 2.5×10^4 at indicated test temperature prior to test.

^dPredicted rupture life based on average behavior.

^eSpecimen tested at Battelle's Columbus Laboratory for initial period prior to moving to ORNL.

^fSaddle forgings.

The creep strain^{1,2} incurred in modified 9Cr-1Mo steel as a function of time under constant load and temperature was described by

$$e_c = a t^{1/3} + \dot{e}_m t, \quad (1)$$

where

e_c = creep strain (%),

a = primary creep strain constant (%/h^{1/3}),

\dot{e}_m = minimum creep rate (%/h).

Additionally, the minimum creep rate was described as a function of stress and temperature by

$$\log \dot{e}_m = C_h + 0.02549 \sigma + 2.974 \log \sigma - 35180/T \quad (600^\circ\text{C} < T < 650^\circ\text{C}), \quad (2)$$

and

$$\log \dot{e}_m = C_h + 3.574 + 0.02549 \sigma + 2.974 \log \sigma - 38,300/T \quad (371^\circ\text{C} < T < 600^\circ\text{C}) \quad (3)$$

where

σ = stress (MPa),

T = temperature (K).

The parameter C_h is a "lot constant" that reflects the creep strength of a specific lot of material. The average value of C_h was 27.391, while the "minimum strength" value, defined as average plus 1.65 times the standard error of estimate in $\log \dot{e}_m$, was 28.075. Equations (2) and (3) were determined from an overall data base of 127 tests on 23 lots of material.

The primary creep strain constant was given by

$$\log a = C_h + 0.005712 \sigma + 1.2626 \log \sigma - 10,099T, \quad (4)$$

where the average value of C_h was 7.038, and the minimum strength value was 7.302. All logarithms are base 10.

Predicted rupture lives given in Table 5 were made assuming average behavior and estimated using the following equation.

$$\log t_r = C_h - 0.0231\delta - 2.385 \log \sigma + 31,080/T, \quad (5)$$

where

$\log t_r$ = rupture life (h),

σ = stress (MPa),

T = temperature (K).

Logarithms are again in base 10. The parameter C_h is a "lot constant" that reflects the relative strengths of different lots of material, assuming that the stress and temperature dependence is the same for all lots. The average value of C_h was -23.737.

Table 6 presents a status report of currently ongoing and completed tests on weldments. Appendix 2 summarizes details of the welding procedures used in making the weldments. Table 7 gives comparisons of measured and predicted, Eq. (4), rupture life assuming average life of basic material. Stress ratios are also given for weldment and base material. The numerator is the applied engineering stress in the creep-rupture test while the denominator is the stress calculated with Eq. (5) using the measured rupture life. This value is then plotted in several figures reported herein.

Appendix 3 gives examples of quantitative microscopy performed on several heats, and is illustrative of the complex microstructure seen in this material under high magnification.

DISCUSSION

Figure 2 compares predicted rupture life using Eq. (5) and actual measured rupture life over the temperature range of 427 to 704°C. Note the excellent agreement between predicted and actual rupture lives. Status of ongoing tests is also shown in Fig. 2. Similarly, Fig. 3 compares isothermal plots of predicted minimum creep rates, Eqs. (2) and (3), and actual measured values. Again note the good agreement between measured and predicted values. Comparisons between measured and predicted

Table 6. Status of creep-rupture tests
of modified 9Cr-1Mo steel welds^a

Test number	Weld number	Heat treatment ^b (°C/°C/°C)	Test temperature (°C)	Stress (MPa)	Test time (h)	Primary creep strain (%)	Minimum creep rate (%h) (10 ⁻⁴)	Total creep strain (%)
23026	PC-58B	1038/760/732	538	186	43,900	0.60	0.17	1.63
24219	PC-129	1038/769/none	593	145	22,196	0.45	0.27	2.33
24279	PC-129	1038/760/732	538	207	20,632	0.15	0.14	0.45
24363	PC-110	1038/621/760	538	179	19,004	0.33	0.25	0.60
24376	PC-132	1038/760/732	538	179	18,359	0.60	0.53	1.13
24625	PC-150	1038/760/732	538	193	14,829	0.16	0.75	1.03
24959	PC-156	1038/760/745	593	83	6,624			0.24
24962	PC-156	1038/760/745	593	83	6,597			0.22
24971	PC-156	1038/760/745	538	207	9,739	0.30	1.29	2.00
24978	PC-156	1038/760/745	538	193	6,093			0.49
25401	PC-111	1038/621/760	538	193.1	3,762			0.62
25403	PC-110	1038/621/760	538	186	3,595			0.79
25405	PC-111	1038/621/760	593	152	2,147			1.97
25409	PC-110	1038/621/760	538	176	3,451			0.83
25410	PC-111	1038/621/760	538	179	3,188			0.42
25411	PC-110	1038/621/760	593	134				6.74
25484	PC-110	1038/621/760	593	110	1,906			0.97
25485	PC-110	1038/621/760	593	104	1,677			0.65
24667	PC-156	1038/760/758	593	124	1,075 ^c	0.35	11.1	2.80
24621	PC-150	1038/760/732	593	110	8,636 ^c	0.22	0.52	
23025	PC-58B	1038/760/732	538	207	26,800 ^c	0.12	0.58	6.3
24038	ETEC	1038/ / 732 DMW/304SS	649	48	13,647 ^c	0.12	0.28	2.7
24293	PC-132	1038/760/732	538	207	9,268 ^c	0.82	2.72	11.6
24666	PC-156	1038/760/745	593	145	499 ^c	0.25	23.8	4.3
24551	PC-150	1038/760/732	593	124	5,037 ^c	0.30	0.07	1.2
24722	PC-156/3C	1038/760/745	593	103	3,215 ^c	0.32	1.18	0.67
24545	PC-150	1038/760/732	593	145	1,504 ^c			
24631	PC-150	1038/760/732	649	76	711 ^c			
23979	PC-110	1038/621/760	593	172	168 ^c			
23992	PC-110	1038/621/760	593	145	1,080 ^c			
23999	PC-110	1038/621/760	593	124	2,277 ^c			
24005	PC-110	1038/621/760	593	172	1,502 ^c			
24013	PC-81	1038/621/732-40h	649	62	5,085 ^c			
24278	PC-132	1038/760/732	593	145	580 ^c			
23791	PC-93	1038/760/732	593	110	9,835 ^c			
25493	PC-111	1038/621/760	593	138.9	1,173			0.44
25535	PC-111	1038/621/760	538	165.5	523			0.17
24006	PC-110	1038/621/760	593	145	8,087 ^c			

^aTest time and total creep strain as of April 2, 1987.

^bASME Code Case 1973 specified the following heat treatment:

Normalized Tempered PWHT
1038-1090°C / min. 732°C / min. 704°C

^cRuptured.

Table 7. Comparison of measured and predicted rupture lives for modified 9Cr-1Mo Steel weldments.

Test number	Weld number	Heat treatment ^a	Process	Test temperature (°)	Stress (MPa)	Rupture strain (%)	Rupture life (h)	Predicted rupture life ^b (h)	$\frac{t_r \text{ measured}}{t_r \text{ predicted}}$ (%)	Stress ratio, weldment/base (MPa/MPa)
23025	PC-58B	1038/760/732	SMA	538	207	6.46	26,800	19,100	140	207/206 (1.0)
24293	PC-132	1038/760/732	SMA	538	207	11.79	9,268	19,100	48	207/222 (0.93)
24722	PC-156	1038/760/746	SA	593	103	2.67	4,707	95,200	5	103/143 (0.72)
24551	PC-150	1038/621/732	GTA	593	124	1.33	5,037	20,100	25	124/142 (0.87)
24667	PC-156	1038/760/746	SA	593	124	2.94	1,075	20,100	5	124/166 (0.75)
24666	PC-156	1038/760/746	SA	593	145	4.60	499	5,578	9	145/177 (0.82)
24621	PC-150	1038/621/760	GTA	593	110	1.21	8,636	55,462	16	110/135 (0.81)
25411	PC-110	1038/621/760	GTA	593	134	6.74	760	9,357	8	134/169 (0.79)
25405	PC-111	1038/621/760	GTA	593	152	7.6	2,147	3,381	63	152/158 (0.96)
23026	PC-158B	1038/760/732	SMA	538	186	(ongoing) ^c	43,900	99,966	44	186/198 (0.94)
24376	PC-132	1038/760/732	SMA	538	179	(ongoing) ^c	18,359	161,126	11	179/211 (0.84)
24959	PC-156	1038/760/745	SA	593	83	(ongoing) ^c	6,624	654,636	1	83/141 (0.59)
24962	PC-156	1038/760/745	SA	593	83	(ongoing) ^c	6,597	654,636	1	83/141 (0.59)
24971	PC-156	1038/760/745	SA	538	207	(ongoing) ^c	9,739	19,100	51	207/216 (0.96)
24978	PC-156	1038/760/745	SA	538	193	(ongoing) ^c	6,093	63,409	10	193/228 (0.84)
24219	PC-129	1038/760/none	GTA	593	145	(ongoing) ^c	22,196	5,578	398	145/128 (1.1)
24279	PC-129	1038/760/732	GTA	538	207	(ongoing) ^c	20,632	19,100	108	207/210 (0.99)
24363	PC-110	1038/621/760	GTA	538	179	(ongoing) ^c	19,004	161,469	12	179/211 (0.84)
24625	PC-150	1038/760/732	GTA	538	193	(ongoing) ^c	14,829	6,228	238	193/214 (0.90)
25401	PC-111	1038/621/760	GTA	538	193	(ongoing) ^c	3,762	6,228	60	193/236 (0.82)
25403	PC-110	1038/621/760	GTA	538	186	(ongoing) ^c	3,595	100,105	4	186/236 (0.79)
25405	PC-111	1038/621/760	GTA	593	152	(ongoing) ^c	2,147	3,384	63	152/158 (0.75)
25409	PC-110	1038/621/760	GTA	538	176	(ongoing) ^c	3,451	198,402	2	176/235 (0.75)
25410	PC-111	1038/621/760	GTA	538	179	(ongoing) ^c	3,188	161,469	2	179/238 (0.75)
25484	PC-110	1038/621/760	GTA	593	110.3	(ongoing) ^c	4,159	73,402	3	110/160 (0.69)
25485	PC-110	1038/621/760	GTA	593	104.3	(ongoing) ^c	1,677	117,012	1	104/162 (0.64)
24545	PC-150	1038/760/732	GTA	593	145	(ongoing) ^c	1,504	5,578	26	145/164 (0.88)
24631	PC-150	1038/760/732	GTA	649	76	(ongoing) ^c	711	7,026	10	76/104 (0.73)
23979	PC-110	1038/621/760	GTA	593	172	(ongoing) ^c	168	834	20	172/196 (0.88)
23992	PC-110	1038/621/760	GTA	593	145	(ongoing) ^c	1,080	5,578	19	145/168 (0.86)
23999	PC-110	1038/621/760	GTA	593	124	(ongoing) ^c	2,277	25,941	9	124/158 (0.78)
24005	PC-110	1038/621/760	GTA	593	172	(ongoing) ^c	1,502	834	180	172/164 (1.05)
24013	PC-81	1038/621/732(40 h)	SA	649	62	(ongoing) ^c	5,085	25,059	20	62/78 (0.79)
24278	PC-132	1038/760/732	SMA	593	145	(ongoing) ^c	580	5,578	10	145/194 (0.75)
23791	PC-93	1038/760/732	SA	593	110	(ongoing) ^c	9,835	75,128	13	110/139 (0.79)
25493	PC-111	1038/621/760	GTA	593	139	(ongoing) ^c	1,173	8,603	14	139/168 (0.83)
25535	PC-111	1038/621/760	GTA	538	166	(ongoing) ^c	523	396,388	0.01	166/266 (0.62)
24006	PC-110	1038/621/760	GTA	593	145	(ongoing) ^c	8,078	5,578	145	145/140 (1.03)

^aASME Code Case 1973 specifies the following heat treatment:
 Normalized Tempered PWHT
 1038-1090°C / min. 732°C / min. 704°C

^bPredicted using the rupture equation for wrought material.

^cOngoing.

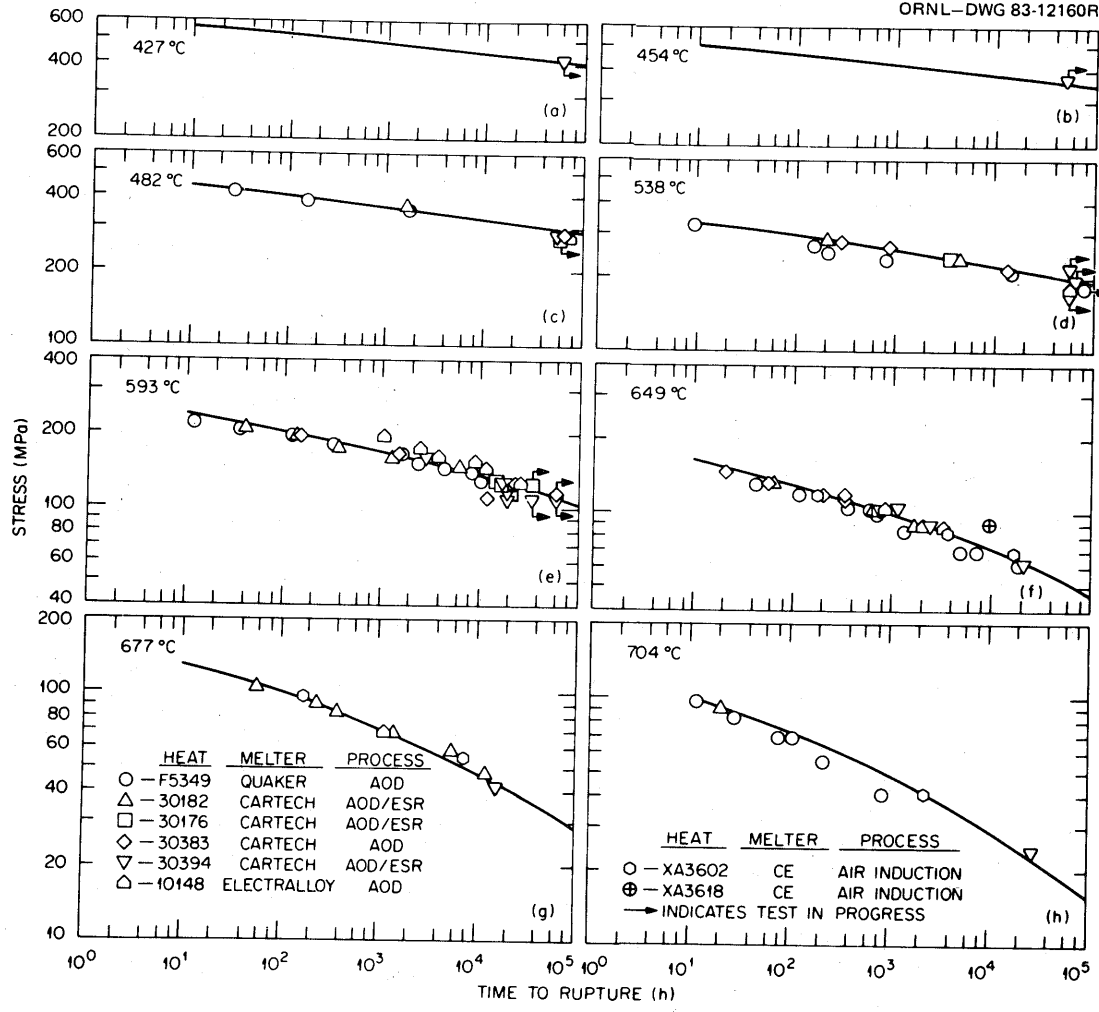


Fig. 2. Stress-rupture data for commercial heats of modified 9Cr-1Mo steel tested in the normalized and tempered condition. Average curves from the time-temperature parameter are also included in these plots.

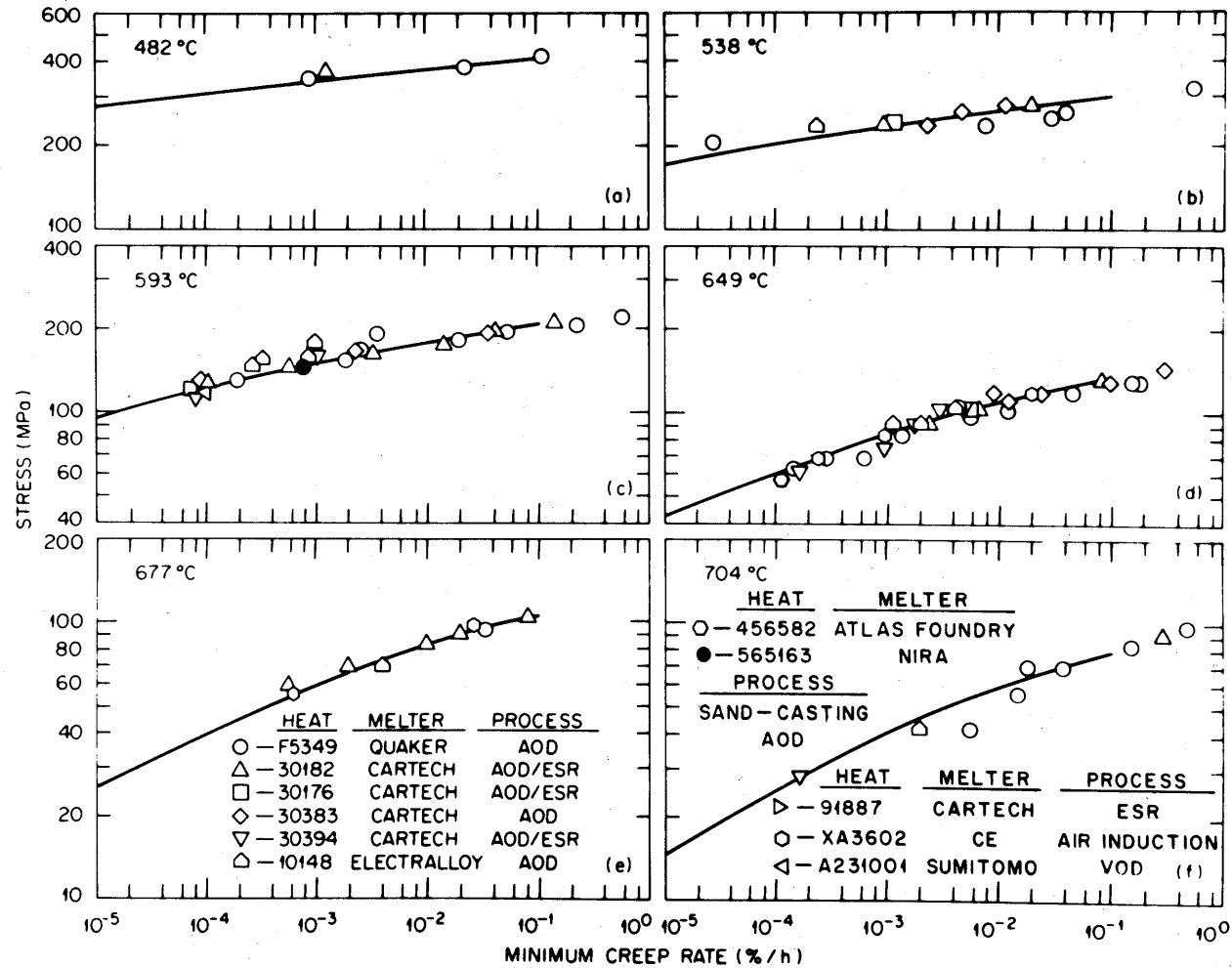


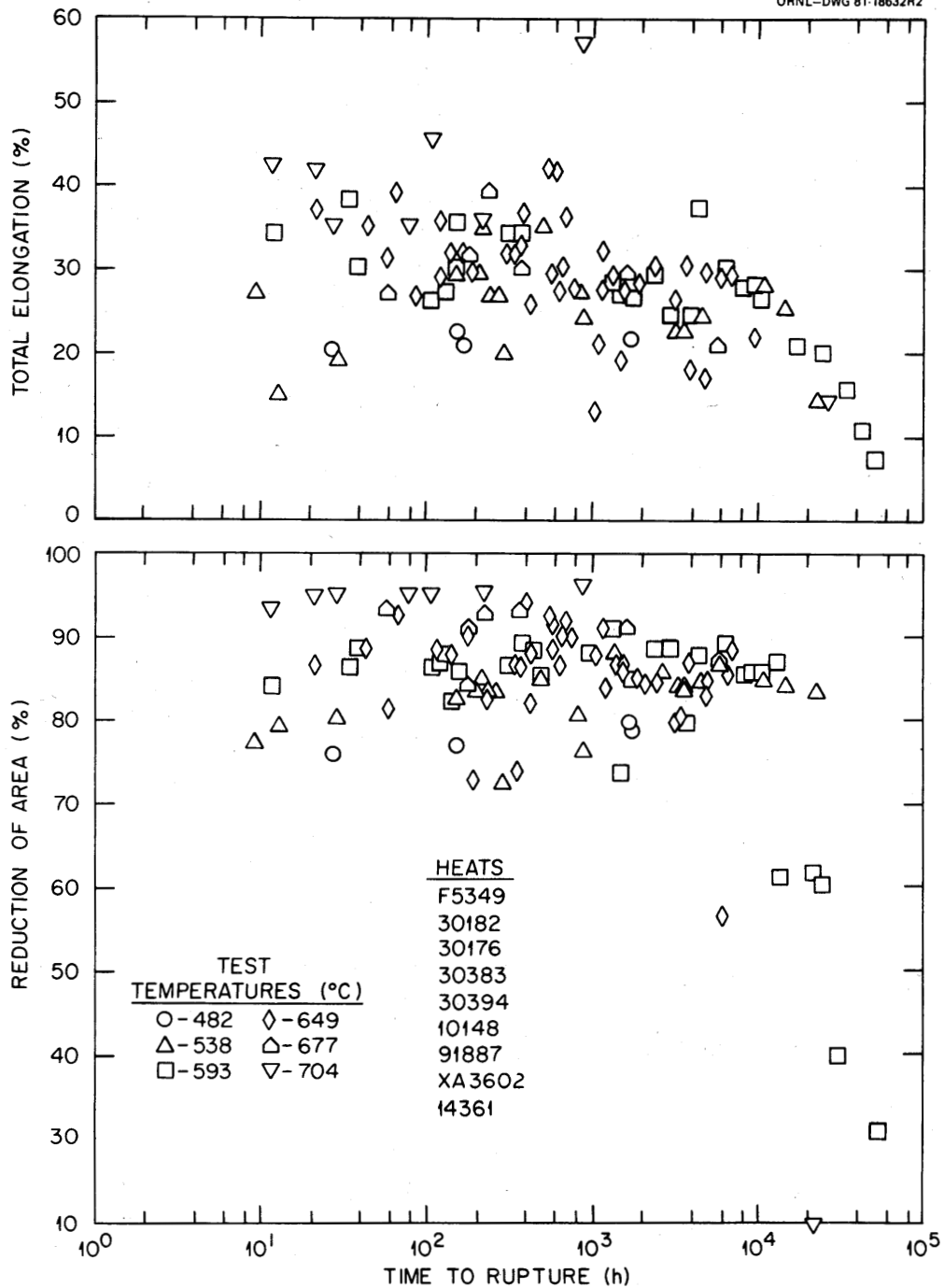
Fig. 3. Stress-minimum creep rate data for commercial heats of modified 9Cr-1Mo steel tested in the normalized and tempered condition. Average curves from the time-temperature parameter are also included in these plots.

creep response given in Appendix 1 generally indicate good agreement between predictions and experimental creep measurements particularly at temperatures at or in excess of 482°C. Figure 4 shows reduction-of-area as a function of rupture time to 50,000 h. Note that with increased rupture time that there is a decrease in rupture ductility in the temperature range of 593 to 704°C which was not apparent in previously reported short-term results.² The heat showing this reduced ductility was 30394/30383. Normally, a decrease in rupture ductility with increased rupture life is indicative of an embrittlement process or intergranular rupture. Figure 4(b) shows the fracture surface of a base material specimen that failed after nearly 50,000 h of test time. The photograph shows no indication of intergranular separation to this test time. It should be noted that reduction-of-area values of 30 to 40% in the range of 50,000 h at 593°C are quite good in comparison to the reference heats of types 304 and 316 stainless steels [see Fig. 4(c) for comparison with type 304 stainless steel] which showed values of less than 10% under similar test conditions. This comparison continues to support our conclusion that modified 9Cr-1Mo steel has increased resistance to intergranular rupture under creep strain conditions in comparison to the austenitic stainless steels. Results from creep-fatigue tests also support this conclusion.¹⁰ However, Fig. 4(c) shows that an extrapolation of creep ductility values for modified 9Cr-1Mo can give values similar to those of type 304 stainless steel in the range of 100,000 to 200,000 h. This would indicate that a strain limit for this material may be necessary, but additional long-term data are needed to justify such a conclusion.

In Figs. 5 through 8 comparisons are given of rupture data and an early form of the rupture equation. This equation is very similar to Eq. (5) and was written as

$$\log t_r = -24.244 - 0.02374\sigma - 2.4871 \log \sigma + 31,876/T . \quad (6)$$

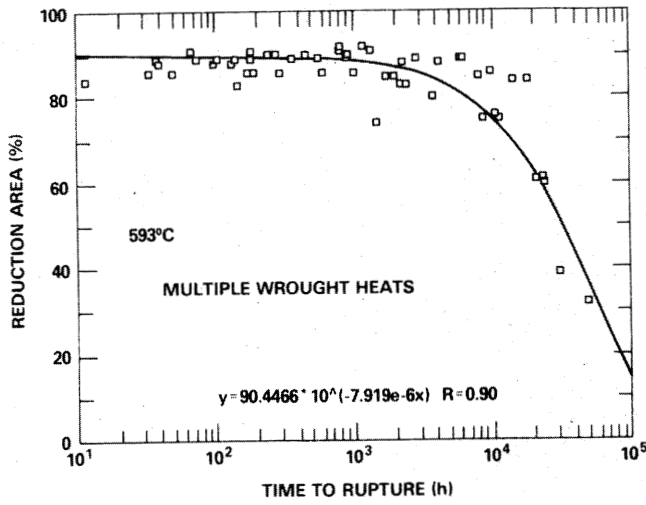
$\log t_r - 31,876/T$ is plotted as the abscissa in Figs. 5 through 8 where t_r , σ , and T have the same meaning and units as defined for Eq. 5. Figure 5 shows no degradation in rupture life following pre-creep isothermal



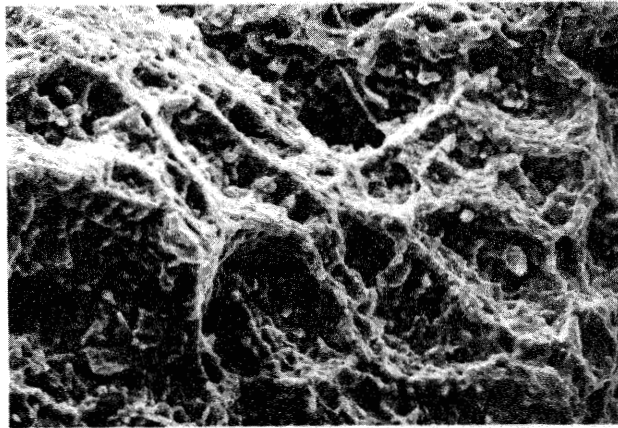
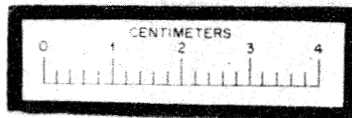
(a)

Fig. 4. (a) Creep-rupture ductility data as a function of rupture time at various temperatures for commercial heats. (b) Reduction of area data from long-term creep-rupture tests at 593°C indicating reduced ductility at test times in excess of about 20,000 h. (c) Reduction of area vs time to failure for multiple wrought heats of modified 9Cr-1Mo and type 304 stainless steel.

ORNL-DWG 87-13973



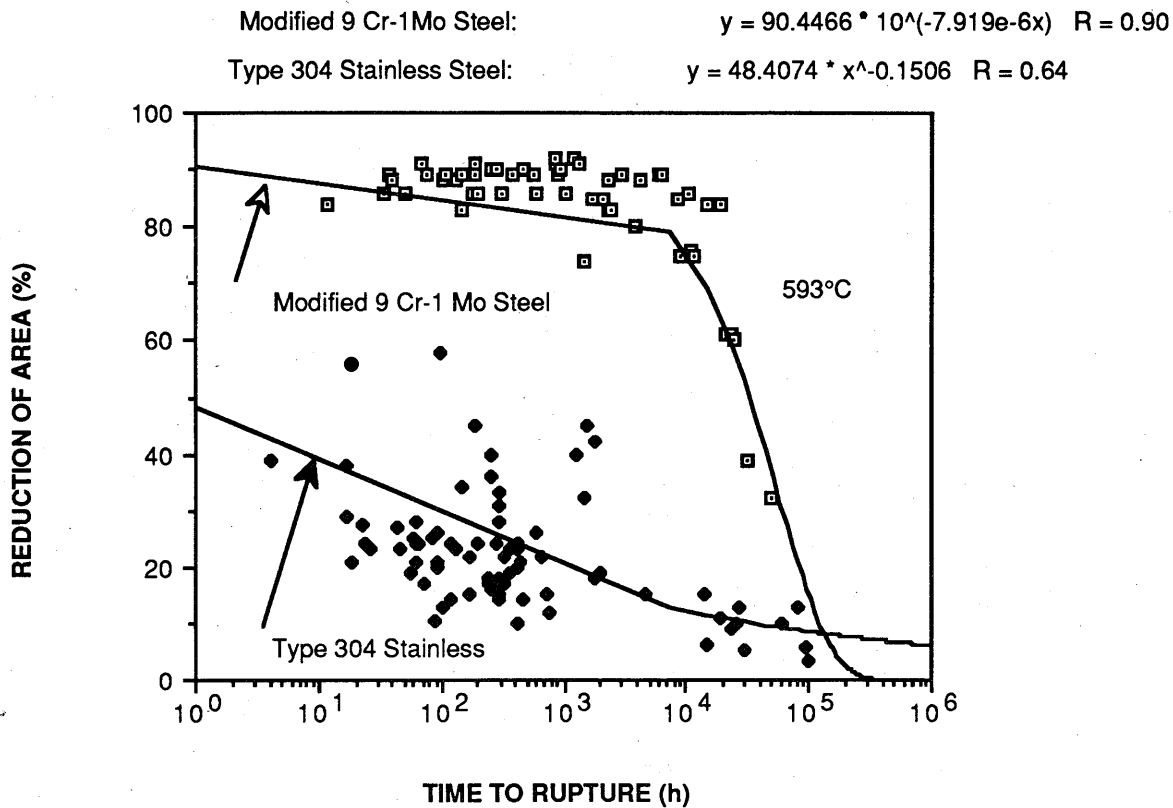
TEST NO. 22855
TIME TO RUPTURE: 49,514 h (5.7 years)
REDUCTION OF AREA: 32%
TEMPERATURE: 593°C



20
μm

(b) **FRACTURE SURFACE**

Fig. 4 (cont'd)



(c)

Fig. 4 (cont'd)

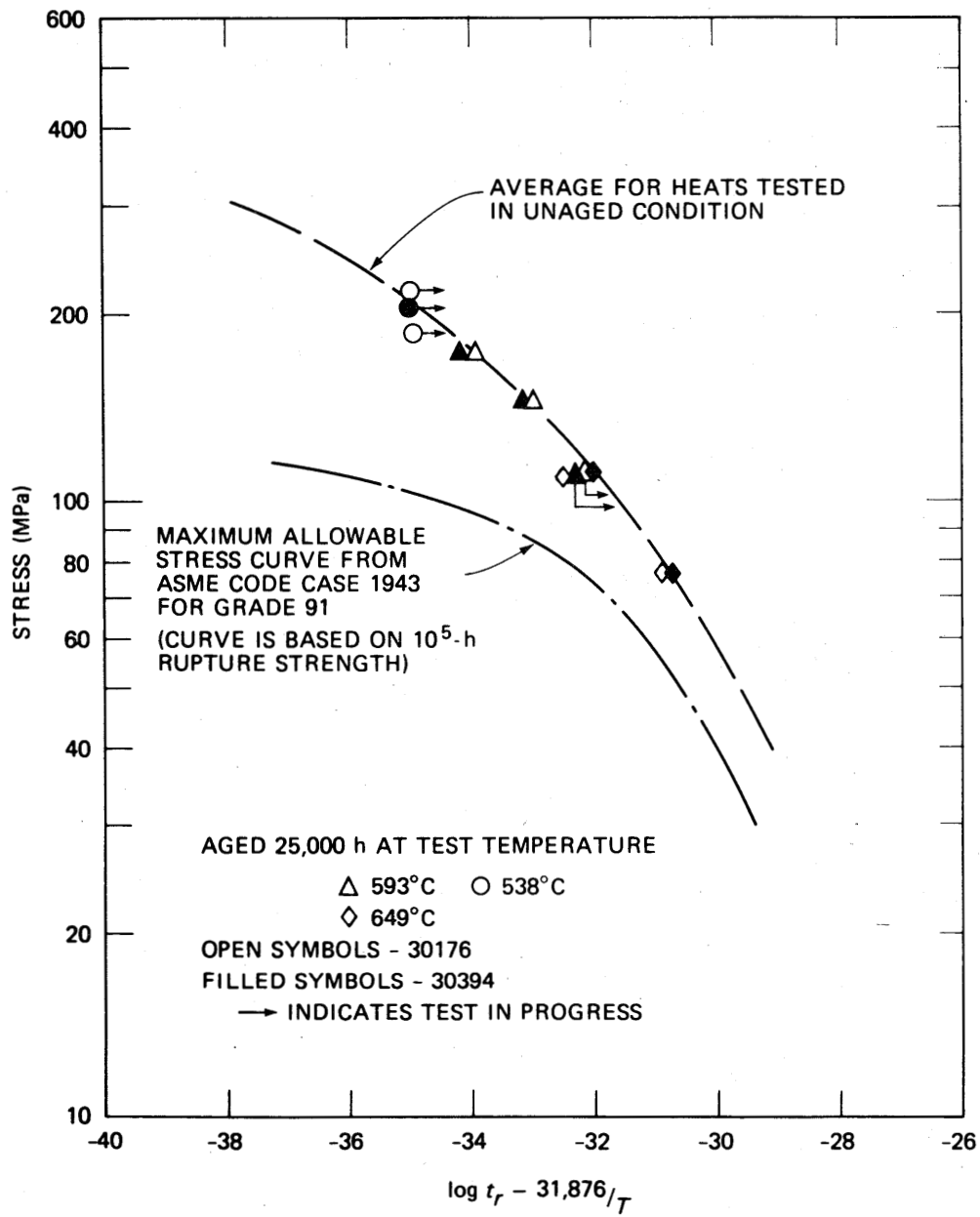


Fig. 5. Effect of aging for 25,000 h on creep-rupture life of modified 9Cr-1Mo steel.

aging in the temperature range of 538 to 649°C. Figure 6 compares rupture life of specimens taken from sand castings (elbow, steam chest, and valve body) forms with average behavior of wrought material, a somewhat lower rupture life is apparent for the castings. In Fig. 7, results are plotted from specimens taken from a saddle forging and tested in the range of 538 to 649°C. Again, similar rupture life to that of commercial wrought heats is apparent. Finally, results from test specimens taken from heats of material melted by Japanese suppliers, i.e., Sumitomo Metal Industries and Nippon Kokan K.K. (NKK), are again compared in Fig. 8 to average behavior of wrought commercial heats melted in the United States. Similar rupture life is apparent.

Figure 9 is a plot of the 593°C rupture data generated on the heats indicated. Included also are data from heat 91887 which was out of specification with respect to silicon and niobium content. The slightly higher niobium content is thought to be responsible for the increased strength at this temperature as well as at 649°C. Comparisons are also shown for other ferritic alloys as indicated which show the improved strength of modified 9Cr-1Mo steel. The creep-rupture data reported herein continue to support the rupture equation extrapolations, i.e., Eqs. (5) and (6) and therefore the long term 10^5 h extrapolations and comparisons to other materials shown in Fig. 10 are believed to be valid.

Figures 11 through 13 compare rupture data from transverse weldments as well as all weld metal specimens. The weldments were made by the shielded metal arc (SMA), submerged arc (SA), and the gas tungsten arc (GTA) processes.⁶ Note that weldment filler material was either standard or modified 9Cr-1Mo steel in terms of chemical composition.

Plotted in these figures are stress values and times to failure for the specimens. The stress values for the weld metal or weldments, however, have been normalized by dividing by the rupture strength of base material corresponding to the time to failure of the weldment. Such a process facilitates a comparison between base and weldment creep strength. Also shown for comparison purposes is two-thirds of the average stress-to-rupture which is the basis for Section VIII of the ASME Code stress allowables. The data given in Figs. 11 through 13 indicate that the rupture life of weldments can be inferior to that of base material particularly at high stress levels or short rupture times. However, in all cases the data fall on or above the Section VIII stress allowable values.

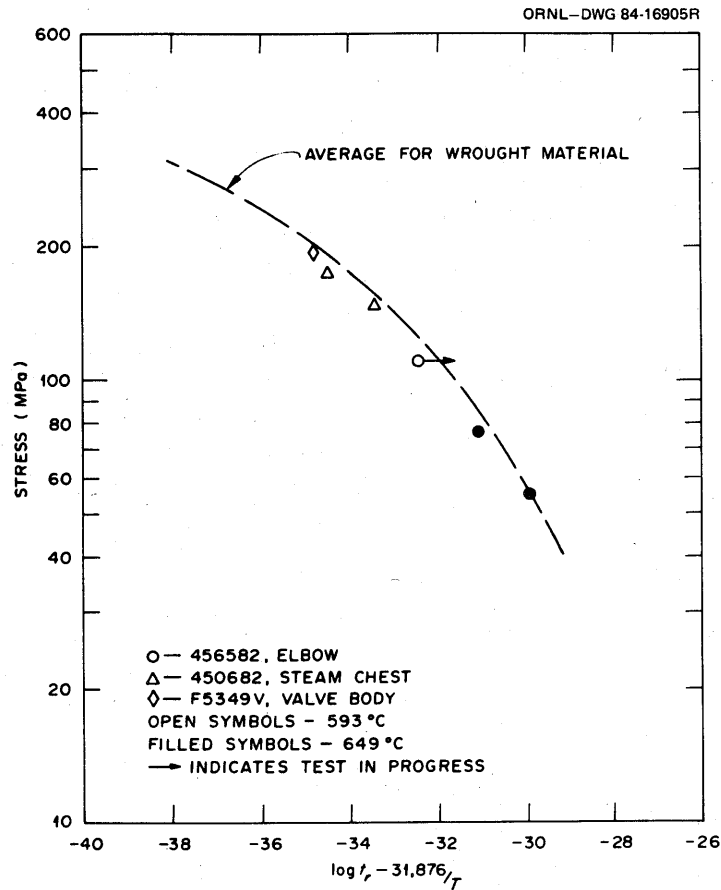


Fig. 6. Comparison of creep-rupture strength of modified 9Cr-1Mo sand castings with average curve for wrought material.

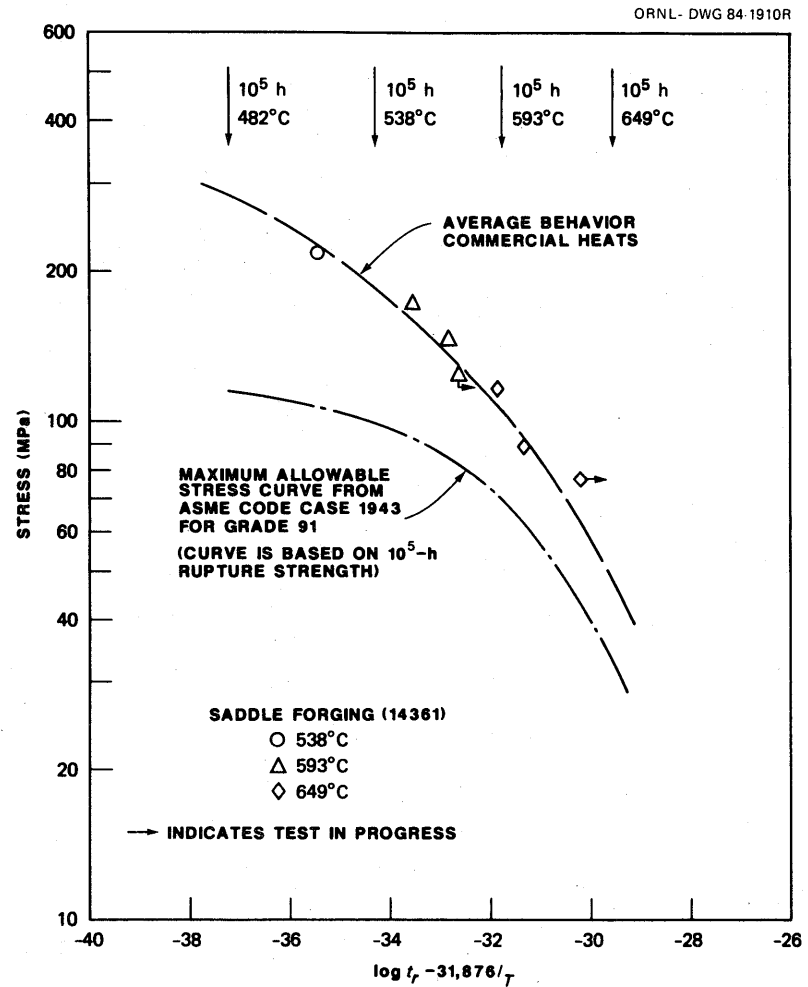


Fig. 7. Comparison of creep-rupture data on saddle forging with average curve developed from model for various product forms of several commercial heats. Maximum allowable design stress curve from ASME Code Case 1943 for Grade 91 is also included for comparison.

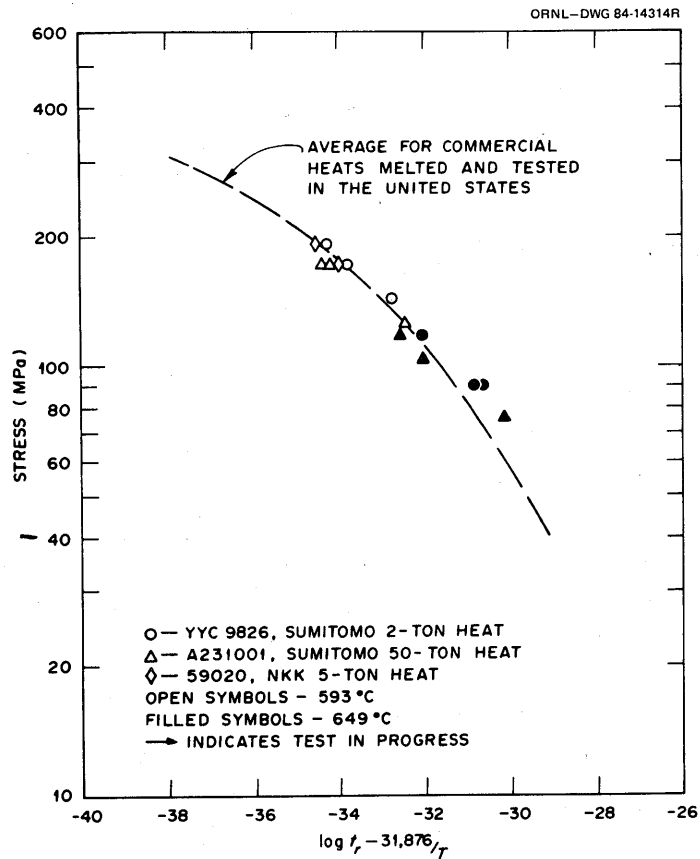


Fig. 8. Comparison of creep-rupture data on heats of modified 9Cr-1Mo steel melted and fabricated in Japan with average curve for commercial heats melted and tested in the United States.

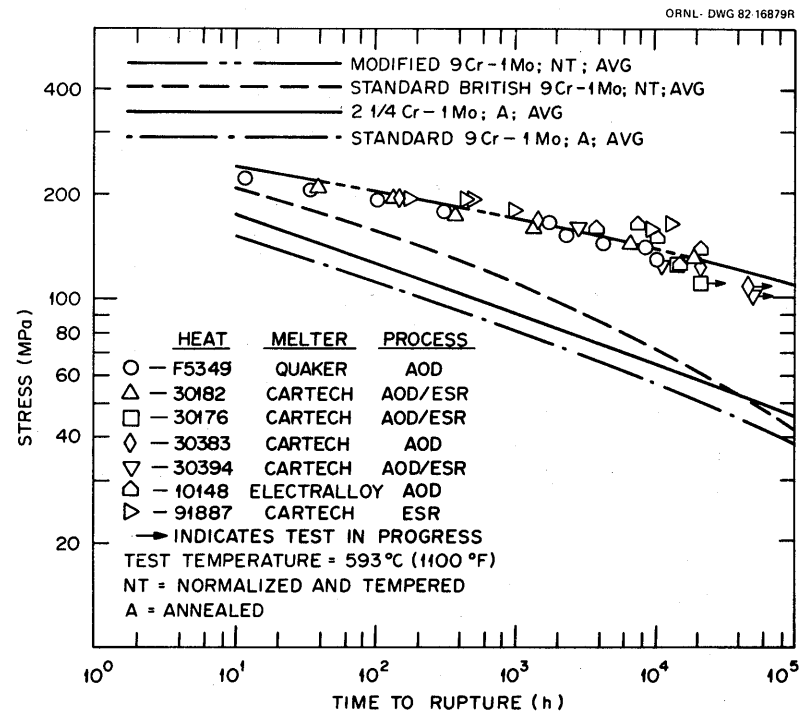


Fig. 9. Stress-rupture plot at 593°C comparing data on commercial heats of modified 9Cr-1Mo steel (tested in normalized and tempered condition) with average curves for standard British 9Cr-1Mo steel tested in normalized and tempered condition and standard American 9Cr-1Mo steel and 2.25Cr-1Mo steel tested in annealed conditions.

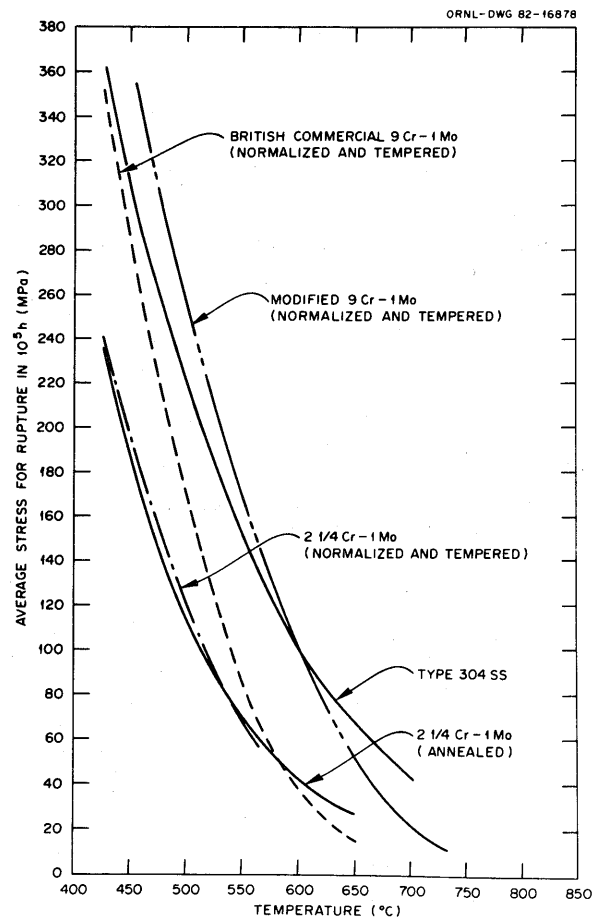


Fig. 10. Variation of 10^5 creep-rupture strength with temperature for several materials.

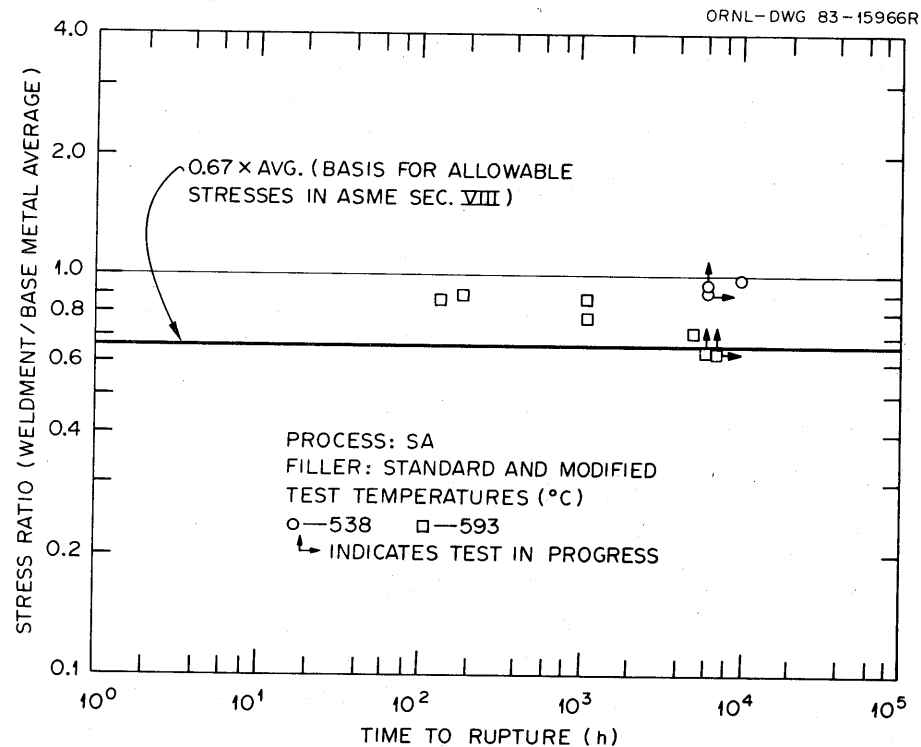


Fig. 11. Stress ratio (weldment to base metal average) as a function of time to rupture for SA weldments of both standard and modified 9Cr-1Mo filler wire compositions. Data are for test temperatures of 538 and 593°C. Stress ratios of unity, representing equal strength, and 0.67, the criterion for allowable stresses in ASME Code, Sect. VIII, are also included.

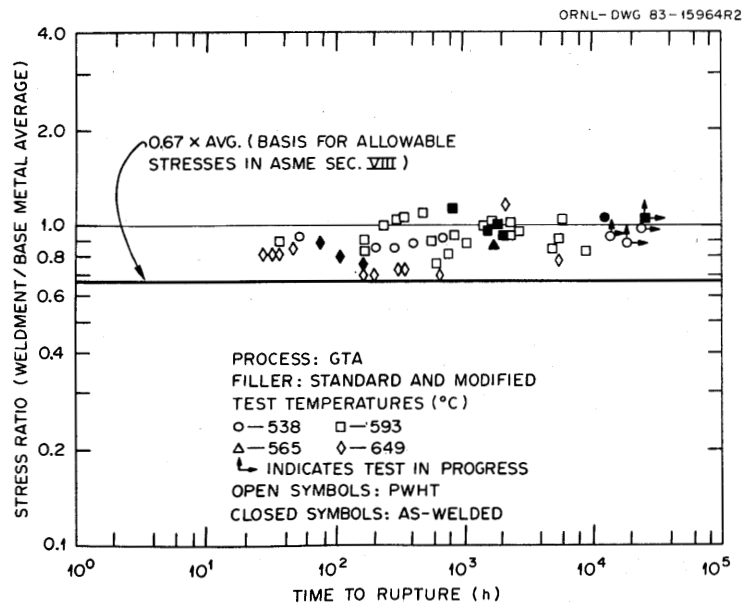


Fig. 12. Stress ratio (weldment to base metal average) as a function of time to rupture for GTA weldments of both standard and modified 9Cr-1Mo filler wire compositions. Data are for test temperatures of 538, 593, 565, and 649°C. Stress ratios of unity, representing equal strength, and 0.67, the criterion for allowable stresses in ASME Code, Sect. VIII, are also included.

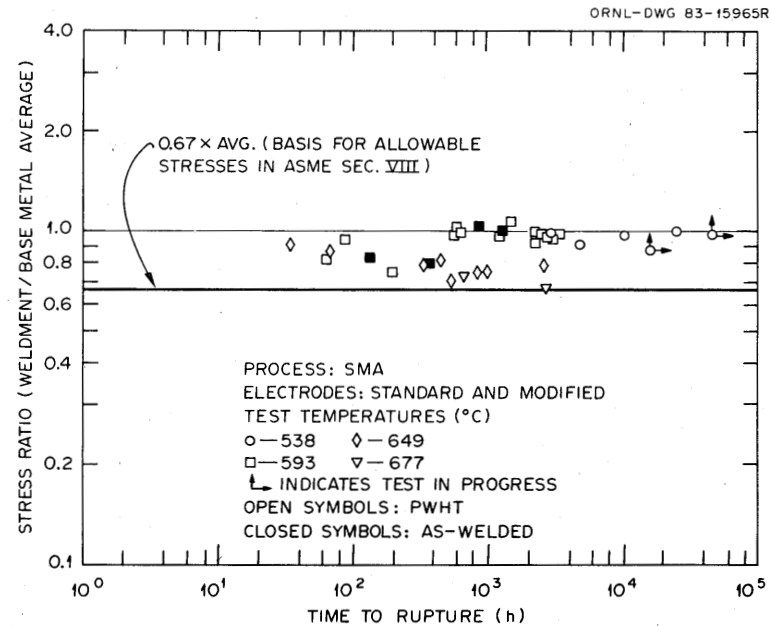


Fig. 13. Stress ratio (weldment to base metal average) as a function of time to rupture for SMA weldments of both standard and modified 9Cr-1Mo filler wire compositions. Data are for test temperatures of 538, 593, 649, and 677°C. Stress ratios of unity, representing equal strength, and 0.67, the criterion for allowable stresses in ASME Code, Sect. VIII, are also included.

Data obtained from all weldment tests are combined in Figs. 14 and 15. The rupture strength is again normalized by dividing by the base material average, Fig. 14, or minimum strength, Fig. 15. Weldments of this material given the standard heat treatment, i.e., normalizing at 1038°C, tempering at 760°C, followed by a PWHT at 732 to 760, show reduced creep-rupture life times in comparison to base material particularly at fairly short test times (see Fig. 14) because of a soft zone that occurs in the HAZ in the base material,¹¹ Fig. 16. Failure always occurs in this region which is the weak link or soft zone thought to be due to carbide coarsening in this region due to overtempering.

A modified tempering treatment was developed that tends to minimize the hardness variation across the weldment.¹² The heat treatment consists of the standard normalization procedure followed by tempering at 621°C. Following welding the PWHT is performed at 760°C. Figure 17 shows resultant hardness values after various stages in the heat treatment sequence and indicates that a PWHT at 760 is better than one at 732°C in terms of minimizing hardness variations. Figure 18 compares creep-rupture specimens that were given the standard or modified heat treatment prior to creep testing at 593°C. The top three specimens failed in the weak zone of the HAZ (note the slant fracture appearance since the weld was a V-groove butt weldment). The bottom three specimens were given the modified heat treatment with the 621°C temper as indicated. Note that failure is cup-cone in appearance and that failure now occurs out in the base material. Figures 19 and 20 compare results of creep-rupture tests conducted on specimens taken from weldments that had been given either the standard or modified heat treatment prior to testing at either 538°C (Fig. 19) or at 593°C (Fig. 20). Average and minimum (average - 1.65 × the standard error of the estimate (SEE) behavior of base material are also given for comparison purposes. Figure 20 clearly shows that the modified heat treatment improves the weldment creep-rupture properties with the creep strength now being about equal to that of the base material.

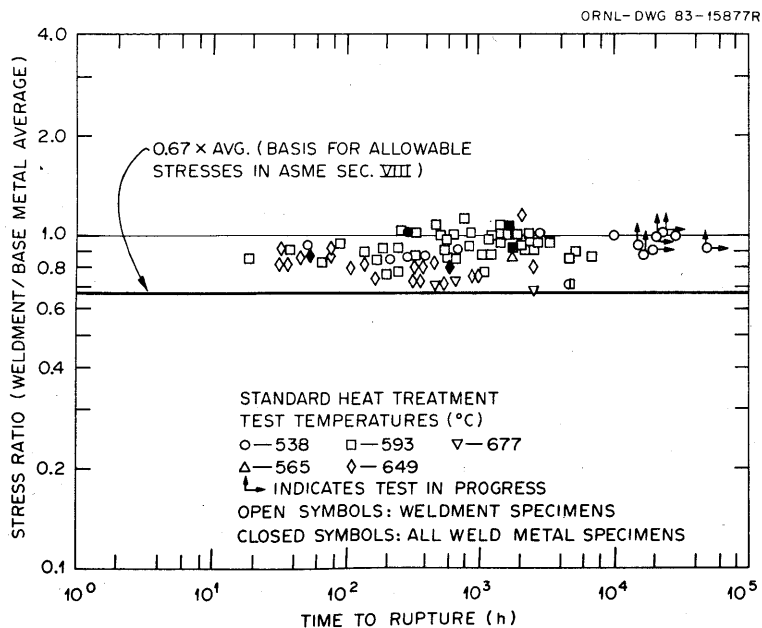


Fig. 14. Stress ratio (weldment to base metal average) as a function of time to rupture. Weldment data are for both the standard and modified 9Cr-1Mo filler wire and for all three welding processes (GTA, SMA, and SA). Data are for test temperatures of 538, 565, 593, 649, and 677°C. Stress ratios of unity, representing equal strengths, and 0.67, representing the ASME Code, Sect. VIII, criteria for allowable stresses, are also included.

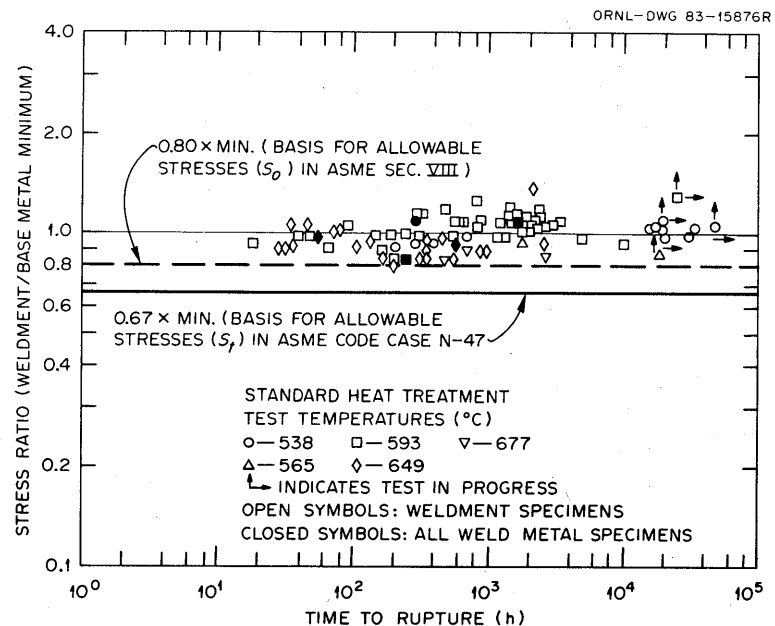


Fig. 15. Stress ratio (weldment to base metal minimum) as a function of time to rupture. Weldment data are for both the standard and modified 9Cr-1Mo filler wire and for all three welding processes (GTA, SMA, and SA). Data are for test temperatures of 538, 565, 593, 649, and 649°C. Stress ratios of unity, representing equal strengths; 0.80, the criterion for allowable stresses in ASME Code, Sect. VIII; and 0.67, the criterion for all allowable stresses in ASME Code Case N-47, are also included.

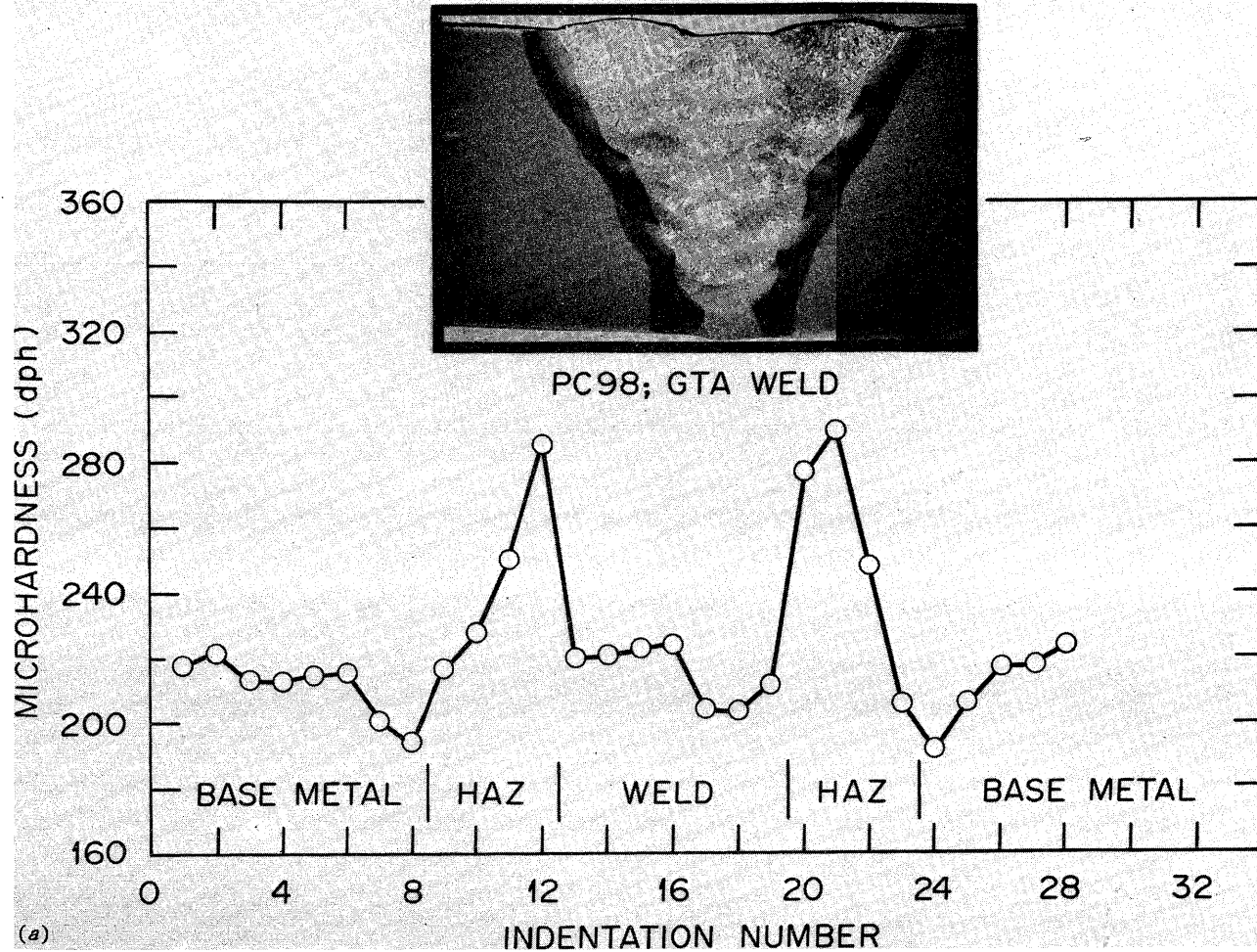


Fig. 16. Hardness profile across several weldments illustrating strong and weak zones. (a) Gas tungsten arc (GTA). (b) Submerged arc (SA). (c) Submerged arc (SA). (d) Shielded metal arc (SMA).

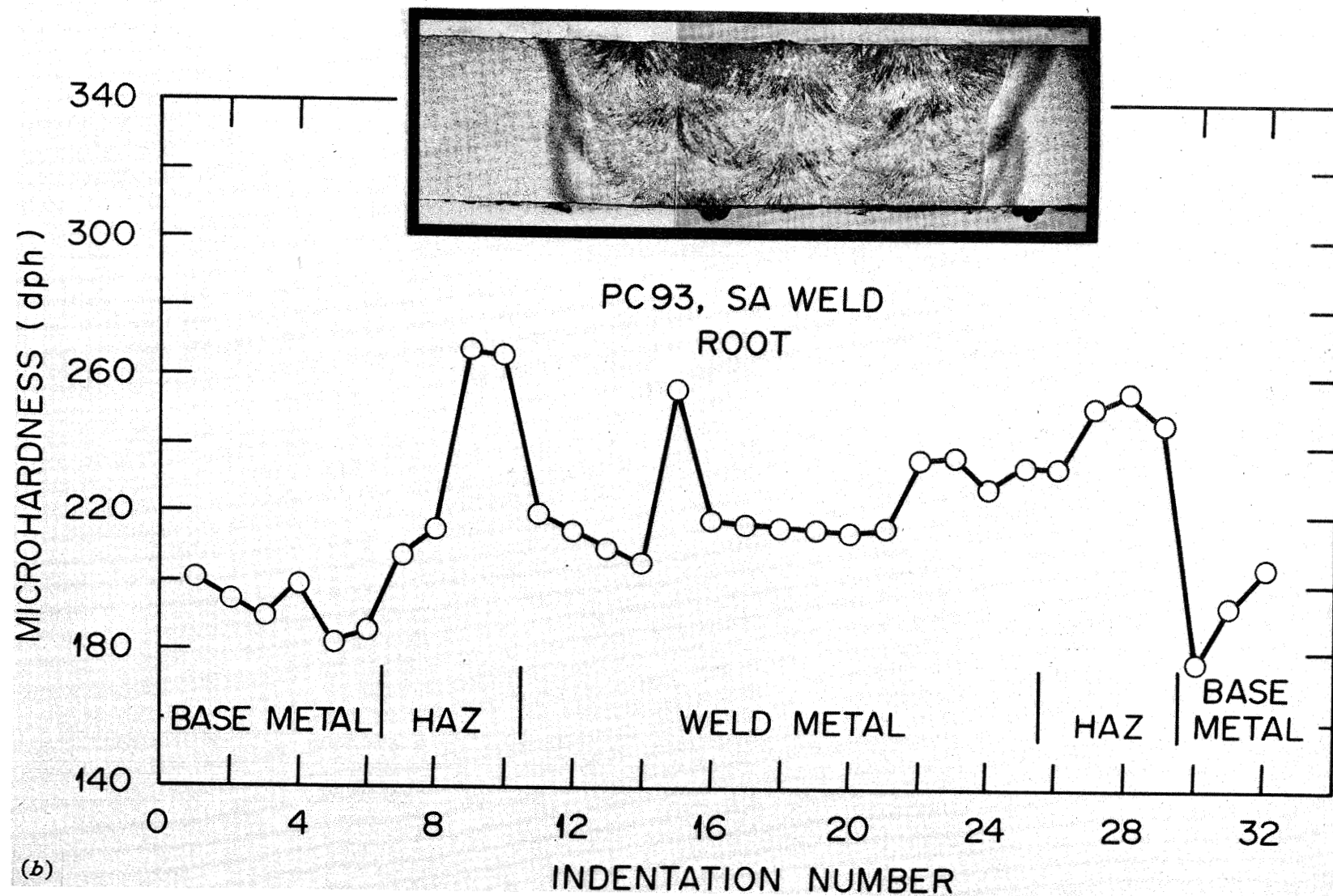


Fig. 16 (cont'd)

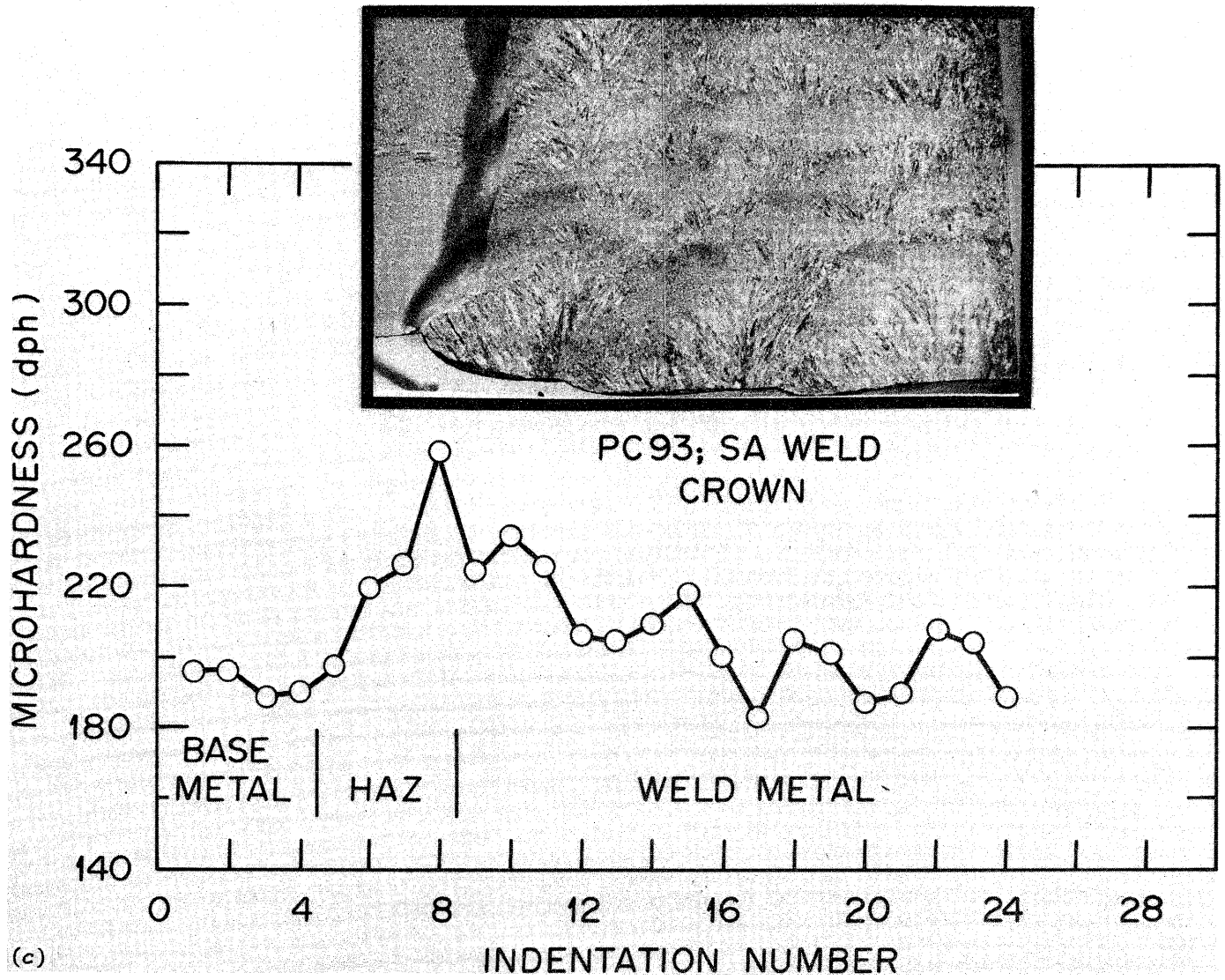


Fig. 16 (cont'd)

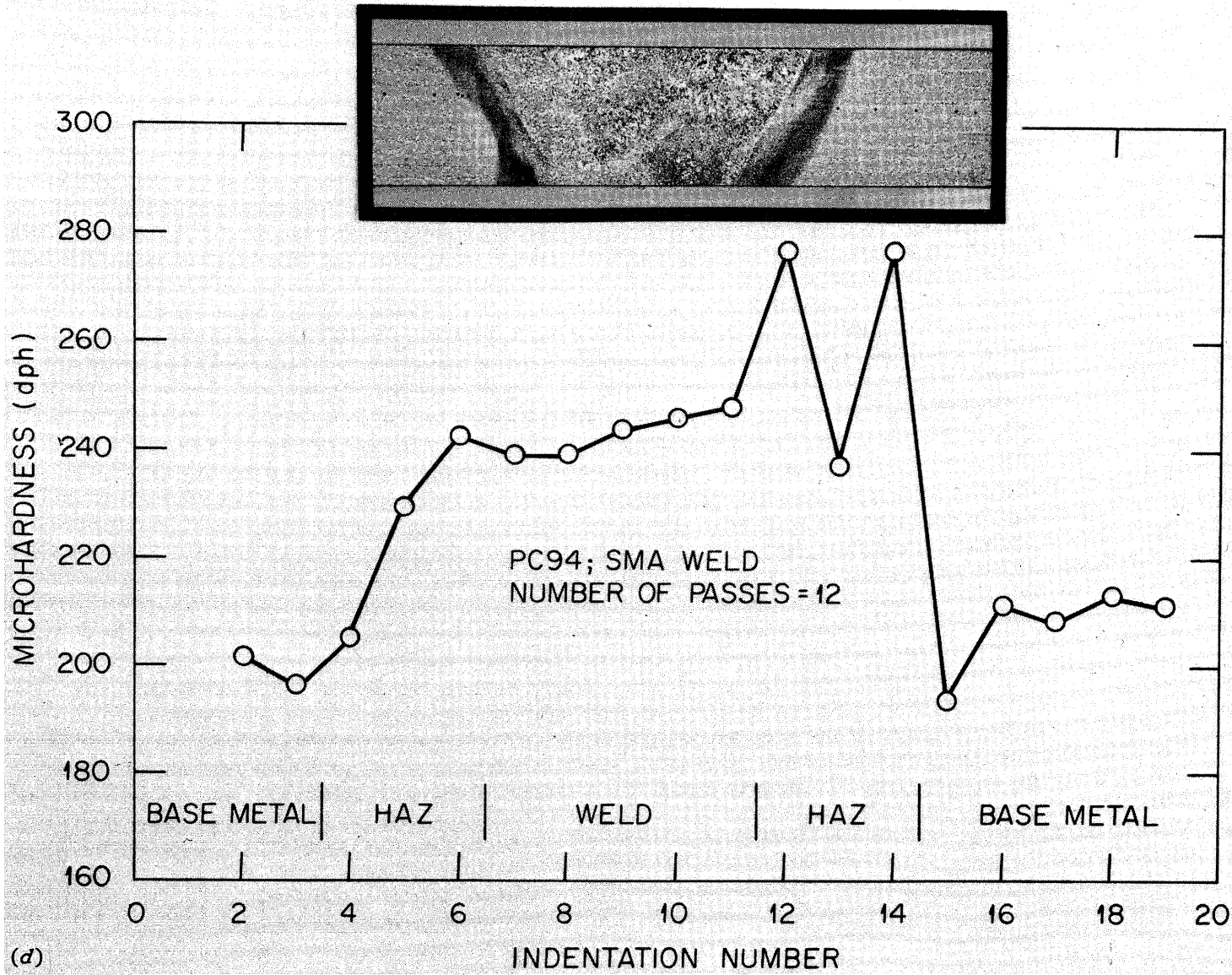


Fig. 16 (cont'd)

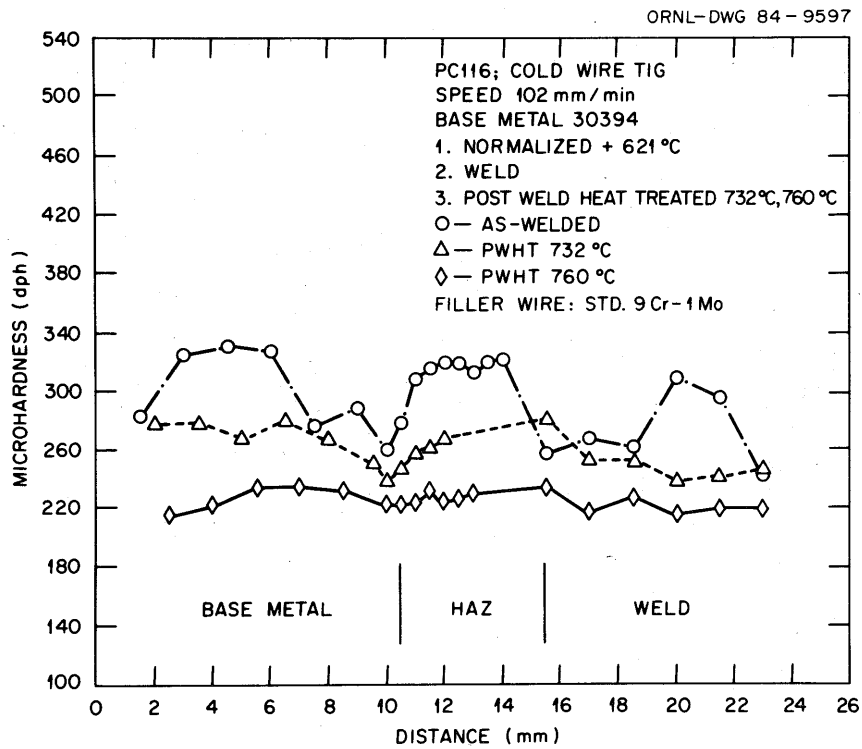
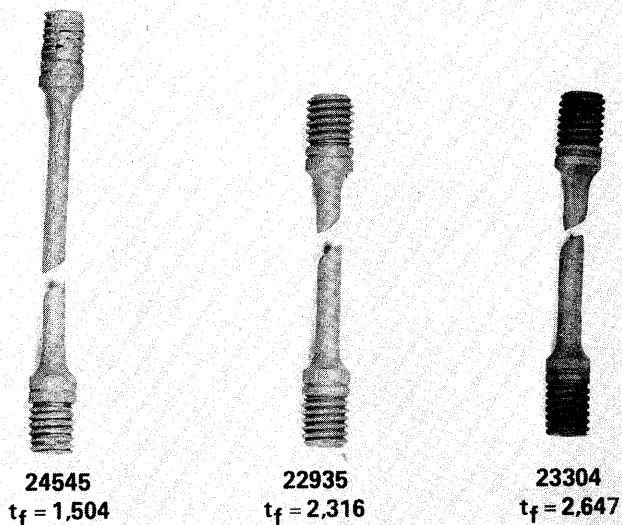


Fig. 17. Hardness traverse data for GTA weld PC-116 showing that a 760°C PWHT is necessary to eliminate the overtempered region in partially tempered base plate.

TEST TEMPERATURE: 593 °C

PRE-TEST HEAT TREATMENT (°C): 1038/760/732



PRE-TEST HEAT TREATMENT (°C): 1038/621/760

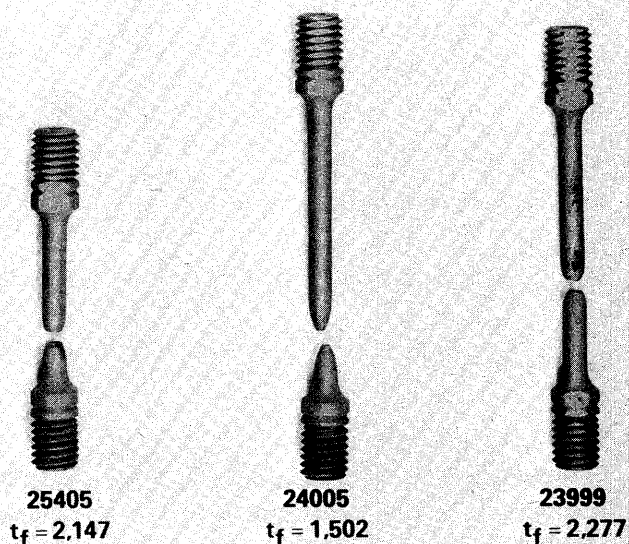


Fig. 18. Comparison of post-tested weldment creep specimens given the standard and modified heat treatment prior to creep testing at 593°C. Note the slant fracture appearance of specimens given the standard heat treatment, i.e., 1038°C/760°C/732°C in comparison to the cup-cone fractures of those given the modified heat treatment, i.e., 1038°C/621°C/760°C.

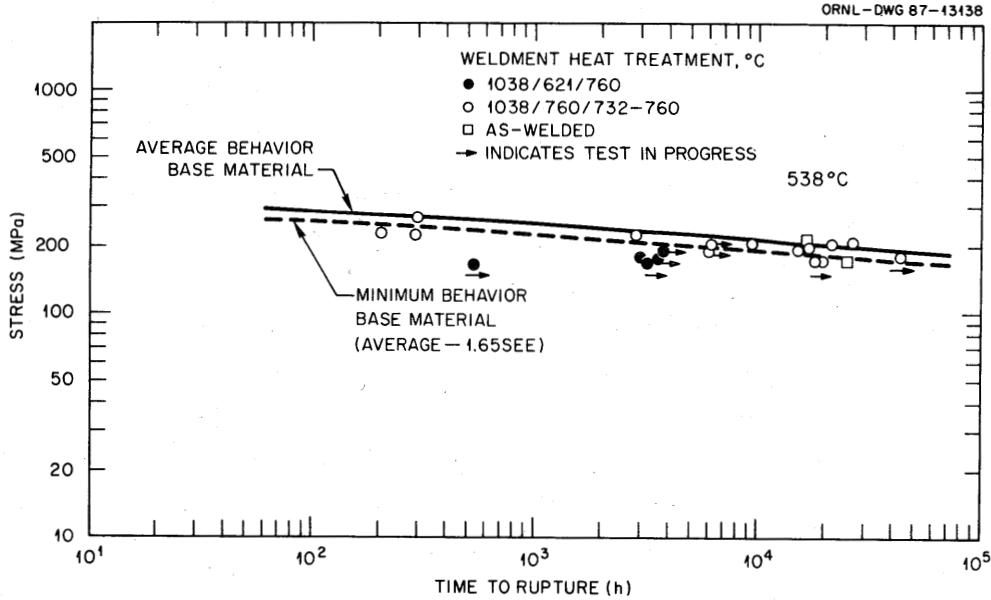


Fig. 19. Stress-rupture properties of specimens take across weldments with base, heat-affected-zone, and weld metal all within gage section of the specimen unless specified otherwise. Weldments prepared by SA, SMA, and GTA processes.

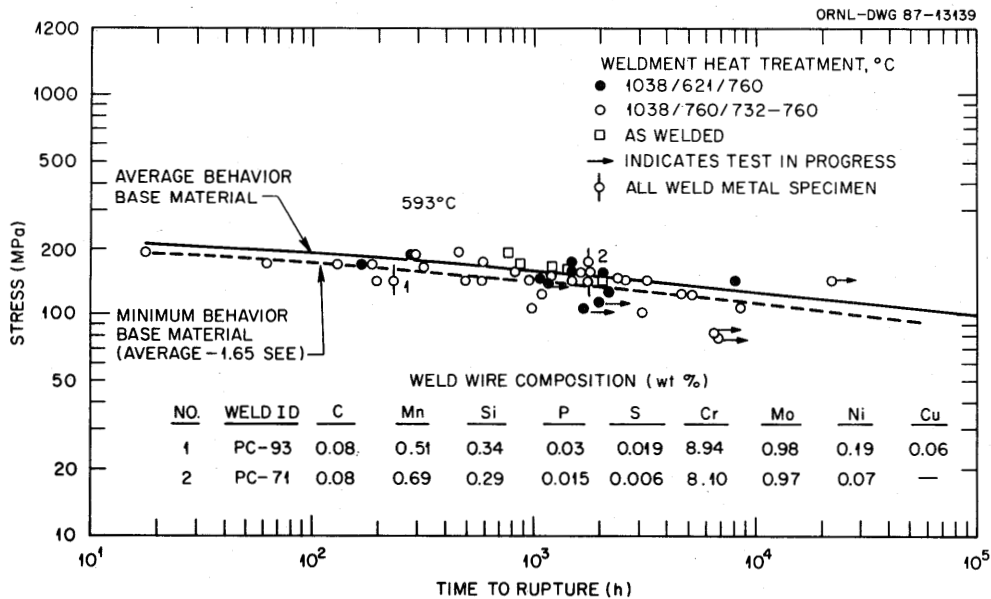


Fig. 20. Stress-rupture properties of specimens taken across weldments with base, heat-affected-zone, and weld metal all within gage section of the specimen unless specified otherwise. Weldments prepared by SA, SMA, and GTA processes.

CONCLUSIONS

Results of long-term creep and creep-rupture tests currently ongoing or recently completed are reported for modified 9Cr-1Mo steel and its weldments. Commercially supplied base material was from many suppliers and included multiple product forms such as plate, pipe, castings, and a forging. Weldments were made by several methods including SA, GTA, and SMA. Base material was tested in the normalized and tempered condition. Weldment specimens were generally taken transverse to the weld fusion line such that specimens contained base, HAZ, and weld metal. Weldment specimens were taken from material given either a standard heat treatment, (i.e., normalized at 1038°C, tempered at 760°C, and PWHT at 732 to 760°C) or a modified heat treatment, (i.e., normalized at 1038°C, tempered at 621°C, and PWHT at 760°C). The following are specific conclusions from this ongoing effort.

1. Predictions of rupture behavior of base material using previously developed rupture equations are very good over the temperature range of 427 to 704°C and to test times of about 68,000 h.
2. Generally good agreement was found in predicting creep deformation response of base material particularly at temperatures in excess of 427°C.
3. Plots of creep-rupture ductility for base material measured as total elongation or reduction of area indicate that these values decrease with test times in excess of 10 to 20,000 h in the temperature range of 593 to 649°C.
4. Thermal aging of base material for 25,000 h (2.9 years) in the temperature range of 538 to 649°C results in no decrease in rupture life when tested at those same temperatures.
5. Available creep-rupture data taken from specimens cut from sand castings indicate a slight decrease in rupture life in the temperature range of 593 to 649°C in comparison to wrought material. Specimens taken from a saddle forging and tested in the range of 538 to 649°C show similar rupture lives to that of the average behavior of other wrought product forms.
6. Increasing the niobium content to 0.15 wt %, which is beyond the allowed range of 0.06 to 0.1 wt %, increases the rupture strength in this alloy.

7. A comparison between average creep-rupture life of commercially melted material processed in the United States and Japan indicated similar behavior.

8. Specimens taken from weldments in the transverse direction such that the gage length contained base, HAZ, and weld metal that had been given the standard heat treatment showed reduced stress-rupture lives in comparison to base material similarly heat treated. Failure occurred in a soft zone in the HAZ along a line parallel to the fusion line resulting in a slant fracture appearance of the ruptured specimens. These were the results generally found for tests with initial stress levels such that failure occurred in several thousand hours. For specimens tested at 538°C and loaded at somewhat lower stress levels such that failure occurred after much longer test times, there was an indication that rupture life improved.

9. Weldment material given the modified heat treatment showed improved rupture lives over that given the standard heat treatment. Weldment material given the modified heat treatment showed rupture lives similar to that of base material.

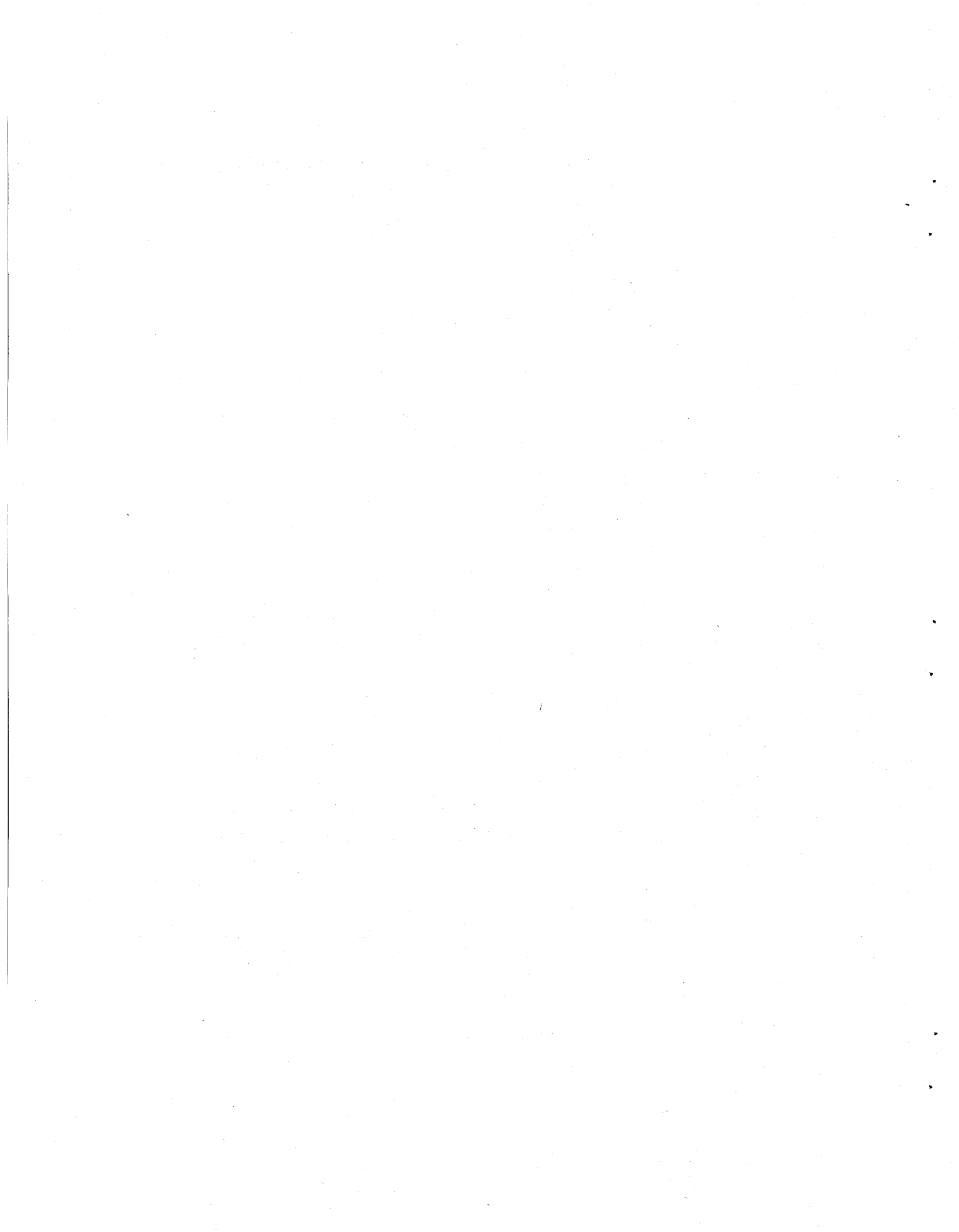
ACKNOWLEDGMENTS

The authors would like to thank H. E. McCoy and R. W. Swindeman for reviewing the manuscript, and M. R. Upton for preparing the manuscript. The authors would also like to thank R. Baldwin and H. D. Upton for conducting the tests.

REFERENCES

1. J. R. DiStefano et al., *Summary of Modified 9 Cr-1 Mo Steel Development Program: 1975 - 1985*, ORNL-6303, October 1986.
2. V. K. Sikka, M. G. Cowgill, and B. W. Roberts, "Creep Properties of Modified 9 Cr-1 Mo Steel," pp. 413-23 in *Proceedings of Topical Conference on Ferritic Alloys for Use in Nuclear Energy Technologies* held in Snowbird, Utah, on June 19-23, 1983, ed. J. W. Davis and D. J. Michel, The Metallurgical Society of AIME, Warrendale, Penn., 1984.

3. V. K. Sikka and M. D. Hart, *Characterization of Modified Cr-1 Mo Steel Extruded Pipe*, ORNL-6154, April 1985.
4. V. K. Sikka, *Characterization of Modified 9 Cr-1 Mo Steel Sand Castings*, ORNL/TM-9573, April 1985.
5. V. K. Sikka and P. Patriarca, *Analysis of Weldment Mechanical Properties of Modified 9 Cr-1 Mo Steel*, ORNL/TM-9045, May 1984.
6. J. F. King, V. K. Sikka, M. L. Santella, J. F. Turner, and E. W. Pickering, *Weldability of Modified 9 Cr-1 Mo Steel*, ORNL-6299, September 1986.
7. G. C. Bodine and R. E. McDonald, "Laboratory and Pilot Commercial Process/Product Development of Modified 9 Cr-1 Mo Ferritic Alloy," pp. 9-20 in *Ferritic Steels for High-Temperature Applications, Proceedings of ASM International Conference on Production, Fabrication, Properties, and Applications of Ferritic Steels for High-Temperature Applications, Warren, Pa., Oct. 6-8, 1981*, ed. A. K. Khare, American Society for Metals, Metals Park, Ohio, 1983.
8. V. K. Sikka, R. E. McDonald, and J. H. Smith, *Fabrication, Evaluation, and Inspection of Cold-Reduced and Cold-Drawn Tubes of Modified 9 Cr-1 Mo Steel*, ORNL/TM-8009, February 1982.
9. A. K. Khare and V. K. Sikka, "Evaluation of Modified 9 Cr-1 Mo Steel Forging," pp. 303-27 in *Proceedings of Symposium on Steel Forgings, Williamsburg, Va., November 28-30, 1984*, STP 903, American Society for Testing and Materials, Philadelphia, September 1986.
10. C. R. Brinkman, J. P. Strizak, and M. K. Booker, *Smooth- and Notched-bar Fatigue Characteristics of Modified 9 Cr-1 Mo Steel*, ORNL-6330, February 1987.
11. V. Biss, *Metallographic Investigation of Soft Regions Near Heat Affected Zones of Modified 9 Cr-1 Mo, HT-9, and 2.25 Cr-1 Mo Steel Weldments*, Report J-4747, AMAX Materials Research Center, Ann Arbor, Mich., Mar. 8, 1982.
12. V. K. Sikka, "Method for Welding Chromium Molybdenum Steels," U.S. Patent 4,612,070, Sept. 16, 1986.



Appendix 1

CREEP CURVES

The following illustrations are creep curves (total strain) versus time for modified 9Cr-1Mo steel (Figs. A1.1-A1.8). They represent results of ongoing (early 1987) tests (i.e., Figs. A1.1, A1.3, A1.4 and A1.5) as well as tests that have been completed (i.e., Figs. A1.2, A1.6, A1.7, A1.8 and A1.9). Also included for comparison are predictions of the creep response from the creep equation developed in 1984. Figures A1.6 through A1.9 also show a macro-photograph of the applicable ruptured specimen.

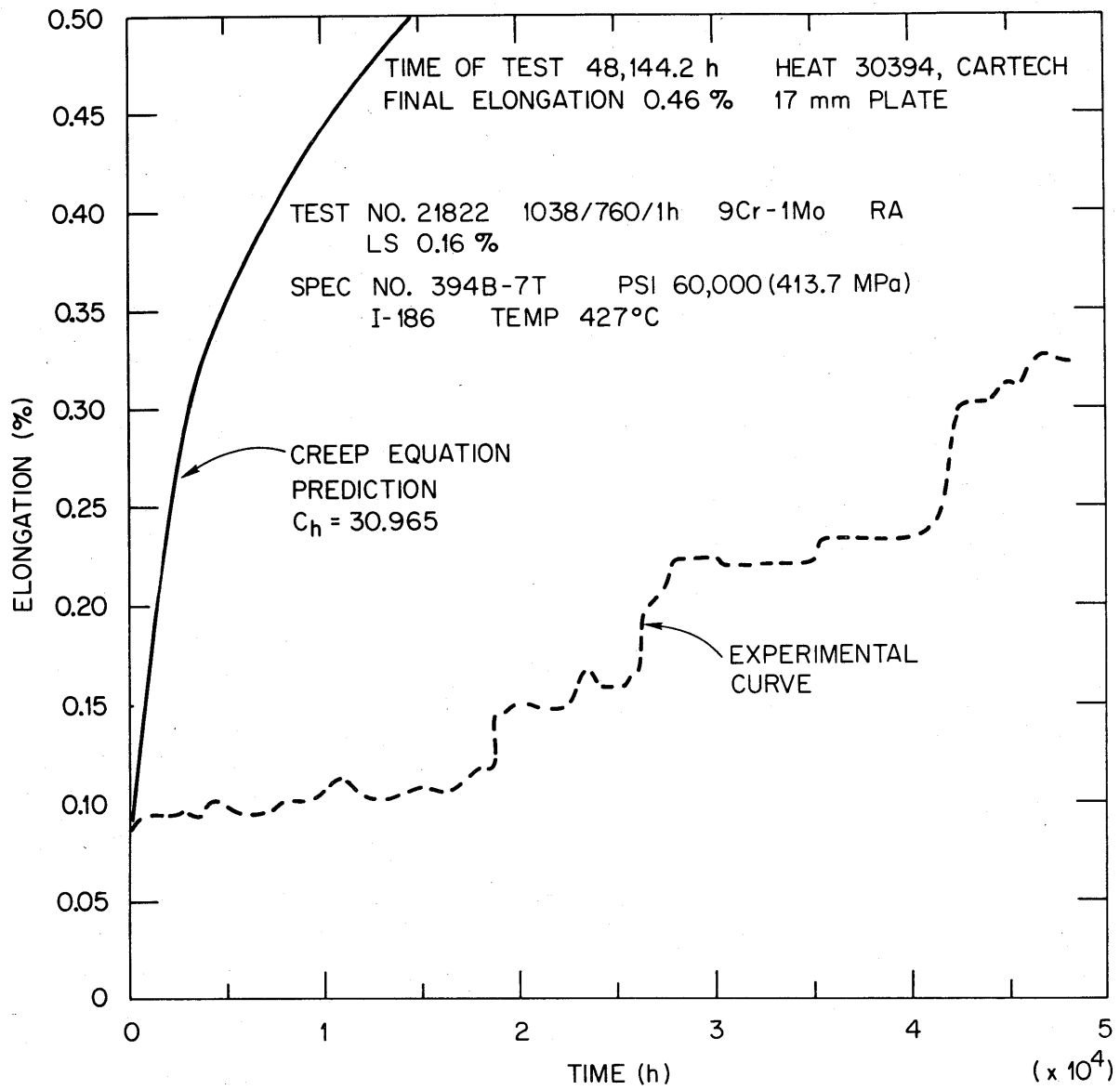


Fig. A1.1

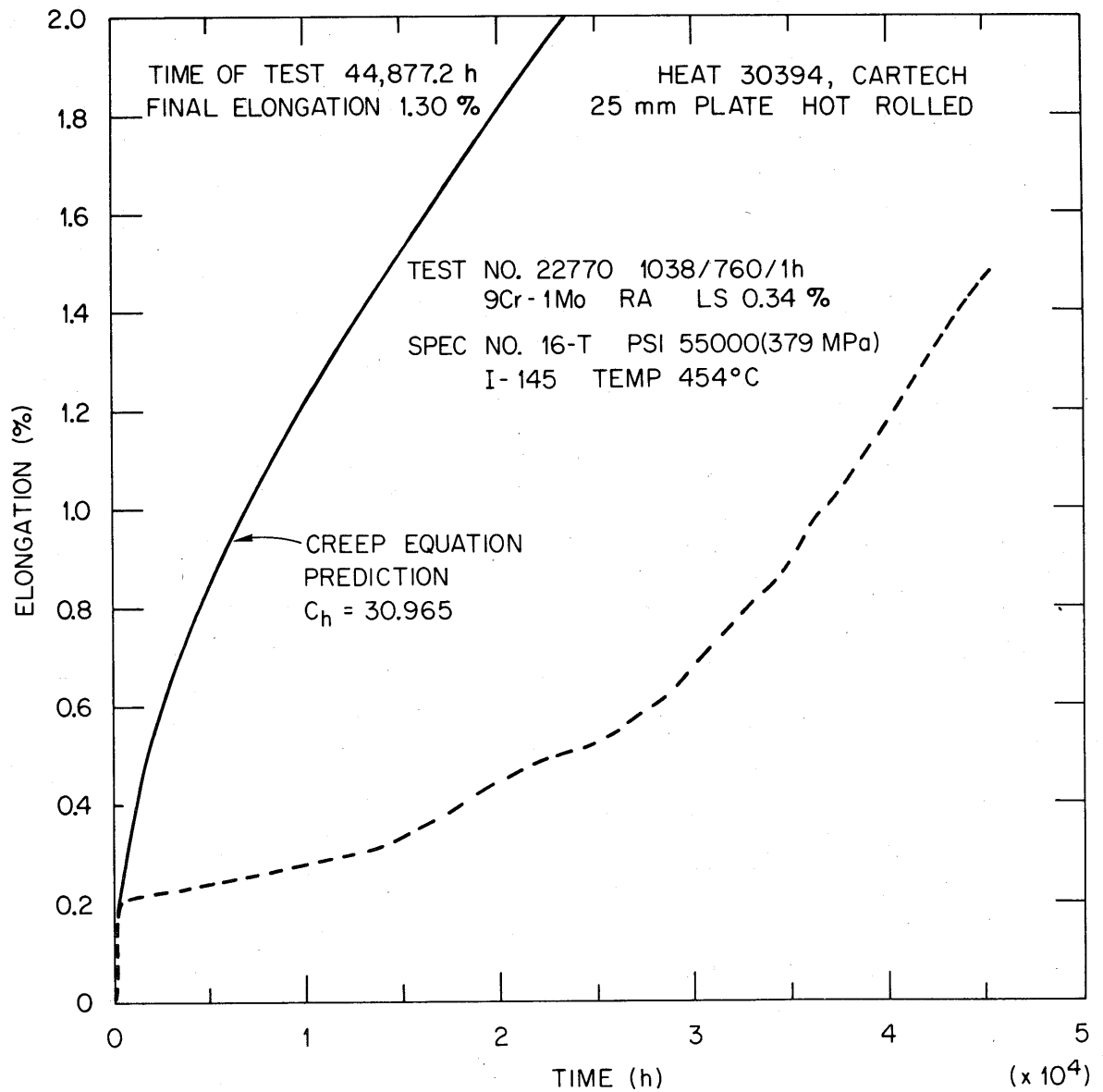


Fig. A1.2

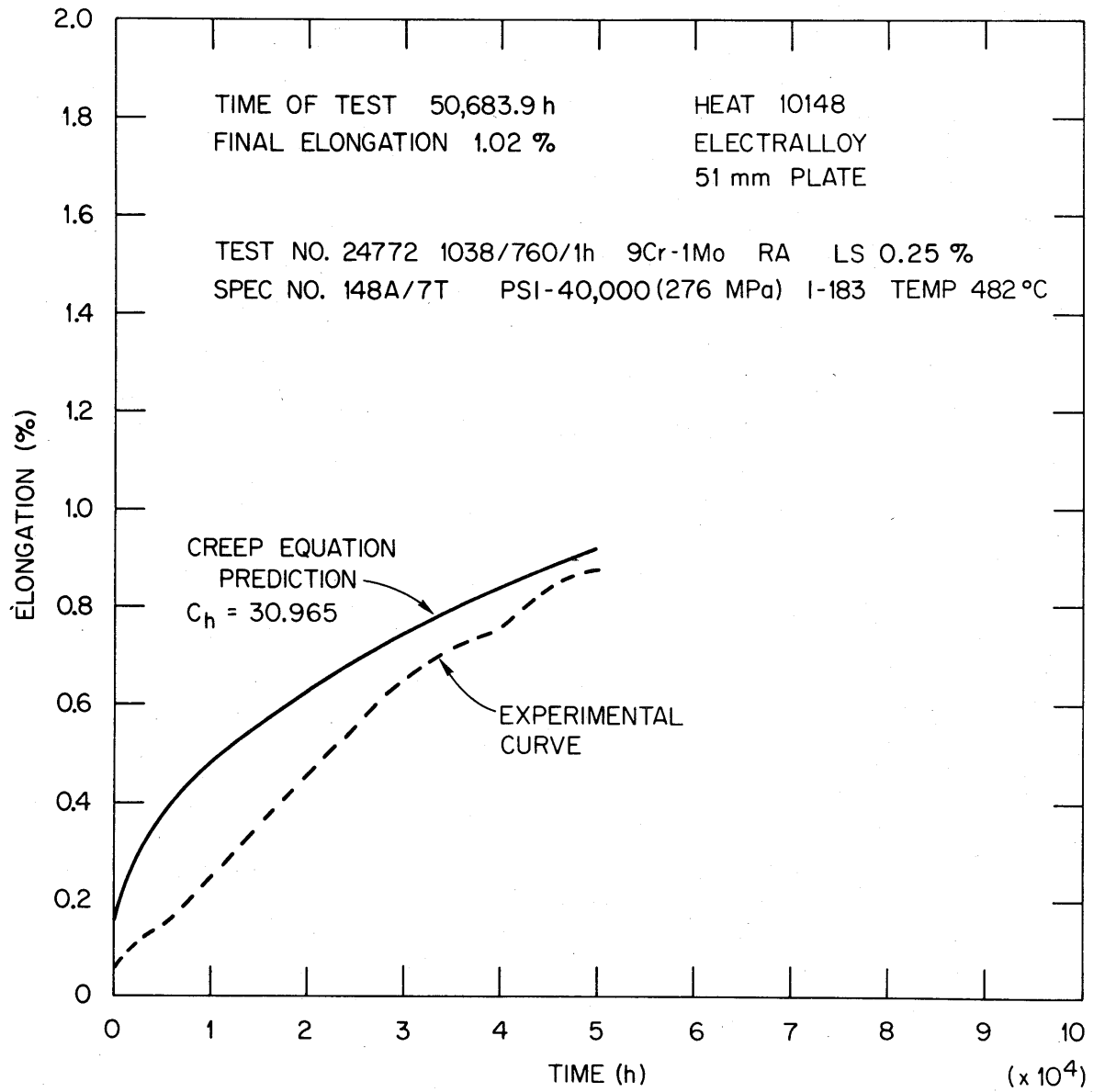


Fig. A1.3

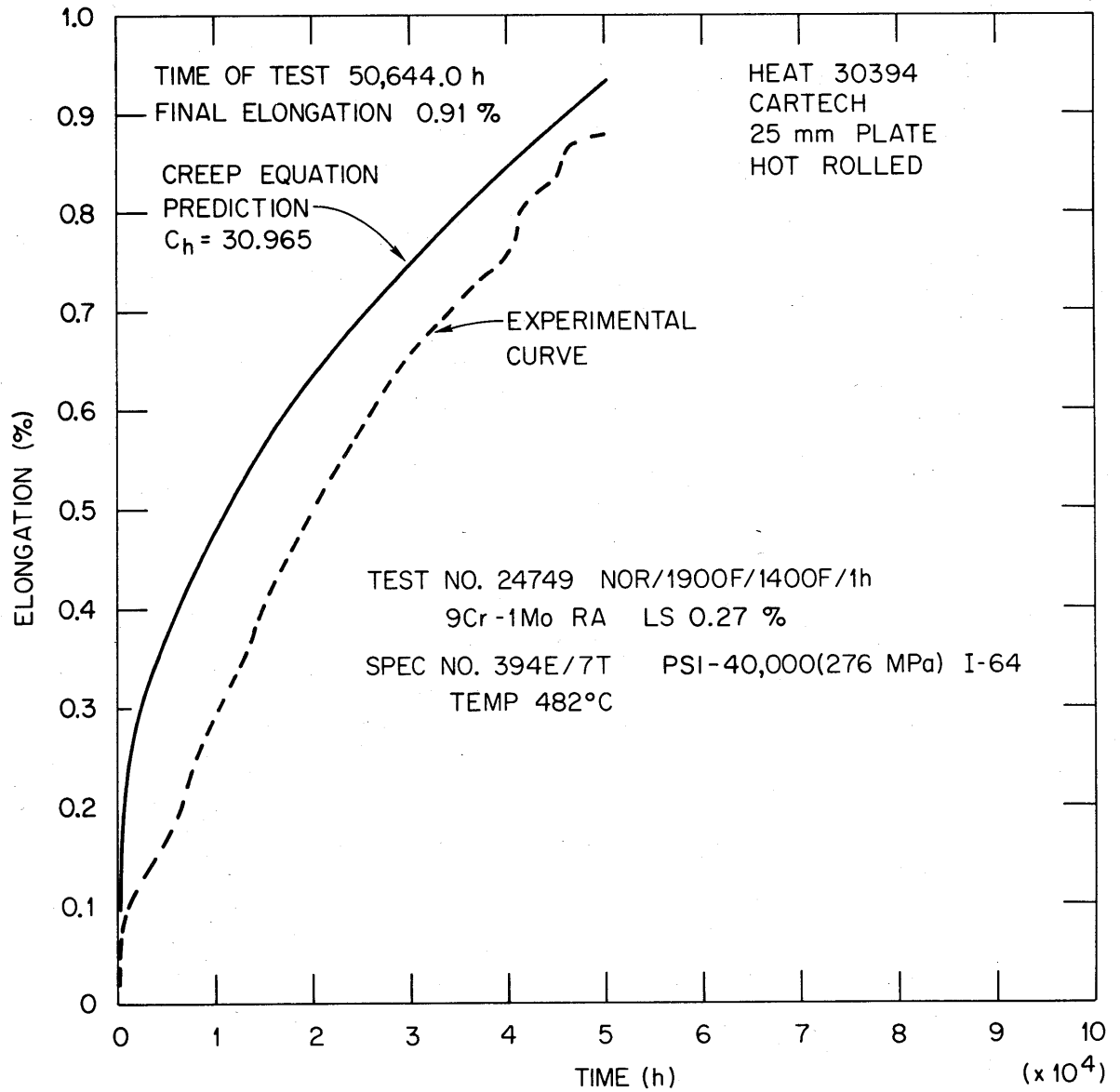


Fig. A1.4

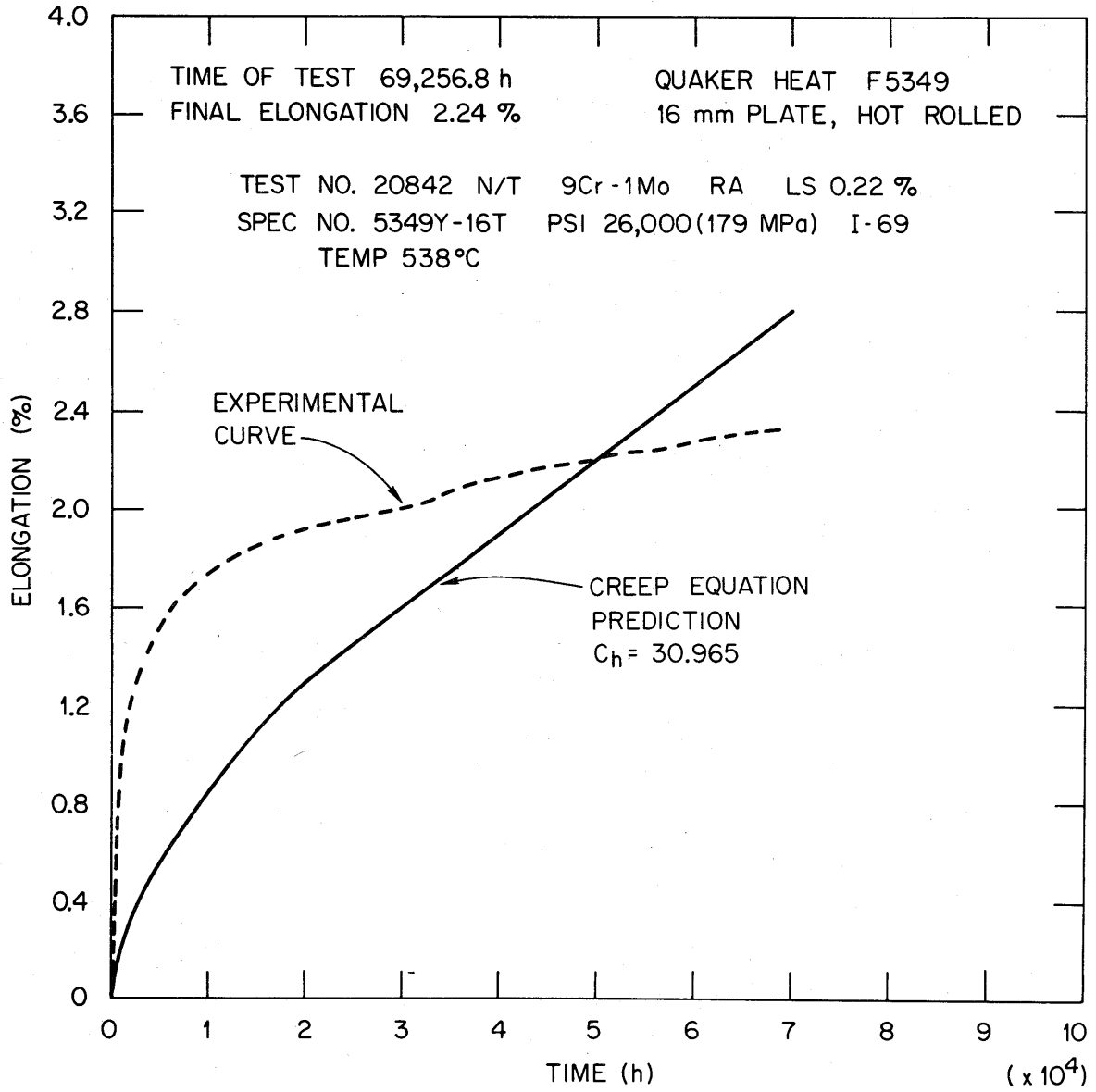


Fig. A1.5

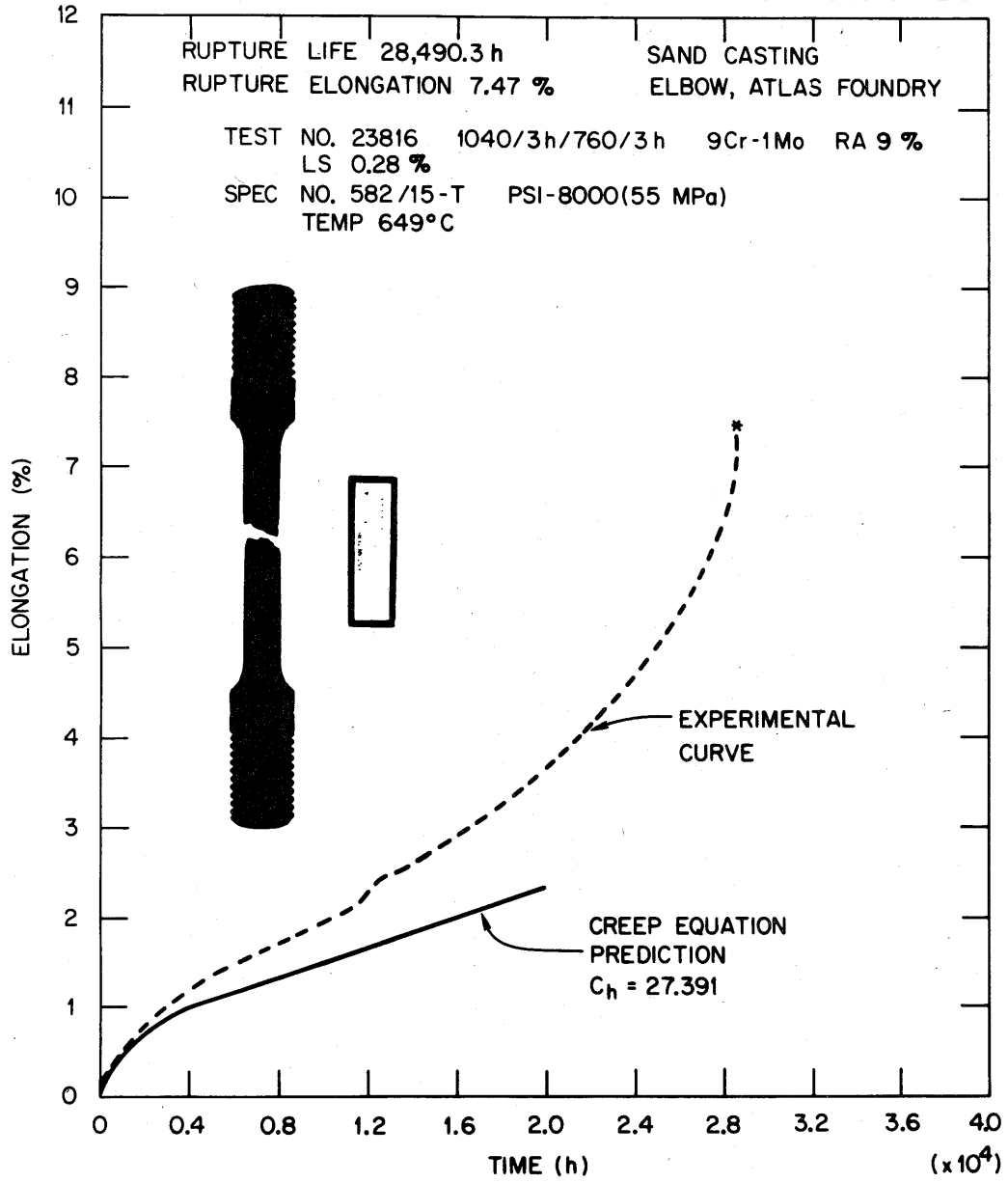


Fig. A1.7

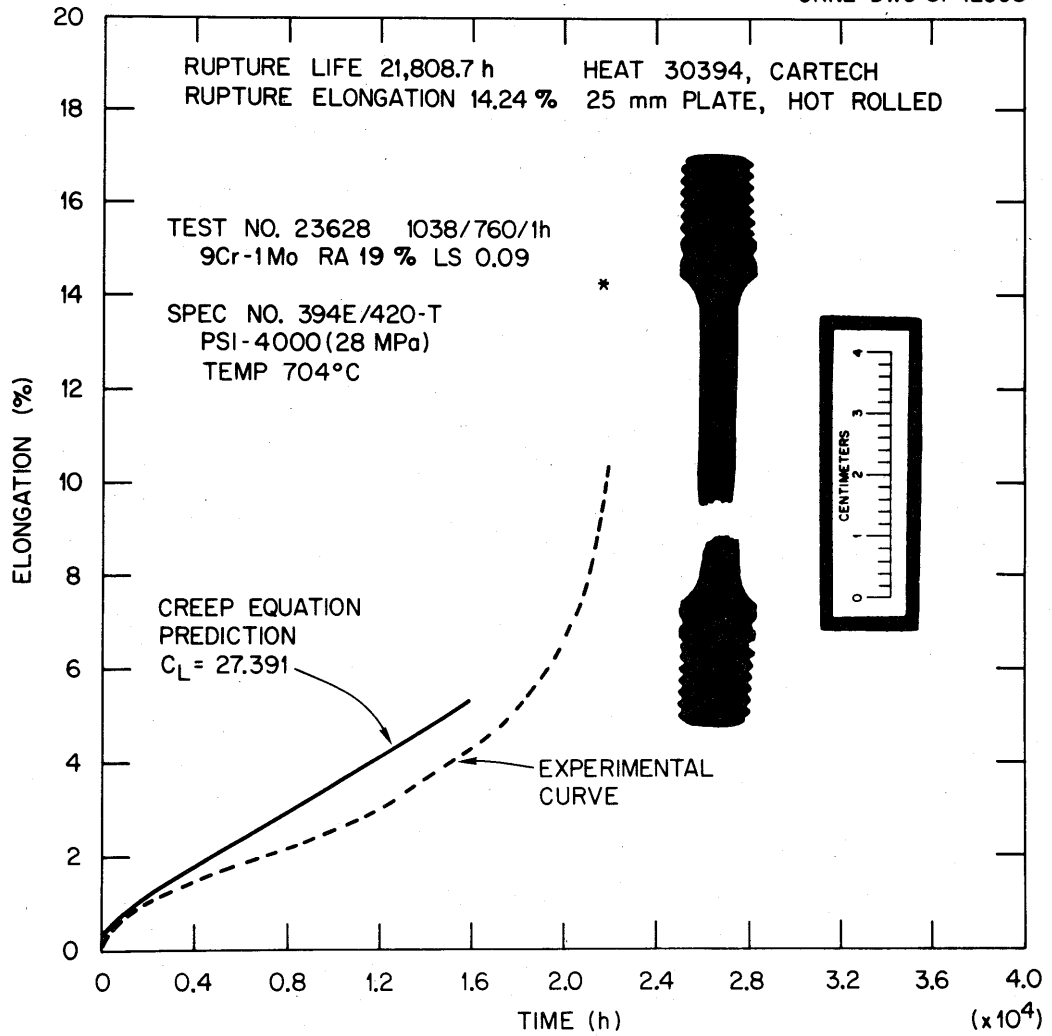


Fig. A1.8

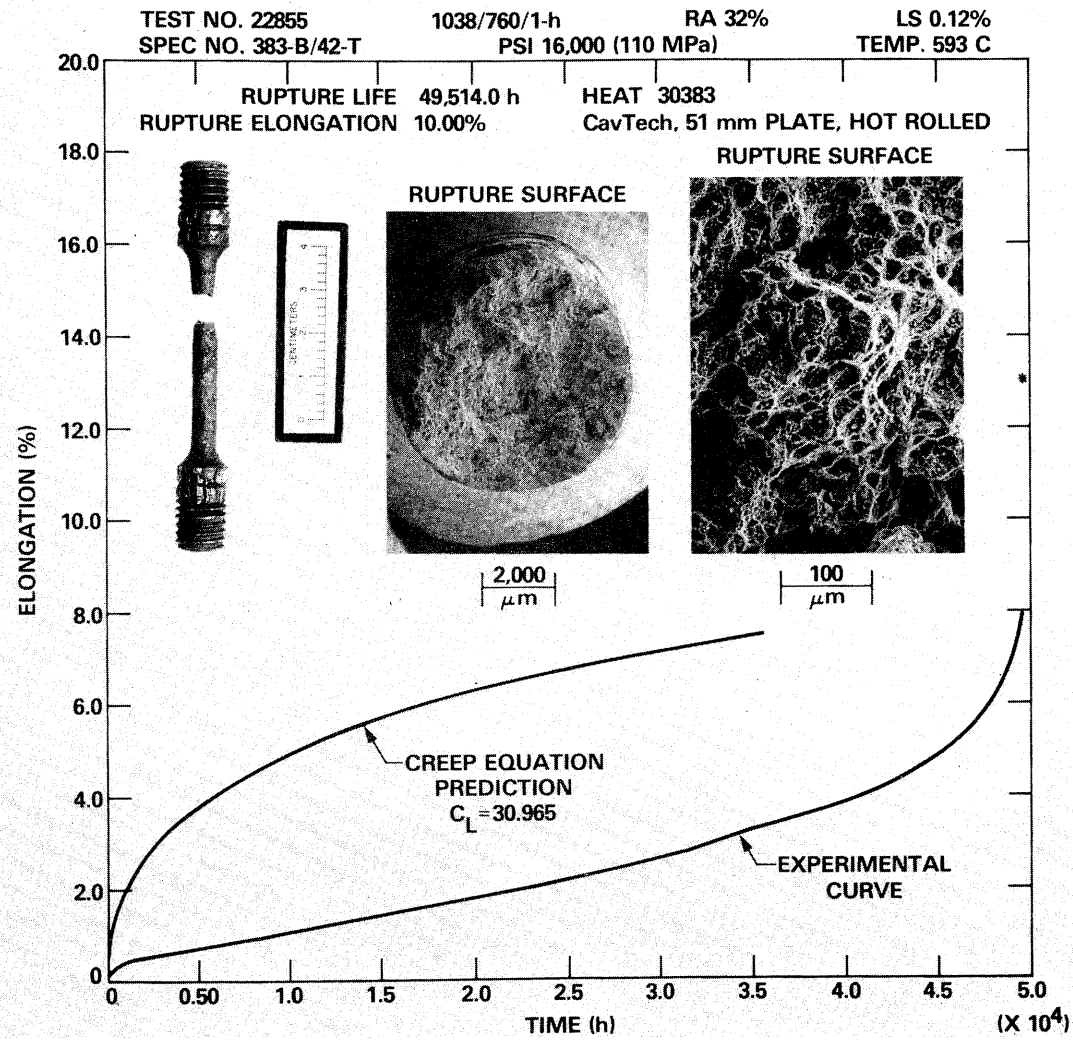


Fig. A1.9

Appendix 2

WELDMENT DATA

Table A2.1 summarizes details of the welding procedures used in the preparation of weldments of modified 9Cr-1Mo steel. Weldments were prepared by the gas tungsten arc (GTA) process, the shielded metal arc (SMA) process, and the submerged arc (SA) process.

Table A2.2 contains results of creep-rupture tests conducted on specimens taken across weldments such that the gage section contains base, heat-affected-zone, and weld metal unless otherwise indicated. The heat treatment indicated gives the normalization/tempering/and PWHT temperature (e.g., 1038/760/704°C).

Table A2.1. Welding procedures for modified 9Cr-1Mo steel

Weld	Process	Base metal	Heat	Thickness	Temper (°C)	Time (h)	Filler metal	Weld wire	Heat	Flux/Gas	PWHT (°C)	Time (h)	Remarks
PC-109	SAW	Mod.	10148	51			ER505	735	D3612F-505	OP-76	760	1.0	
PC-110	GTAW	Mod.	30176	25	621	1.0	ER505	715	33669	3He-1Ar	760	1.0	Cold wire
PC-111	GTAW	Mod.	30394	25	621	1.0	ER505	715	33669	3He-1Ar	760	1.5	Cold wire
PC-112	SAW	Mod.	10148	51	621	1.5	ER505	735	D3612F-505	OP-76	760	1.5	
PC-113	SAW	Mod.	10148	51	621	1.5	ER505	735	D3612F-505	OP-76	760	1.5	Macros show weld metal cracking.
PC-114A	SAW	Mod.	10148	51	593	1.5	ER505	735	D3612F-505	OP-76	760	1.5	Flux baked at 400°C. Cracking as in PC-113.
PC-114	Same as PC-114A	except for PWHT								OP-76	732	1.5	Same as PC-114A.
PC-115A	SAW	Mod.	10148	51	649	1.5	ER505	714	33569	OP-76	760	1.5	Flux baked at 200°C. No weld metal cracks.
PC-115	Same as PC-115A	except for PWHT								OP-76	732	1.5	Same as PC-114A.
PC-116	GTAW	Mod.	30176	25	621	1.0	ER505	715	33669	3He-1Ar	*	*	See full noted for details.
PC-117A	GTAW	Mod.	30176	10	760	1.0	ER505	715	33669	3He-1Ar	760	1.0	Half of plate was not PWHT.
PC-117B	GTAW	Same as PC-117A.								3He-1Ar	760	1.0	Half w/no PWHT. Surface buttering was added.
PC-118A	GTAW	Mod.	30176	10	621	1.0	ER505	715	33669	3He-1Ar	760	1.0	Half w/no PWHT.
PC-118B	GTAW	Same as PC-118A								3He-1Ar	760	1.0	Half w/no PWHT. Surface buttering added.
PC-119	SAW	Mod.	10148	51	621	1.5	ER505	743	21078	OP-76			Weld terminated due to flux adherence.
PC-120	GTAW	Mod.	30176	25	760	1.0	ER505	744	21078	3He-1Ar	760	1.0	Cold wire.
PC-121	GTAW	Mod.	30176	25	621	1.0	ER505	744	21078	3He-1Ar	760	1.0	Cold wire.
PC-122	GTAW	Mod.	30394	10	621	1.0	ERNiCr3				200°C preheat		Dissimilar weld to 316 SS. 9Cr buttered w/filter.
PC-123	GTAW	Mod.	30384	10	621	1.0	ERNiCr3				200°C preheat		Dissimilar weld to 316 SS. 9Cr buttered w/filter.
PC-124	GTAW	Mod.	30394	10	621	1.0	ERNiCr3				No preheat		Dissimilar weld to 316 SS. 9Cr buttered w/filter 1/4.
PC-125	GTAW	Mod.	30394	10	621	1.0	ERNiCr3				No preheat		Dissimilar weld to 316 SS. 9Cr buttered w/filter 1/2.
PC-126	GTAW	Mod.	30394	10	760	1.0	ERNiCr3				200°C preheat		Dissimilar weld to 316 SS. 9Cr buttered w/filter.
PC-127	GTAW	Mod.	30394	10	760	1.0	ERNiCr3				200°C preheat		Dissimilar weld to 316 SS. 9Cr buttered w/filter 1/2.
PC-128	SMAW						E505	739	M-10565		760	1.0	
PC-129	GTA	Mod.	30176	25				742					
PC-130	GTAW	Mod.	30176	10		1.0	ER505	751	3L27971	Ar	732	1.0	Two root passes made with std. electrode.
PC-131	SAW	Mod.	30176	25	1150	1.0	ER505				732	1.0	PC-131A - PWHT of 760°C/1 h. Jap electrode.
PC-132	SMAW	Mod.	30176	25	760	1.0	ER505	752			732	1.0	PC-132A - PWHT of 760°C/1 h. Jap electrode.
PC-133	GTAW	Mod.	30176	25	760	1.0	ER505	744	21078	Ar			On hold.
PC-134													
PC-135													
PC-136	GTAW	Mod.	30176	25	760	1.0	ER505	744	21078	3He-1Ar	732	1.0	Half with PWHT of 760°C/1 h.
PC-137													
PC-138	SAW	Mod.	30176	25	760	1.0	ER505	743	21078	Ind-24	732/746/760		
PC-139	SAW	Mod.	30176	25	760	1.0	ER505	743	21078	Ind-24	732/746/760		
PC-140	GTAW	Mod.	30394	25	760	1.0	ER505	744	21078	3He-1Ar			
PC-141	GTAW	Mod.	30176	25	760	1.0	ER505	744	21078	3He-1Ar			For mechanical testing by subcontractors.
PC-142	SAW	Mod.	30176	25	621	1.0	ER505	742	21078	Ind-24			For mechanical testing by subcontractors.
PC-143	SAW	Mod.	30176	25	621	1.0	ER505	742	21078	Ind-24			High heat input - excessive penetration.
PC-144	GTAW	Mod.	30176	13	621	1.0	ER505	742	21078				Lower H than PC-142.
PC-147	SAW	Mod.	30176	25	621	1.0	ER505	742	21078	Ind-24	746	4.0	9Cr-1Mo buttering - effect on overtemper zone.
PC-148	SAW	Mod.	30176	25	621	1.0	ER505	742	21078	Ind-24	746	4.0	To qualify procedure and welding materials.
PC-149	GTAW	Mod.	30176	25	621	1.0	ER505	758	21648	Ar			To qualify procedure and welding materials.
PC-150	GTAW	Mod.	30176	25	621	1.0	ER505	758	21648	Ar			To qualify welding materials.
PC-151	SAW	Mod.	30176	25	621	1.0	ER505	758	21648	Ar			To qualify manual GTAW procedure.
PC-152	GTA	Mod.	30176	25	760	1.0	ER505	758	21648	Ind-4	745	4.0	0.5g FeMn added per pass.
PC-153	GTA	Mod.	30176	25	760	1.0	ER505	758	21648	Ar	none		Stress corrosion cracking test.
PC-154	GTA	Mod.	30176	25	760	1.0	ER505	758	21648	Ar	none		Stress corrosion cracking test.
PC-155	GTA	Mod.	30176	25	760	1.0	ER505	758	21648	AR	none		Stress corrosion cracking test.
PC-156	SAW	Mod.	30176	25	760	1.0	ER505	758	21648	L0091	745	1.0	Charpy V-notch testing - AC current.
PC-157	SAW	Mod.	30176	25	760	1.0	ER505	758	21648	L0091	745	4.0	Charpy V-notch testing - DC+ current.
PC-158A	SAW	Mod.	30176	25	760	1.0	ER505	758	21648		774	4.0	Charpy V-notch testing - AC current.
PC-158B											732		
PC-93	SAW	Mod.		200	760			714	33669		732		
PC-81	SAW	Mod.	30393		760			692	C2626				

A2.2. Results of creep-rupture tests on weldments
of modified 9Cr-1Mo steel

Test	Weld	Heat treatment (°C/°C/°C)	Test temperature (°C)	Stress (MPa)	Test time (h)	Reduction of area (%)	Comments
22945	30394L	As-welded	538	221	12,158	75	
22948	30394L	As-welded	538	207	16,328	87	
22946	30394L	As-welded	538	179	24,994	24	
22949	30394L	As-welded	565	172	1,759	84	
22950	30394L	As-welded	565	124	18,067	25	
22938	30394L	As-welded	593	159	1,457	70	
22937	30394L	As-welded	593	145	2,091	73	
23102	30394L	As-welded	649	90	162	71	
20997	PC-4	1038/760/760	538	234	290	75	
20991	PC-4	1038/760/760	649	117	35	73	
20993	PC-4	1038/760/760	649	83	307	49	
20998	PC-5	1038/760/760	649	117	27	81	
21003	PC-5	1038/760/760	649	83	194	73	
21236	PC-9	1038/760/732	538	234	201	73	
21215	PC-9	1038/760/732	649	117	30	68	
21225	PC-9	1038/760/732	649	83	308	38	
22995	PC-10	1038/760/732	593	172	238	60	
22981	PC-10	1038/760/732	593	159	538	55	
21257	PC-10	1038/760/732	649	117	45	54	
21492	PC-13	1038/760/732	538	276	288	83	
21418	PC-13	1038/760/732	649	117	53	83	
21490	PC-13	1038/760/732	649	83	560	80	
21519	PC-16	1038/760/732	538	276	2,834 ^a		All weld metal
23233	PC-16	1038/760/732	649	117	10,505 ^a		All weld metal
22093	PC-32	1038/760/732	538	276	50	84	
22099	PC-32	1038/760/732	538	234	683	82	
22086	PC-32	1038/760/732	538	234	385	84	
22060	PC-32	1038/760/732	593	193	35	73	
21954	PC-32	1038/760/732	649	159	2,038	78	
22072	PC-32	1038/760/732	593	103	164	77	
22434	PC-36	As-welded	593	771	771	771	
22478	PC-36	1038/760/732	593	193	292	41	
22549	PC-36	1038/760/732	593	159	1,850	6	
22559	PC-36	1038/760/732	593	193	461	10	
23489	PC-90	1038/760/732	593	172	586	9	
23493	PC-90	1038/760/732	593	145	2,548	48	
23498	PC-90	1038/760/732	649	131	34	16	
23485	PC-90	1038/760/732	649	117	78	7	
23486	PC-90	1038/760/732	649	90	450	16	
23497	PC-90	1038/760/732	649	76	840	1	
23703	PC-93	1038/760/732	593	145	238	85	
23549	PC-93	1038/760/732	593	145	1,070	79	
23543	PC-94	1038/760/732	649	76	882	18	
23634	PC-94	1038/760/732	677	55	667	34	
23630	PC-94	1038/760/732	677	41	2,578	74	
23540	PC-95	1038/760/732	593	145	2,223	52	
23551	PC-95	1038/760/732	649	69	2,521	14	
23644	PC-102	1038/760/732	593	145	2,468	49	
23632	PC-102	1038/760/732	649	76	510	49	
22530	PC-39	1038/677/760	593	193	298	20	

Table A2.2 (cont'd)

Test	Weld	Heat treatment (°C/°C/°C)	Test temperature (°C)	Stress (MPa)	Test time (h)	Reduction of area (%)	Comments
22550	PC-39	1038/677/760	593	159	1,448	11	
22529	PC-39	1038/677/760	649	117	72	28	
22534	PC-39	1038/677/760	649	103	103	25	
22596	PC-42	1038/760/704	593	193	18	84	
22609	PC-42	1038/760/704	593	159	320	86	
22627	PC-42	1038/760/704	593	145	1,036	85	
22836	PC-45	1038/760/760	593	159	2,318	10	
22860	PC-45	1038/760/760	593	124	4,765	28	
22916	PC-52	1038/760/732	593	159	813	24	
22934	PC-52	1038/760/732	593	159	1,538	17	
22935	PC-52	1038/760/732	593	145	2,319	22	
23022	PC-58B	1038/760/732	593	172	555	76	
23023	PC-58B	1038/760/732	593	159	1,203	53	
23034	PC-58B	1038/760/732	593	145	2,647	41	
23161	PC-59	As welded	593	172	858	43	
23115	PC-59	As welded	593	159	1,268	20	
23116	PC-59	As welded	649	103	133	16	
23124	PC-59	As welded	649	90	357	11	
23236	PC-63	1038/760/732	593	172	582	16	
23295	PC-63	1038/760/732	593	145	3,364	9	
23457	PC-63	1038/760/732	649	90	334	17	
23285	PC-71	1038/760/732	538	207	17,202	30	
23271	PC-71	1038/760/732	593	172	132	59	
23283	PC-71	1038/760/732	593	172	186	58	
23276	PC-71	1038/760/732	593	172	1,627	32	
23430	PC-71	1038/760/732	593	145	1,785	36	
23366	PC-74	1038/760/732	593	172	63	77	
23385	PC-74	1038/760/732	593	145	198	75	
23884	PC-75	1038/760/732	593	172	1,460	3	
23386	PC-75	1038/760/732	593	145	2,643	7	
23709	PC-80	1038/760/732	677	55	4,924	25	
23501	PC-90	1038/760/732	538	234	2,783	72	
23504	PC-90	1038/760/732	538	207	15,279	80	
23502	PC-90	1038/760/732	593	193	86	62	

^aTest discontinued before rupture.

Appendix 3

MICROSTRUCTURAL ANALYSIS OF 9Cr-1Mo STEEL
(HEATS 91887 AND XA3370)

The following is discussion concerning detailed quantitative microscopy performed on heats 91887 (commercial) and XA3370 (experimental). The chemical compositions of these are provided in Table A3.1.

Table A3.1. Average of top and bottom ingot chemical composition
(chromium equivalent numbers are also listed in this table)

Heat	Content (%)																				σ - Ferrite			
	C	Si	Mn	S	P	Cr	Mo	W	Nb	V	Ti	Ni	N	Total Al	B	Zr	Cu	Co	As	Sn	O	CrE	expected	found (%)
71887	0.097	0.08	0.38	0.005	0.007	9.22	1.01	<0.01	0.15	0.22	<0.01	0.08	0.038	0.003		<0.001	0.01	0.018			0.005	10.1	no	0
XA3370	0.0515	0.02	0.350	0.0085	0.0055	8.250	0.79	<0.01	0.045	0.11	<0.01	0.05	0.0380	0.0030	<0.01	<0.001	0.020	0.0155	<0.001	<0.001	0.0095	8.9	no	0

The heats were examined in the normalized and tempered condition (i.e., 1 h at 1038°C followed by air cool to 760°C, held for 1 h, and air cooled to room temperature) by R. W. Carpenter and P. S. Sklad of Oak Ridge National Laboratory. The following are their observations.

1. Low magnification-low contrast electron microscopy

The general microstructure of both alloys is shown in Fig. A3.1 (91887) and Fig. A3.2 (XA3370). It can be seen that both are composed of small subgrains whose dislocation density is variable. These subgrains are much smaller than the prior austenite grain size. The prior austenite boundaries are decorated with precipitates in both alloys, presumably carbides (see below). The prior austenite boundary precipitates are larger and less numerous in XA3370 than in 91887. Qualitative examination of large precipitate distribution showed that the concentration of nonaustenite boundary precipitate was higher in alloy 91887. An example of such precipitates is shown in Fig. A3.3; it is seen that these precipitates often occur on subgrain boundaries and that their size is about 1500 Å.

2. Chemical precipitate extractions

Chemical extractions of the precipitates were made to determine the amount of precipitate present in each alloy and for X-ray diffraction identification of precipitate phases. The results are given in Table A3.2. The precipitates identified were the same in both alloys: MC and $M_{23}C_6$. Alloy 91887 contained more precipitate, consistent with microstructural observation and alloy composition. Reference lattice constants for NbC and VC (ASTM files) are 4.4702 and 4.16 Å, respectively. The smaller MC unit cell determined for alloy 91887 (Table A3.2) is consistent with the larger vanadium concentration in that alloy. It is also probable that these precipitates contain other metallic constituents, especially Mo. This probability is based on experience with similar precipitates in austenitic stainless steel. Preferred orientation of precipitate particles on X-ray specimens rendered measurement of the relative concentration of MC and $M_{23}C_6$ by

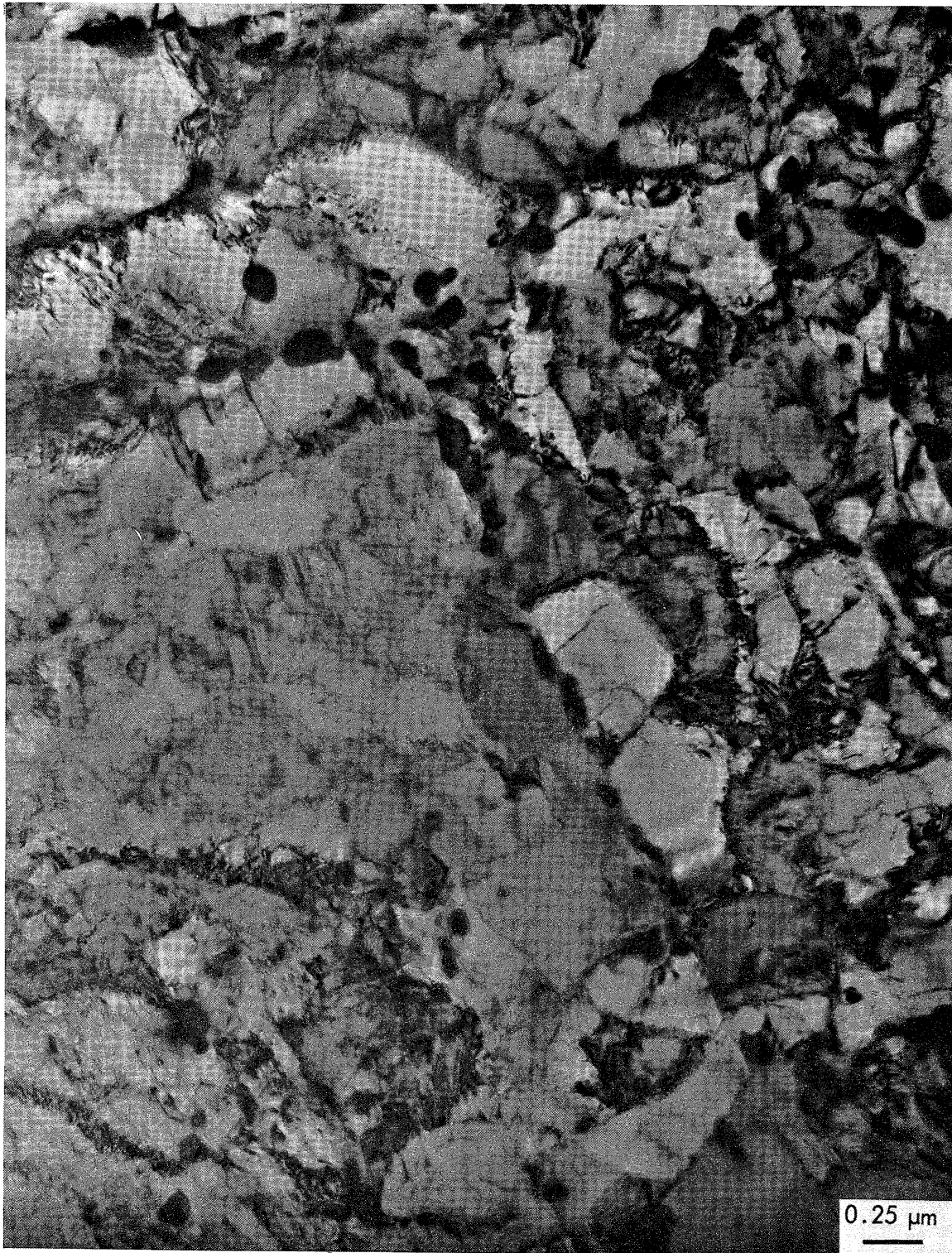


Fig. A3.1. Microstructures of 9Cr-1Mo (91887) showing subgrains as well as precipitates along prior austenitic grain boundaries.



Fig. A3.2. Microstructure of 9Cr-1Mo (XA3370) showing subgrains as well as grain boundary precipitates along prior austenite boundaries.



Fig. A3.3. Micrograph of 9Cr-1Mo (91887) illustrating the distribution of precipitates in locations other than at prior austenite boundaries.

Table A3.2

Alloy 91887	Alloy XA3370
0.92 wt% precipitate	0.57 wt% precipitate
MC: $a_0 = 4.42 \text{ \AA}$	MC: $a_0 = 4.46 \text{ \AA}$
$M_{23}C_6 = 10.63 \text{ \AA}$	$M_{23}C_6 = a_0 = 10.59 \text{ \AA}$

peak intensity ratios inconclusive. The precipitate concentrations detected indicate that a significant fraction of the niobium and vanadium in the alloys was contained in precipitates.

3. Low magnification-high contract microscopy

The defect structure in the alloys is shown in more detail in Fig A3.4 (91887) and Fig. A3.5 (XA3370). In both cases the average dislocation density is high, but the distribution is rather heterogeneous.

Subgrain structure is more evident in these micrographs taken under slightly different imaging conditions. The high dislocation density is particularly well shown in Fig. A3.5, in which a bend contour runs from top left to bottom right across the micrograph. Note the presence of some nearly dislocation free subgrains, and variable changes in orientation across subgrain boundaries. The boundary misorientations have not been measured because the ferromagnetism of the specimen interfered with the required procedure.

4. Higher magnification boundary examination

The structure of some of the subgrain boundaries is shown in more detail in Figs. A3.6 and A3.7 (alloy 91887) and Figs. A3.8 and A3.9 (alloy XA3370). In many subgrain boundaries the dislocations are in networks, possibly more regular in alloy 91887. Close examinations of the subgrain boundaries shows that there may be small precipitates on many of the dislocations, particularly in alloy 91887; however, the resolution is poor and precipitate effects cannot positively be distinguished from dynamical contrast oscillations. There was no evidence of acicular platelet formation, microtwinning, or high density dislocation braids, all of which are characteristic of martensitic transformations in iron-base alloys.



Fig. A3.4. Microstructure of 9Cr-1Mo (91887) showing the general dislocation distribution.



Fig. A3.5. Microstructure of 9Cr-1Mo (XA3370) showing heterogeneous dislocation distribution.



Fig. A3.6. Micrograph showing detail of dislocation networks in subgrain boundaries in alloy 91887.



Fig. A3.7. Micrograph showing detail of dislocation networks in subgrain boundaries in alloy 91887.



Fig. A3.8. Micrograph showing detail of dislocation networks in subgrain boundaries in alloy XA3370.

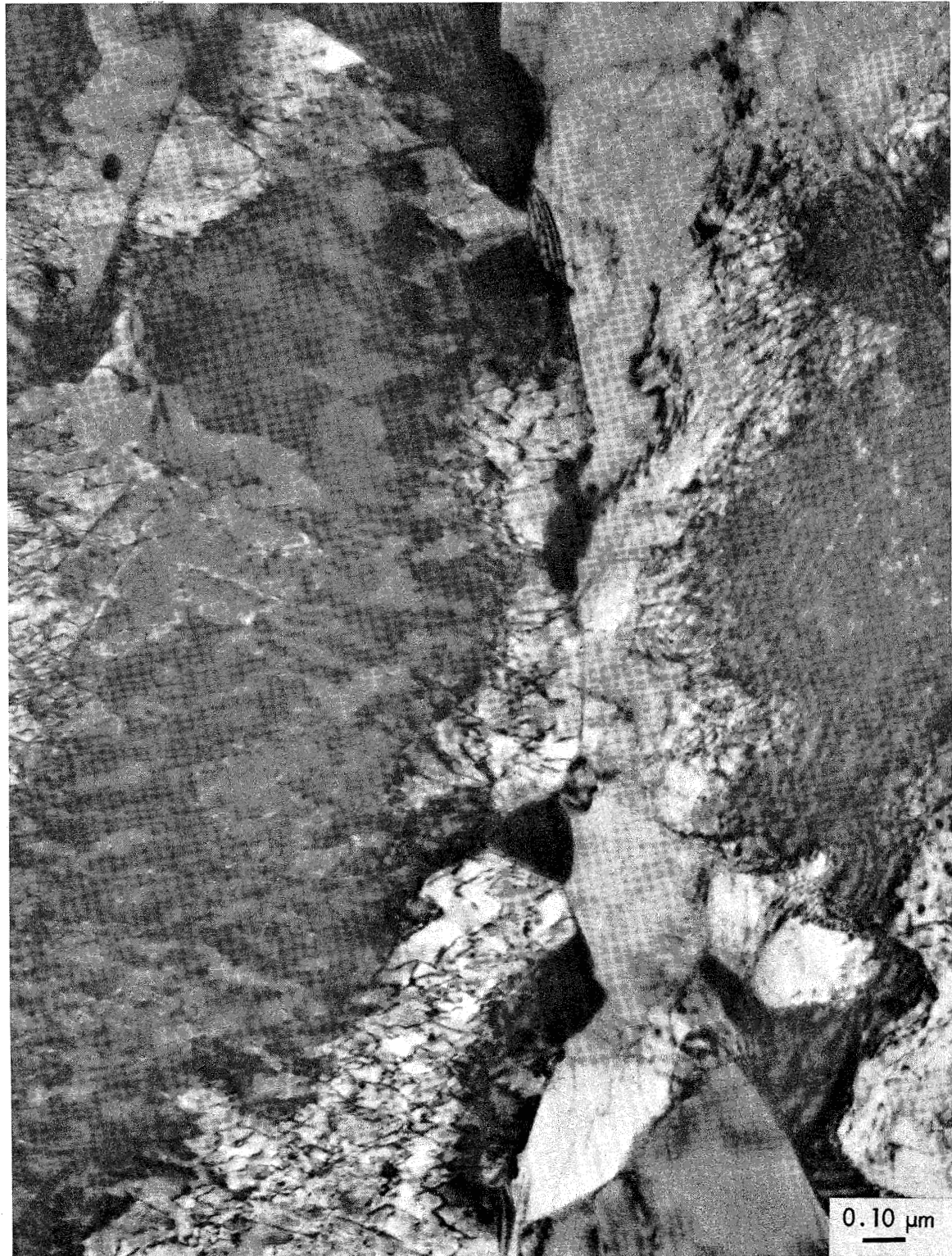


Fig. A3.9. Micrograph showing detail of dislocation networks in subgrain boundaries in alloy XA3370.

5. Energy-dispersive X-ray spectroscopy

Energy-dispersive X-ray spectroscopy was performed on alloy 91887 to check the composition in situ of the large precipitates and to evaluate the method for ferromagnetic specimens. A precipitate examined is shown in Fig. A3.10, taken with the specimen untilted. Upon tilting to the orientation required for X-ray spectroscopy (or image analysis, for that matter), the image quality deteriorated somewhat, as shown in Fig. A3.11. The large precipitate of interest is visible, but finer detail was lost. This resulted from interaction of the now asymmetric specimen magnetic field with the incident beam and the symmetric objective lens field. This effect can be alleviated to a significant extent by using a different specimen preparation method. The X-ray spectra obtained from the precipitate and adjacent matrix are shown in Fig. A3.12. The precipitate does in fact contain a large amount of niobium and a smaller amount of vanadium. The other peaks are to be disregarded at present, since the analysis was performed in situ.

6. Elastic diffuse scattering

In thin regions of the foils elastic diffuse scattering was observed such as that often observed in other alloys in the early stages of precipitation. Dark-field images were taken using elastic diffuse intensity. The results are shown in Fig. A3.13. The small bright contrast in Fig. A3.13(b) is about 50 Å in size and appears to be homogeneously distributed. This is in the proper size range for small precipitates; however, such effects can also result from surface oxide particles formed during specimen preparation. It is only possible to distinguish the two cases using large-angle tilting experiments and dark-field stereo-pairs.

DISCUSSION

The experimental observations described above show that the microstructure of alloy 91887 contains more precipitate than that of alloy XA3370, and that the defect distribution in both alloys is quite similar, with alloy 91887 probably having more regular dislocation arrays in the subgrain boundaries than alloy XA3370. Neither alloy shows a microstructure characteristic of martensite.

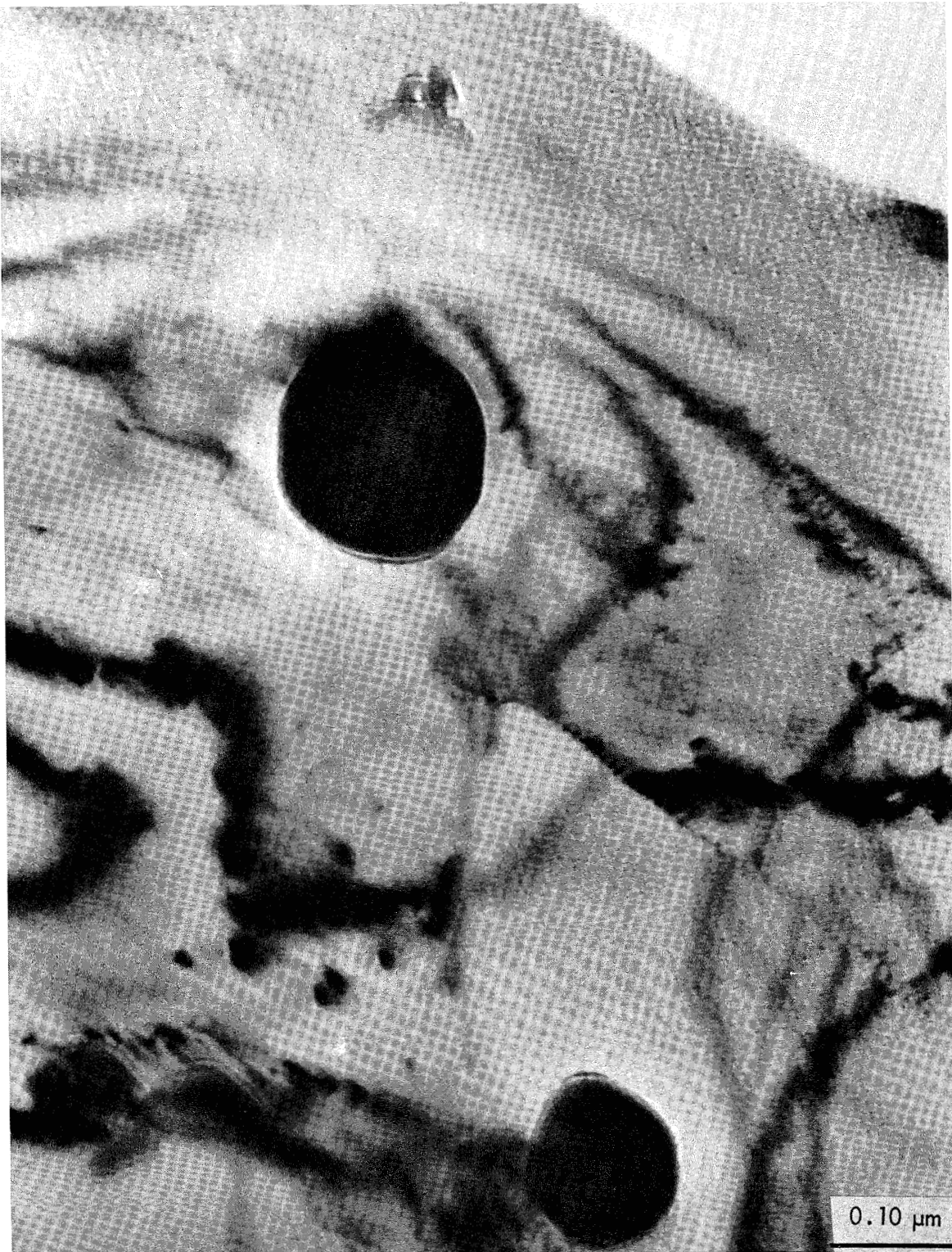


Fig. 3.10. Precipitate examined by in situ energy dispersive X-ray spectroscopy. Specimen is untilted.

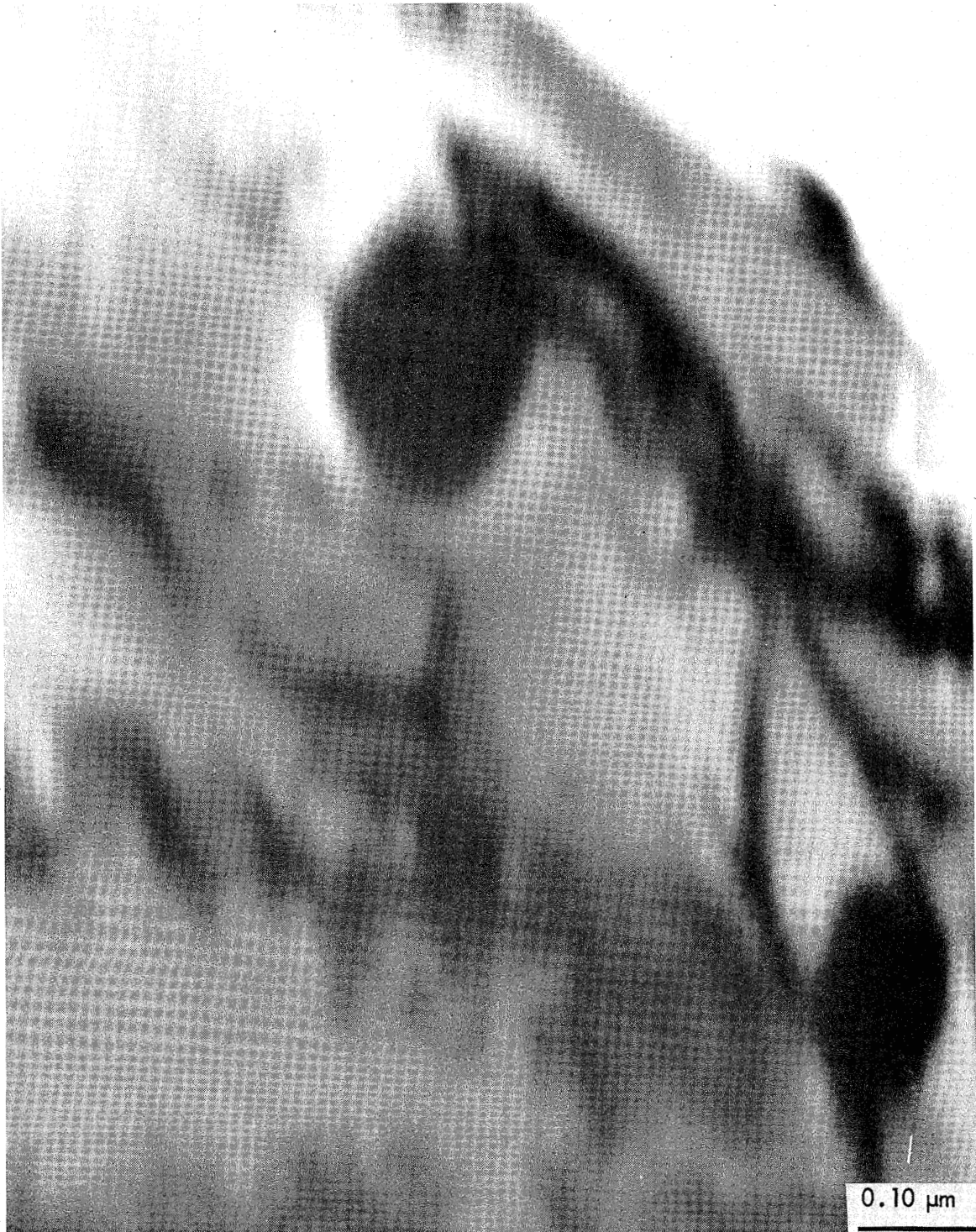


Fig. A3.11. Same precipitate shown in Fig. A3.10 with specimen tilted for X-ray microanalysis. Deterioration of the image quality is due to the interaction of the asymmetric magnetic field of the specimen with the objective lens field.

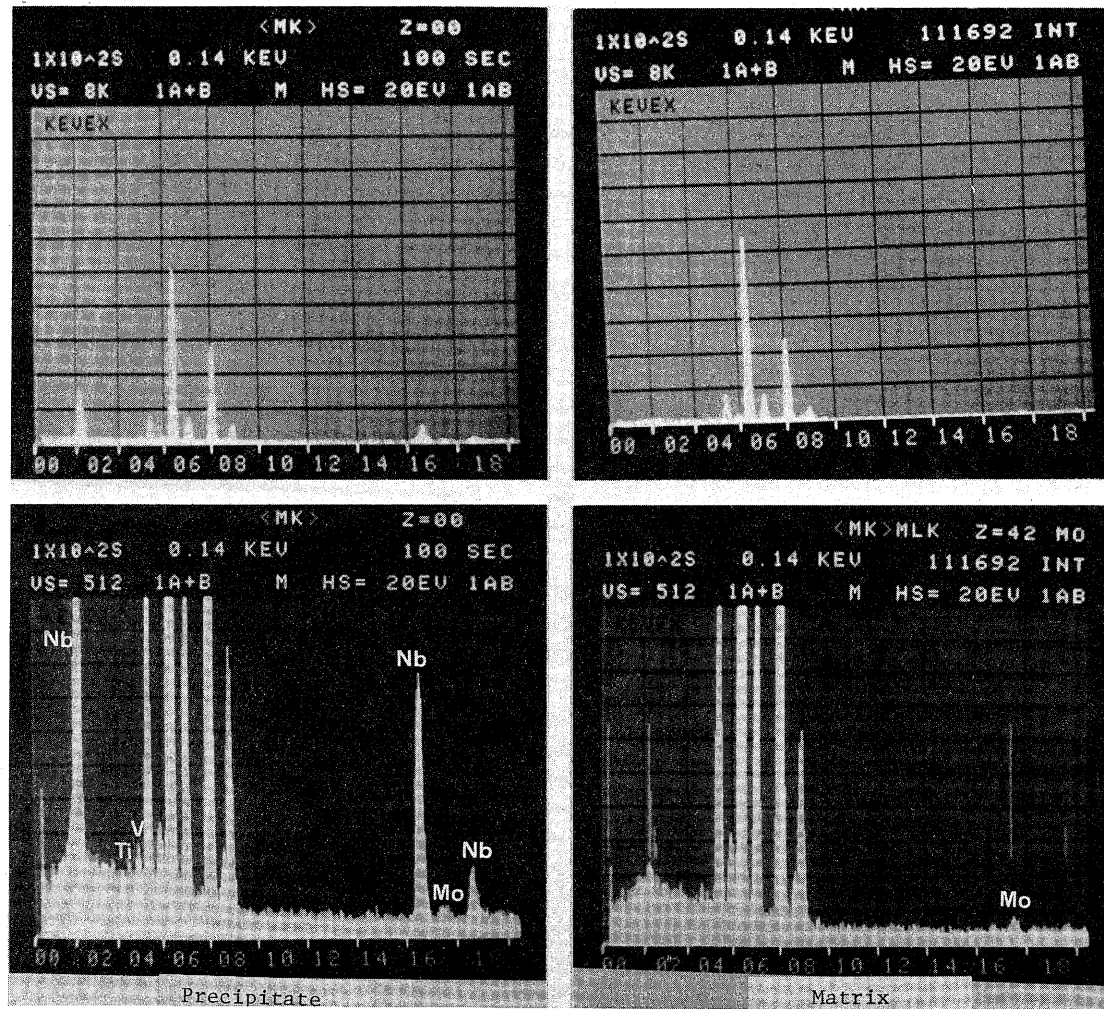


Fig. A3.12. X-ray spectra from MC precipitate analyzed in situ and adjacent matrix. Note the presence of Nb and V in the precipitate. Lower spectra show detail with expanded vertical scale.

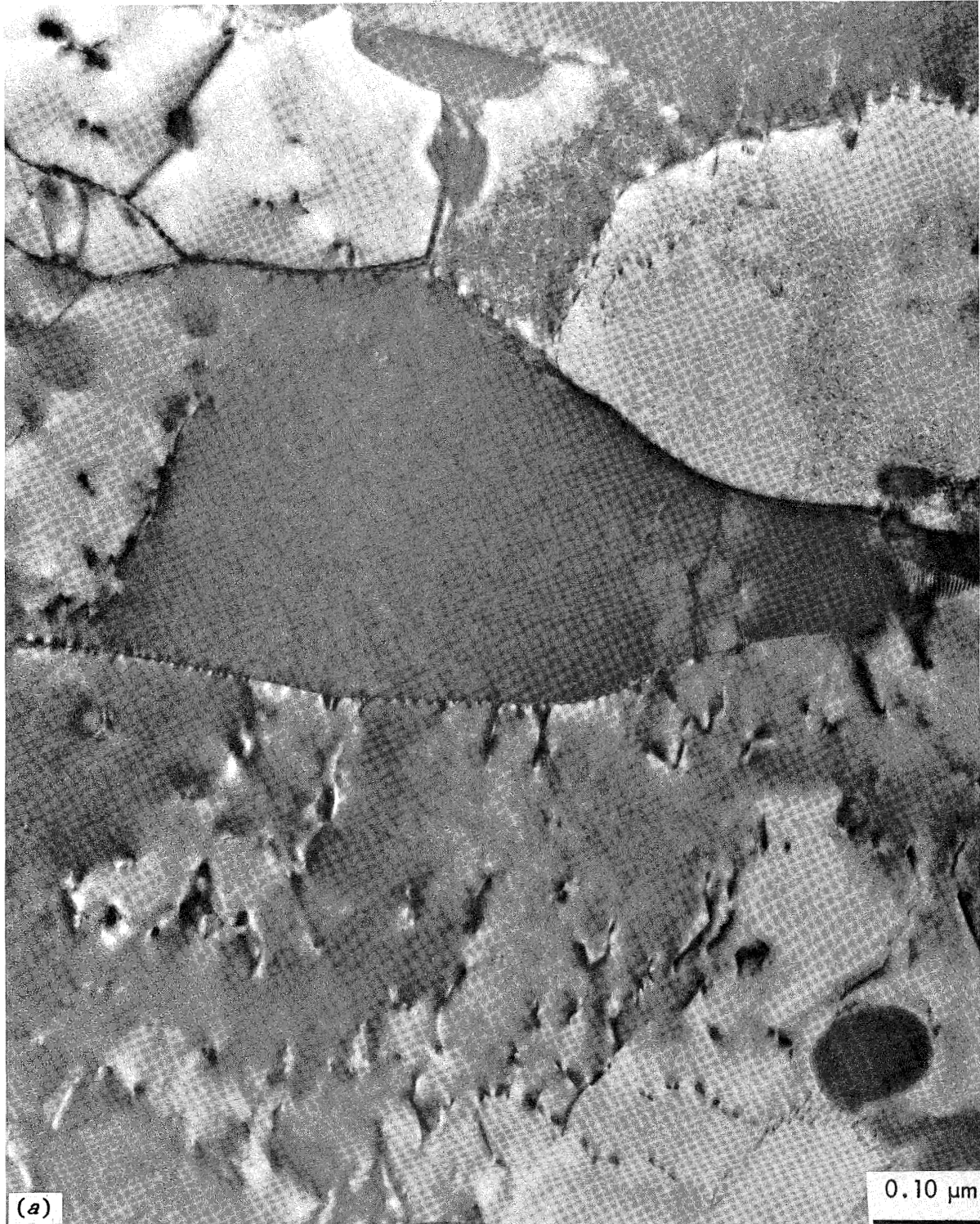


Fig A3.13. (a) Bright field, (b) dark field, and (c) selected area diffraction pattern illustrating the presence of small particles (~ 5 nm) in alloy XA3370. These may be precipitates or surface oxide particles.

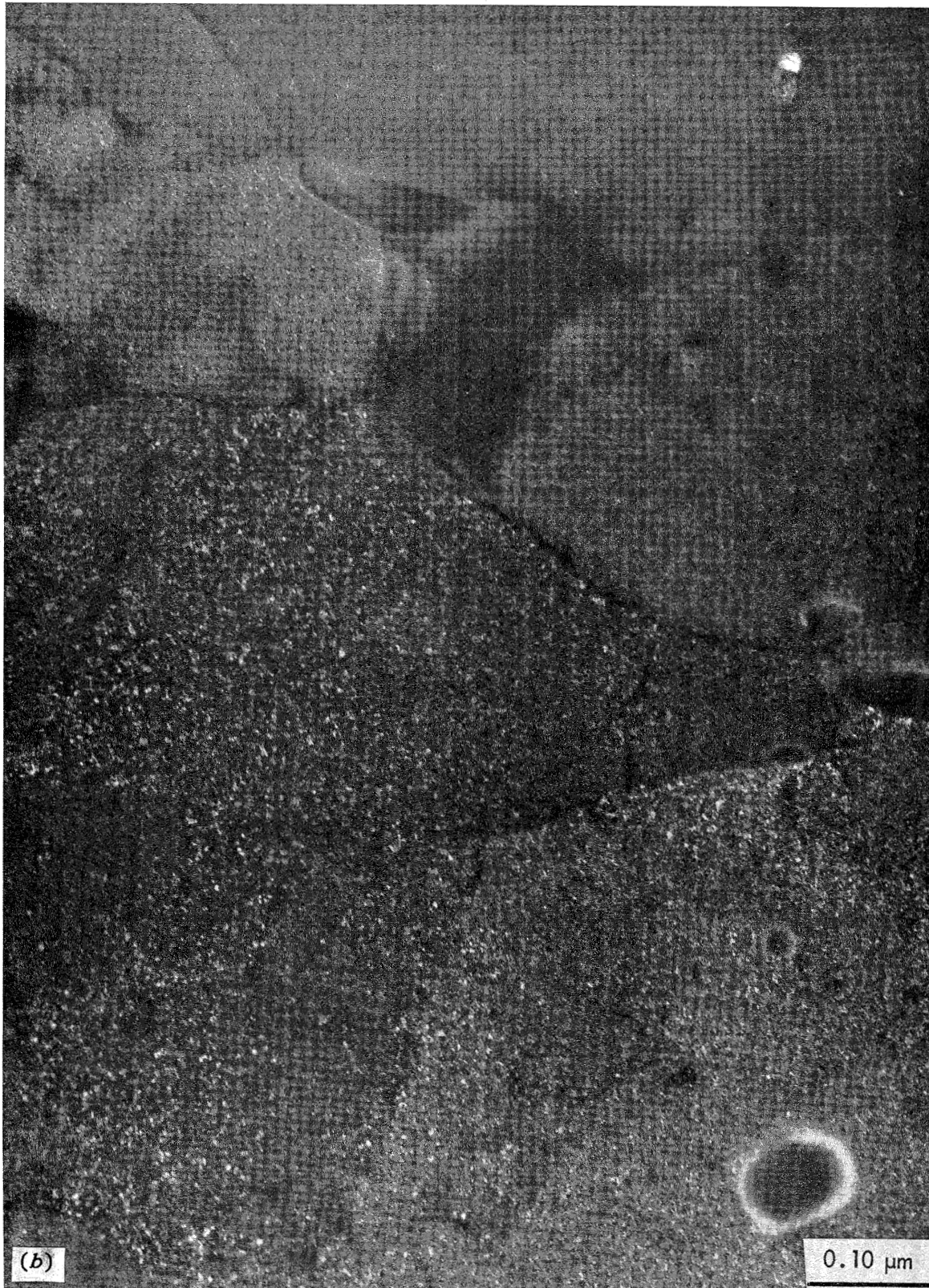
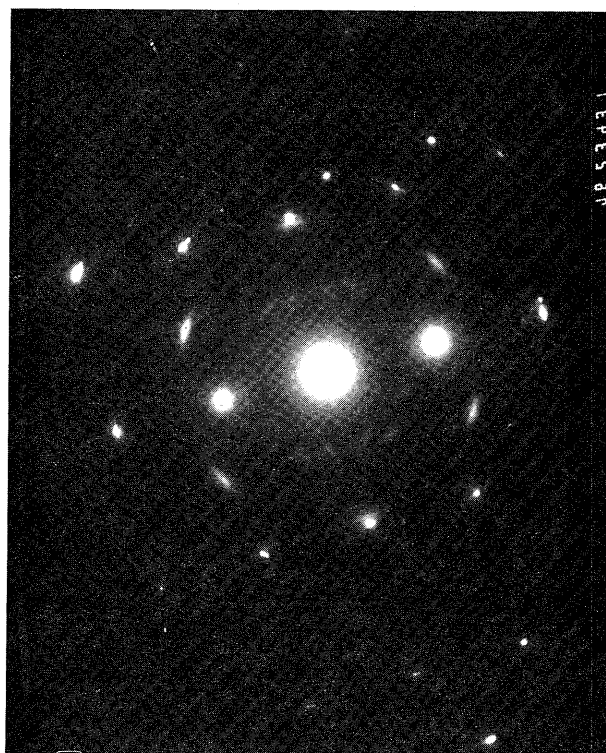


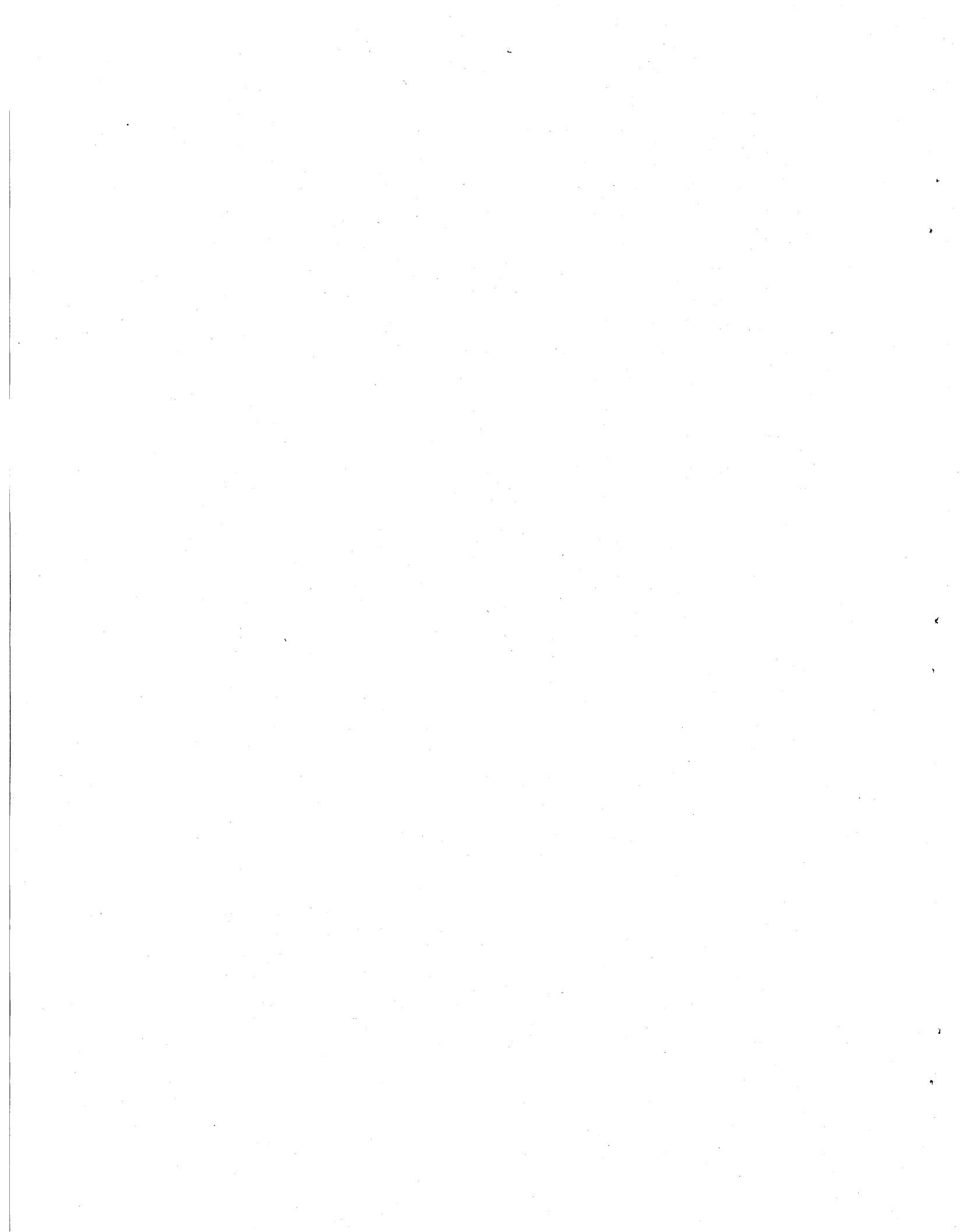
Fig. A3.13 (cont'd)



(c)

Fig. A3.13 (cont'd)

The room-temperature stress-strain behavior of these alloys is similar, and that similarity is reflected in the microstructural observations, which show that the dominant obstacles to dislocation motion are the subgrain boundaries. Dislocation motion stress upon yielding, neglecting lattice friction, will be determined by a characteristic length of dislocation between pinning points. The length between pinning points will be determined by the subgrain size, the dislocation spacing in imperfect cell walls or the dislocation grid spacings in perfect cell walls. Taking these measurements from the micrographs, the shear modulus of both alloys as 82.7×10^3 MPa, and the Burgers vectors to be $b = 1/2 \langle 111 \rangle$ the Orowan contribution to the yield stress is estimated to be 83, 345, and 3,488 MPa for the three cases, respectively. It is clear that dislocations in imperfect cell walls are controlling the room-temperature yield stress of both alloys. It is expected that the incoherent carbide or other precipitates on prior austenite grain boundaries and elsewhere are effective void nucleation sites leading to ductile microvoid fracture at room temperature. It would be useful to examine these fractures in SEM to examine this supposition.



ORNL/TM-10504
 Distribution
 Categories UC-79Th,
 -Tk, -Tr

INTERNAL DISTRIBUTION

- | | | | |
|--------|-------------------------------|--------|-----------------------------|
| 1-2. | Central Research Library | 27-31. | M. L. Santella |
| 3. | Document Reference Section | 32. | W. K. Sartory |
| 4-5. | Laboratory Records Department | 33-37. | V. K. Sikka |
| 6. | Laboratory Records, ORNL RC | 38. | G. M. Slaughter |
| 7. | ORNL Patent Section | 39. | J. O. Stiegler |
| 8. | J. J. Blass | 40. | J. P. Strizak |
| 9. | M. K. Booker | 41. | R. W. Swindeman |
| 10. | R. A. Bradley | 42-44. | P. T. Thornton |
| 11-15. | C. R. Brinkman | 45. | J. R. Weir |
| 16. | J. M. Corum | 46. | H. D. Brody (Consultant) |
| 17-21. | J. A. Horak | 47. | G. Y. Chin (Consultant) |
| 22. | R. L. Huddleston | 48. | F. F. Lange (Consultant) |
| 23. | J. E. Jones Jr. | 49. | W. D. Nix (Consultant) |
| 24. | R. R. Judkins | 50. | D. P. Pope (Consultant) |
| 25. | K. C. Liu | 51. | E. R. Thompson (Consultant) |
| 26. | P. L. Rittenhouse | | |

EXTERNAL DISTRIBUTION

52. ARGONNE NATIONAL LABORATORY, 9700 S. Cass Avenue, Argonne, IL 60439
 O. K. Chopra
- 53-54. BABCOCK AND WILCOX COMPANY, Fossil Power Generation Division,
 20 South Van Buren Avenue, Barberton, OH 44203
 M. Gold
 C. C. Schultz
55. BURNS AND ROE, INC., 700 Kinderkamack Road, Oradell, NJ 07469
 C. S. Ehrman
- 56-57. COMBUSTION ENGINEERING, INC., 1000 Prospect Hill Road, Windsor,
 CT 06095
 P.E.C. Bryant
 A. L. Gaines
58. ELECTRIC POWER RESEARCH INSTITUTE, 3412 Hillview Avenue,
 P.O. Box 10412, Palo Alto, CA 94303
 R. I. Jaffee

59. ELECTRIC POWER RESEARCH INSTITUTE-CONSOLIDATED MANAGEMENT ORGANIZATION, Suite 220, One Energy Center, Naperville, IL 60566
D. R. Riley
60. FOSTER WHEELER DEVELOPMENT CORPORATION, 12 Peach Tree Hill Road, Livingston, NJ 07039
M. D. Bernstein
61. GA TECHNOLOGIES, INC., P.O. Box 86508, San Diego, CA 92138
D. I. Roberts
- 62-63. GENERAL ELECTRIC COMPANY, Nuclear Systems Technology Operations, 310 DeGuigne Drive, P.O. Box 3508, Sunnyvale, CA 94088
P. J. Ring
P. Roy
64. HANFORD ENGINEERING DEVELOPMENT LABORATORY, P.O. Box 1970, Richland, WA 99352
L. K. Severud
- 65-66. ROCKWELL INTERNATIONAL, Rocketdyne Division, 6633 Canoga Avenue, Canoga Park, CA 91304
K. Jaquay
W. Veljovich
67. ROCKWELL INTERNATIONAL, Energy Technology Engineering Group, P.O. Box 1449, Canoga Park, CA 91304
H. C. Wieseneck
68. WESTINGHOUSE ELECTRIC CORPORATION, Advanced Energy Systems Division, P.O. Box 10864, Pittsburgh, PA 15236
R. W. Buckman
- 69-75. DOE, Washington, DC 20545
Office of Fossil Energy, Technical Coordination Staff
M. I. Singer

Office of Fusion Energy
T. C. Reuther

Office of Reactor Systems Development and Technology
C. C. Bigelow
N. Grossman
R. J. Neuhold
A. VanEcho

Office of Breeder Technology Projects
Director

76. DOE, Oak Ridge Operations Office, P.O. Box E, Oak Ridge, TN 37831
Office of Assistant Manager for Energy Research and
Development

77-175. DOE, Technical Information Center, P.O. Box 62, Oak Ridge, TN
37831

For distribution as shown in DOE/TIC-4500, Distribution
Categories UC-79Th (Structural Materials and Design
Engineering), UC-79Tk (Components), and UC-79Tr (Structural
and Component Materials Development).

